Instituut voor Ruimtelijk Onderzoek
Institute of Geographical Research

Rapport GEOPRO 1991.01

BEACH MORPHODYNAMIC SYSTEMS OF THE
CENTRAL NETHERLANDS COAST,
DEN HELDER TO HOEK VAN HOLLAND

Andrew D. Short

BEACH MORPHODYNAMIC SYSTEMS OF THE CENTRAL NETHERLANDS COAST, DEN HELDER TO HOEK VAN HOLLAND

ANDREW D. SHORT

Coastal Studies Unit[1]
Department of Geography
University of Sydney
Sydney NSW 2006

and

Department of Physical Geography
University of Utrecht
PO Box 80115
3508 TC Utrecht

August 1990

1   Present address:

         Coastal Studies Unit
         Department of Geography
         University of Sydney
         Sydney NSW 2006
         AUSTRALIA

         FAX: 61 2 692 3644

ABSTRACT

The 120 km long central Netherlands coast consists of an essentially continuous sandy Holocene regressive/transgressive barrier system facing the southern North Sea. The beach and surf zone is composed of predominantly quartz sands which are coarsest at the shoreline (D50 = 286 Um) and fine seaward. Overall shoreface gradients vary between a low of 0.01 in the central region steepening to 0.015 towards dan Helder in the north and Hoek van Holland in the south. Tides are micro-tidal ranging from 1.4 to 1.7 m. The wave climate is a fetch limited strom wave environment generated by onshore winds in the North Sea together with occasional swell. Waves average 1.4 m in height with a period of 5.4 sec. They peak during the winter storms with a January mean Ho = 1.86 m and storm waves to 3 - 4 m. During summer they decrease to a mean of ~ 1.0m.

The interaction of the wave climate with the sandy shoreface has produced a 2 to 3 bar surf zone. Based on aerial photographs, the inner (bar 1) is modally a ridge and runnel/low tide terrace, bar 2 varies between transverse bar and rip and rhythmic bar and beach, while the outer bar 3 where present is rhythmic bar and beach to longshore bar and trough. All bars are characterised by rhythmic topography and rips which increase in spring from a mean of 500 m (bar 1) to 600 m (bar 2) and 900 m (bar 3). Groyne fields occupy 43 km of the coast and with a mean spring of 200 m induce an increase in rip occurrence and decrease in rip spacing.

The morphodynamics of the beach-bar system can be explained in temporal and spatial terms by examining the impact of the wave climate on the shoreface. Temporal variation is controlled both by seasonal variation in wave height and storm frequency and by inter-storm beach recovery. It is proposed that the spatial variation in bar number (2 or 3), bar spacing and rip spacing is related to infragravity standing and edge waves generated by wave groupiness, acting across the two slope regimes (0.01 and 0.015) which produce standing wave lengths which correlate with actual bar spacing and edge wave lengths which correlate reasonably with rip spacings. Both require however field verification. The hierarchy of bar types is empirically explained by decreasing breaker wave heights across the 300-600 m wide surf zone.

Finally a beach model is proposed for the coast consisting of six stages, a fully dissipative end member expected to occur during severe storm surges, two intermediate modal states consisting of the bar types mentioned above, and lower energy intermediate and a reflective member which are unlikely to occur in this wave climate.

BEACH MORPHODYNAMIC SYSTEMS OF THE CENTRAL NETHERLANDS COAST, DEN HELDER TO HOEK VAN HOLLAND

ABSTRACT

BEACH MORPHODYNAMIC SYSTEMS OF THE CENTRAL NETHERLANDS COAST, DEN HELDER TO HOEK VAN HOLLAND

1.   INTRODUCTION

The Netherlands coast is 432 km long of which 82% consists of sandy beach systems. Inlets occupy 79 km (13%) of which 34 km are dyked and 24 km closed. The coast lies in three natural provincies (Fig. 1.1)

A- Waddenzee
B- Eems-Dollard
C- Lauwersmeer
D- IJsselmeer
E- Rijn
F- Maas
G- Schelde
H- Nieuwe Waterweg
I- Brielse Gat
J- Haringvliet
K- Grevelingen
L- Oosterschelde
M- Veerse Gat
N- Westerschelde

1. Zwarte Haan
2. Den Helder
3. Huisduinen
4. Callantsoog
5. Petten
6. Camperduin
7. Bergen aan Zee
8. Egmond aan Zee
9. Castricum aan Zee
10. IJmuiden
11. Bloemendaal aan Zee
12. Zandvoort
13. Noodwijk aan Zee
14. Katwijk aan Zee
15. Wassenaar
16. Scheveningen
17. Rijswijk
18. Ter Heijde
19. Hoek van Holland
20. Rotterdam
21. Cadzand
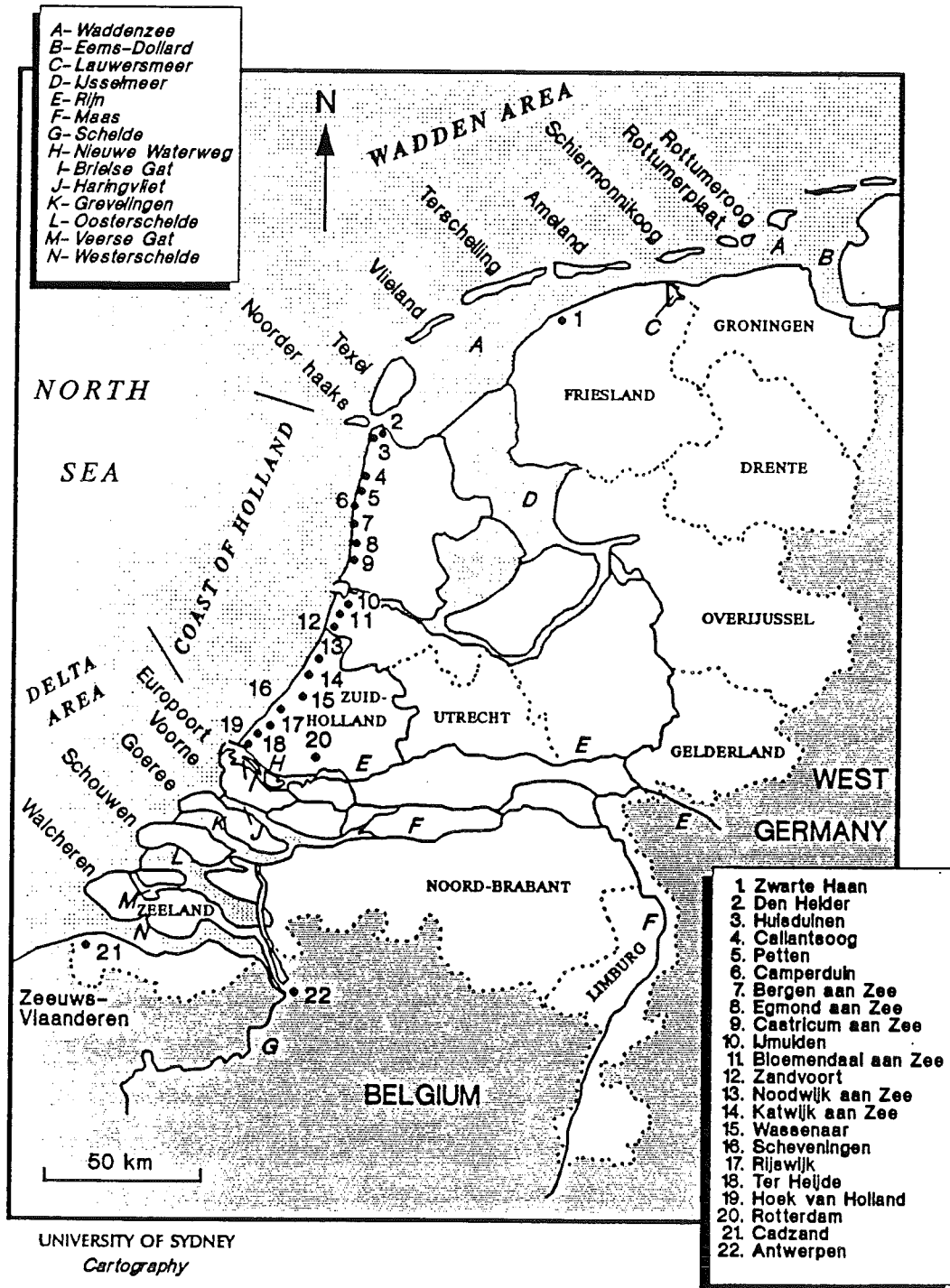22. Antwerpen

UNIVERSITY OF SYDNEY
Cartography

Figure 1.1   The Netherlands showing the three coastal provinces consisting of the Wadden Sea barrier islands and estuaries, the central coast of North and South Holland, and the delta area. Modified from Dillingh and Stolk, 1989.

1

In the north are the seven north and northwest facing Wadden Sea barrier islands with a total sea shore length of 121 km. The central coast consists of a continuous 124 km long, west facing, Holocene barrier. The southern Delta coast of the Zeeland province has a total length of 108 km. It consists of four shore perpendicular delta islands separated by wide, now largely dyked, estuarine systems.
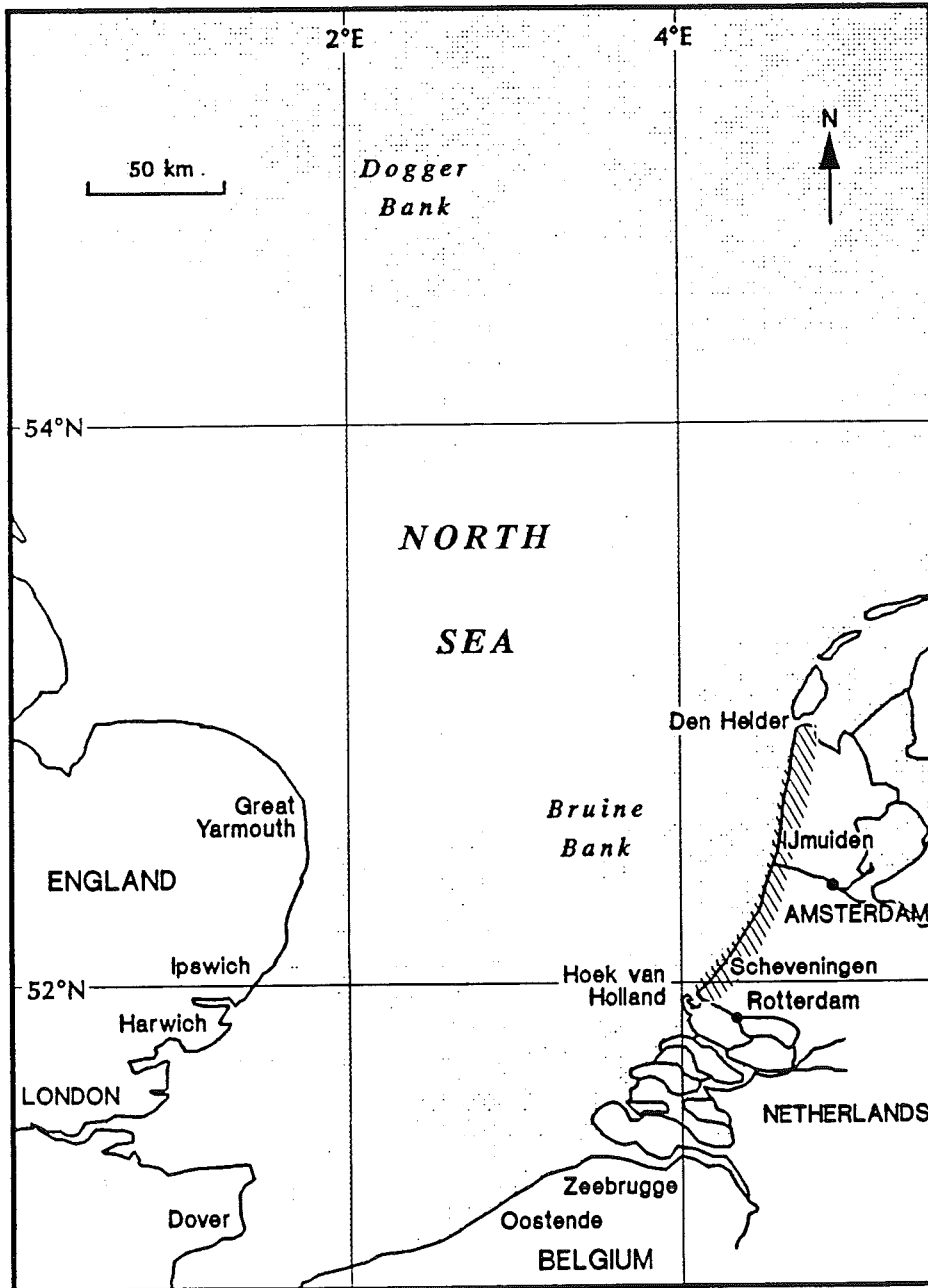

Figure 1.2 The southern North Sea showing the location of the central Netherlands and the coast lying between Den Helder and Hoek van Holland (shaded). To the north are the Wadden Sea barrier islands and tidal inlets and in the south the delta coast of Zeeland.

The entire coast has a west to north orientation and faces the southern North Sea (Fig. 1.2). The contemporary processes affecting the coast are related to wave, tide and wind regimes of the North Sea region interacting with the Netherlands shelf, beach, barrier and estuarine systems. The nature and degree of this interaction varies considerably around the coast in response to changing boundary conditions and processes regimes. The boundary conditions include the orientation particularly to waves and wind; the geomorphology (barrier and estuary); man's impact (dykes, surge barriers, breakwaters, groynes and nourishment) and sediment characteristics. The process regimes include the tide range, tidal and littoral currents, wave climate, wind climate and storm surges. Regional variation in these conditions causes the nature of the shoreline to vary considerably both within and between the three coastal provincies. Stolk (1989) subdivided the three provinces into 20 coastal sectors containing 56 coastal segments. His report provides an overview of the environmental factors that contribute to each sector and segment.

This report is concerned solely with the central Netherlands coast, the provincies of North and South Holland, which contain 124 km of essentially continuous sandy shoreline (Fig. 1.2). The aim of this study is to determine the nature and variability of the beach system that fronts the entire central coast. In particular it assesses the beach morphodynamics including type of beach along the coast, the degree of spatial and temporal variations in beach type and the processes contributing to beach type and its variation. Fig. 1.3-1.5 illustrate parts of the beach systems.

The beach systems are defined as including the subaerial beach and surf zone. Along the central coast this includes the shore parallel bar systems, but not the inner shelf shore connected ridges. It is essentially in the inner, steeper coastal slope (> 1:100) region of the Dutch shoreface as mapped by van Alphen and Damoiseaux (1989). The beach/bar type is defined using the classification of Wright and Short (1985). As each beach type has an inherent morphodynamic system, identification of beach types permits the assessment of beach morphodynamics along the coast. This method is elaborated on in Section 2.2.

The scope of the study is limited to the coast in question, and is also constrained by the nature of the data base. The study utilized entirely existing data. These data therefore dictated the temporal and spatial resolutions of the beach systems and factors contributing to these systems. Assessment of beach type was based on annual aerial photographs taken between 1982 and 1988. These provided complete spatial resolution but limited temporal change to seven annual samples. These samples fortunately indicate a wide, but not necessarily comprehensive range of beach types. These data combined with excellent data on beach profiles, nearshore gradients, coastal sediments and daily wave conditions have been analyzed to present the following preliminary assessment of the beach morphodynamic systems of the central Netherlands coast. The results do indicate the types of systems along the coast, the nature and controls of spatial change in the systems, and to a lesser extent the nature and controls on temporal changes.

3

Figure 1.3   The groyned beach system fronting the village of Callantsoog (km 14) located at km 18. Waves are barely breaking on the outer (bar 3), bar 2 lies as a transverse bar and rip system with groyne controlled rips while the inner bar 1 is welded to the beach. A high but narrow foredune protects Callantsoog from the North Sea (13.7.89).
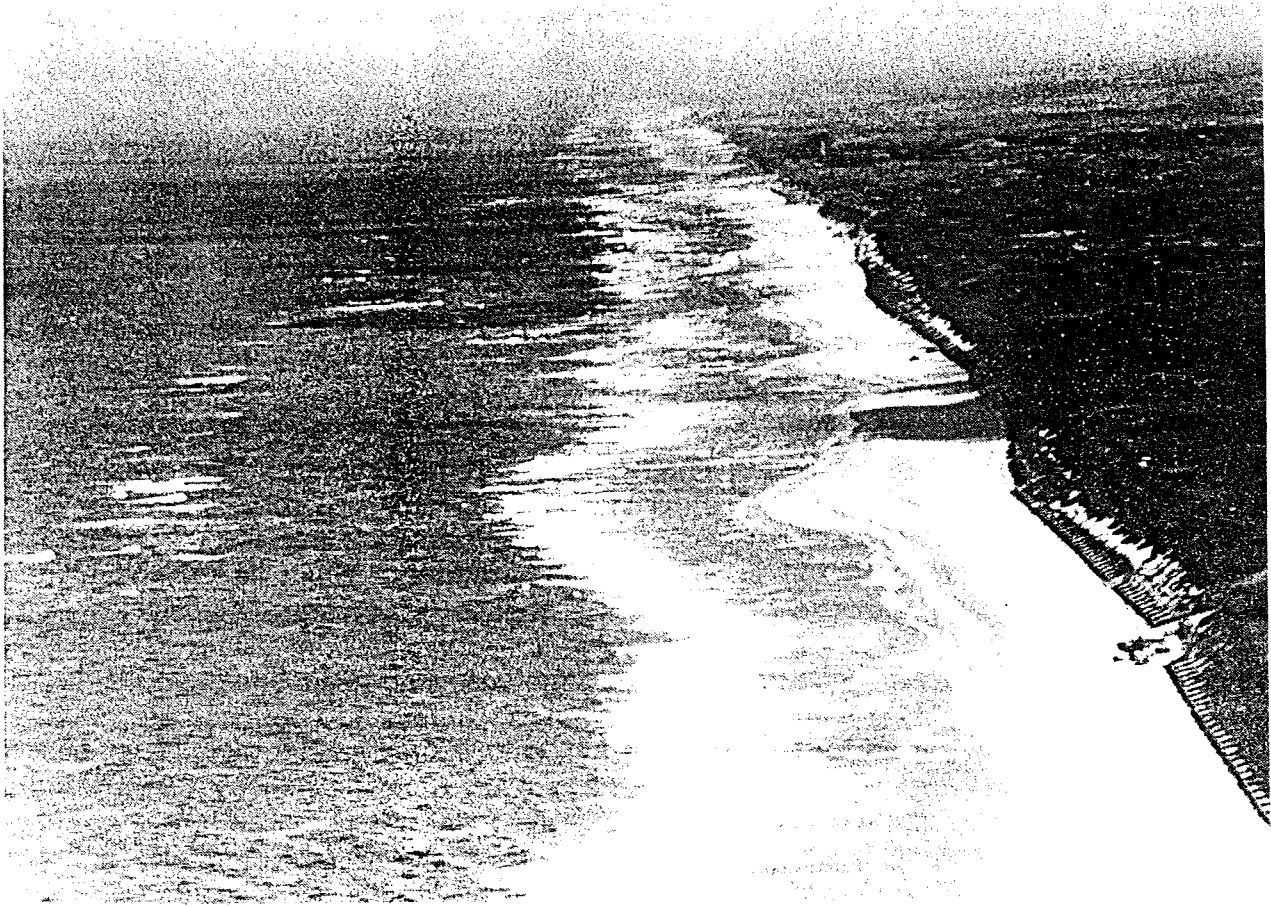
Figure 1.4   Highly rhythmic beach and bar topography immediately south of Egmond aan Zee (km 39). Waves are just breaking on bar 3, bar 2 is highly rhythmic and attached to the beach in places, while attached bar 1 forms rhythmic ridge and runnel systems (13.7.89).
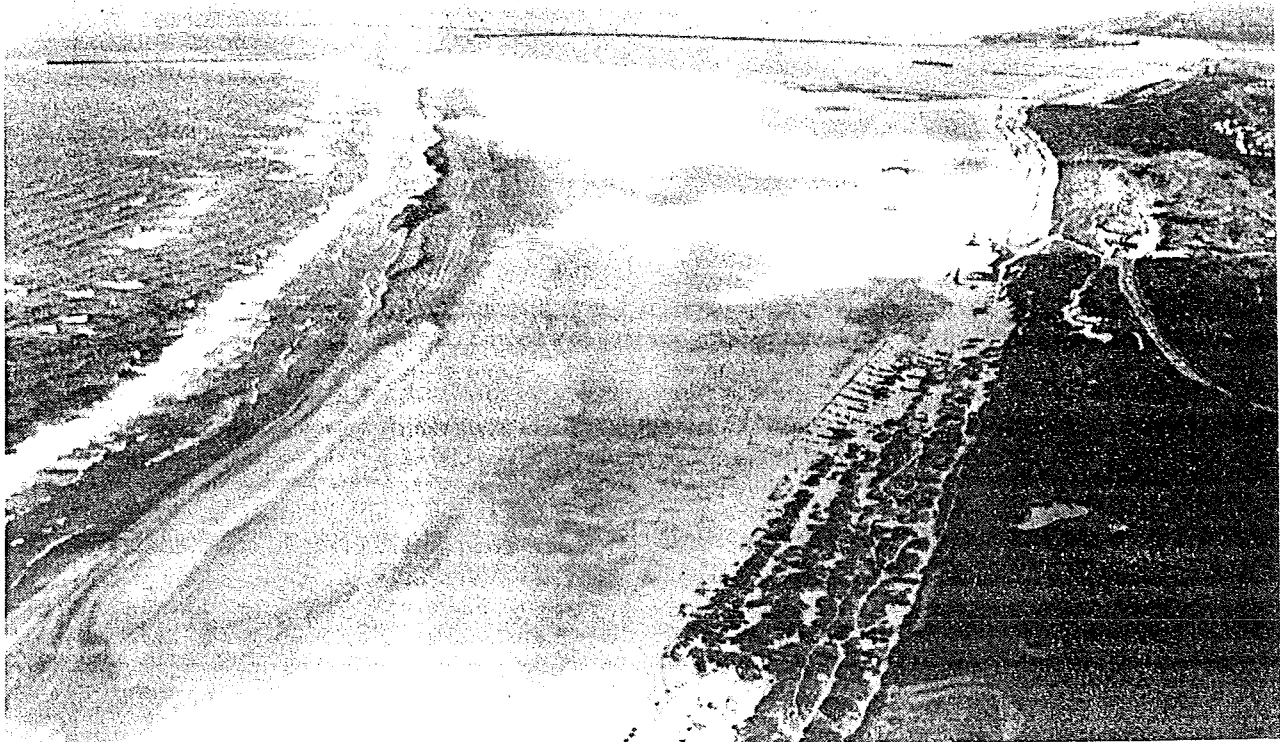

Figure 1.5   The habour moles at IJmuiden (km 56-58) has resulted in substantial shoreline progradation as shown here. Breaker wave height also decreases towards the moles (13.7.89).

2. DATA BASE AND METHODS

2.1 Background

The Netherlands has probably the best studied and best monitored coast in the world. As a result a wealth of data and information exists on coastal evolution, coastal processes and change. Much of this has recently been summarised as a result of two major projects. In 1987 the "Coastal Genesis" project produced a series of reports on coastal behaviour at scales of 5000, 1000 and 100 years. This was followed in 1989 by the "Coast Defence after 1990" project which produced 20 technical reports on all aspects of Netherland's coast defence.

The reports of Stolk et al. (1987) and particularly Stolk (1989) provide an excellent overview and background information on the geological evolution and physical nature of the Netherland coast. Also the report of Dillingh and Stolk (1989) for the European CORINE ' Coastal erosion' project provides a good review of the coast. No attempt will be made in this study to duplicate results published in these reports and elsewhere. Reference will, however, be made to all relevant material and results.

Table 2.1 lists the major data requirements and sources for this study. They are grouped under the headings of location/features, waves, sediment, beach and nearshore profiles and beach morphology. While this study has used solely existing data it has been interpreted, reanalysed and combined in a way to provide a new perspective on the beach morphodynamic systems of the central coast. In particular it represents a first attempt to both identify the beach types along the coast as well as the nature and controls on their variability. In this regard the study has benefited from studies of a similar nature undertaken on the southern Australian coast (Short, 1979, 1980, 1987; Wright and Short 1984; Short and Wright 1985), Israel coast (Bowman and Goldsmith, 1983) and Danish coast (Aagaard, 1988a, 1988b, 1989).

Table 2.1 Major data types and sources - central Netherlands coast

1. Location features breakwaters and dykes	1:25,000 Topographic maps showing all 1 km beach poles, groynes,

2. Sediments:
   * Dune
   * Beach
   * Surf zone
	Kohsiek, 1984
	van Bemmelen, 1988
	van Alphen, 1987

2. Waves:
   1976-1986
   1987-1988
	Rijkswaterstaat, Tidal Waters Division, Roskam, 1988
	KNMI, Division of Oceanographic Research

4. Beach profiles:
   1976-1985
   Nearshore profiles
	Rijkswaterstaat, Tidal Waters Division
	1:10,000 sounding charts, Rijkswaterstaat

5. Beach morphology:
   1982-1988
 	
   1966, 1968, 1970
   and 1971
	Aerial photographs (1:4,000)
	Rijkswaterstaat, Mapping and Survey Division
	Air photo mosaics
	Rijkswaterstaat, North Sea Directorate
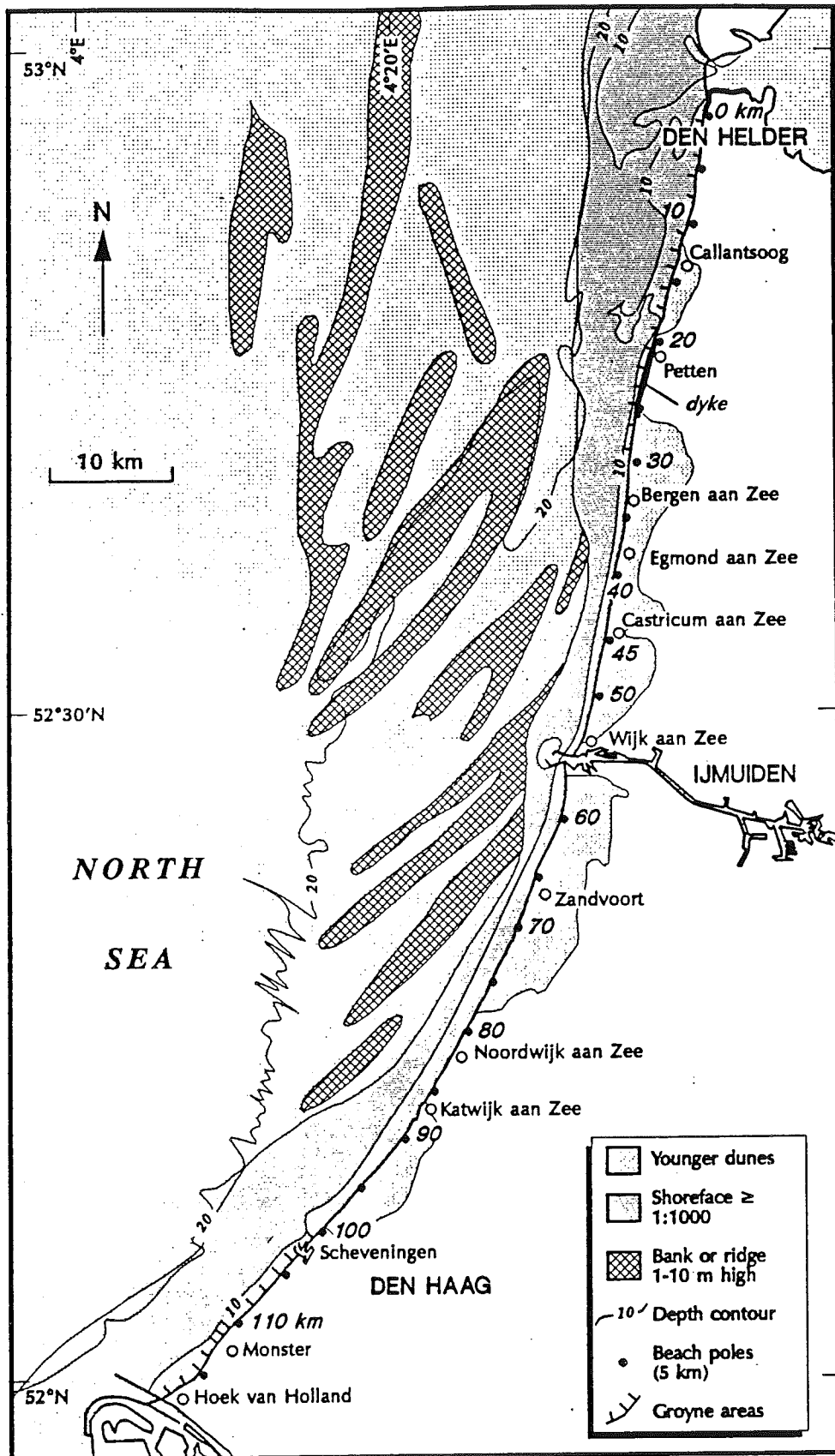
Figure 2.1   The central Netherlands coast and study area, Den Helder to Hoek van Holland. Shown are the location of 5 km beach poles, all major structural features (groynes, breakwaters, dykes), the extent of the coastal slope or shoreface (from van Alphen and Damoiseaux, 1987), 'Younger Dunes' and major towns.

2.2 Sampling

The study of beach morphodynamics requires information on both the morphology or beach type as well as the variables that contribute to morphological change, particularly sediments and coastal processes. For the 124 km long central coast information is also required at a sampling interval that will permit an assessment of longshore or spatial change in beach morphodynamics and over a sufficient period of time to permit assessment of temporal change.

The spatial and temporal sampling procedure adopted by the study was largely pre-determined by the nature and availability of the data. To account for spatial change a minimum 1 km sampling interval was chosen to coincide with the 1 km beach poles along the coast. The location of the 1 km poles are also shown on the 1:25,000 topography maps and are marked on the 1:4,000 aerial photographs. This interval gave 118 sample points for the central coast, extending from km 1 at Den Helder in the north and km 119 at Hoek van Holland in the south (Fig. 2.1). These points or beach pole numbers are used to locate features throughout the report.

Table 2.2 Date and coverage of vertical aerial photographs central Netherlands coast

	Date	Coverage (km)	C/B+W
Vertical Aerial Photographs, 1:4000[1]			
	04.04.82	59- 82	B+W
	09.04.83	26- 55	B+W
	15.04.83	56-118	B+W
	15.05.84	0- 2	B+W
	14.04.84	3- 20	B+W
	11.04.84	56- 97	B+W
	01.02.85	1- 34	B+W .
	24.04.85	35-118	B+W
	25.05.86	26- 58	B+W
	26.05.86	59- 60	B+W
	30.04.86	61-115	B+W
	24.05.87	2- 54	B+W
	09.05.87	55- 97	B+W
	24.04.88	1- 25	C
	22.04.88	26- 55	C
	07.05.88	56-118	C
Aerial Photograph Mosaics, 1:8000[2]			
	28.2.66	108-119	B+W
	16.3.68	86-103	B+W
	17.6.70	86-119	B+W
	14.7.71	86-119	B+W

C = colour
B+W = black and white
1 Source: Rijkswaterstaat, Mapping and Survey Division
2 Source: Rijkswaterstaat, North Sea Directorate

2.3 Beach morphology

The morphology of the beach and bar systems and the location of all rips was obtained from aerial photographs. The date and coverage of the photos is given in Table 2.2. Using the photographs the beach type was recorded continuously for the beach/bar 1, bar 2 and bar 3 (the latter when visible) by visual comparison to the beach model of Wright and Short (1984) shown in Figure 2.2. This data was then sampled at 1 km intervals with a numeric value assigned to each beach type (Table 2.3). For 1988 and parts of 1987 and 1986 a 1:25,000 sketch was made of the beach morphology.

Rip location (± 10 m) was recorded for all rips visible on the 1:4 000 photographs. The rip type (RR, TBR, RBB or LBT, Table 2.3) was given by the beach morphology. In addition rip orientation (north, west/shore normal, south) was recorded as well as rip length for skewed rips. These results are discussed in section 5.

Table 2.3 Classification of beach types

Beach Type[1]	Abbreviation Used in Report	Nominal Value
Reflective	R 1.5	1
Low tide terrace/ridge and runnel	LTT/RR 2.5	2
Transverse bar and rip	TBR 3.5	3
Rhythmic bar and beach	RBB 4.5	4
Longshore bar and trough	LBT 5.5	5
Dissipative	D	6

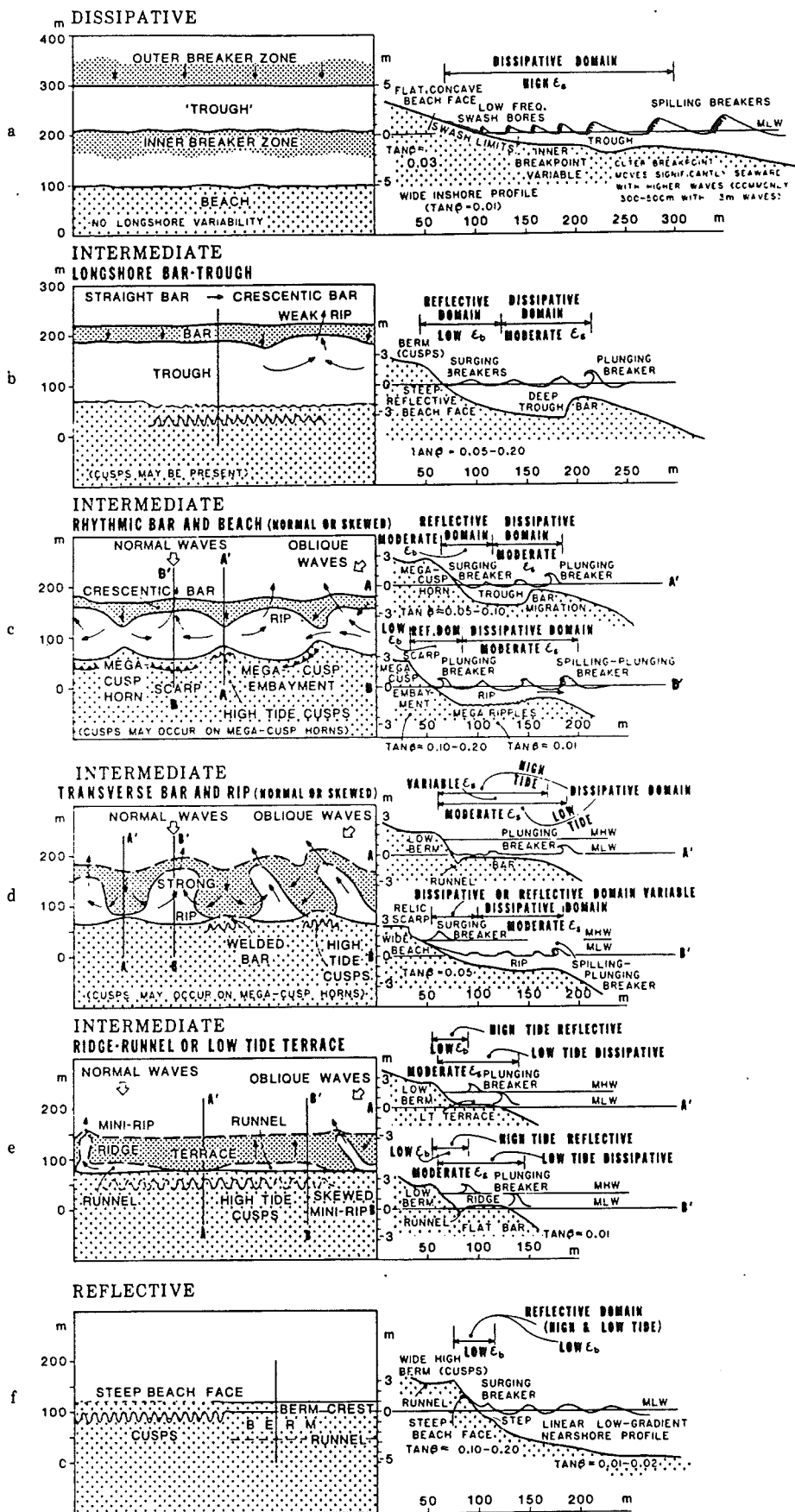1 Based on Wright and Short, 1984

Figure 2.2   The beach model of Wright and Short (1984) showing the three beach types (reflective, intermediate and dissipative) and the six beach states (a-f) used to classify the beach system (see Table 2.3).

10

2.4 Sediments

Beach sediments, in conjunction with waves and tides, determine the beach morphodynamic type (Wright and Short, 1984). In order to assess the nature and spatial variation in sediments along the central coast the results of three recent reports were utilised. The aim was to determine the mean sediment characteristics and the presence, if any, of longshore trends in grain size which could in turn contribute to spatial trends in beach morphodynamics.

Dune sands were analysed by Kohsiek (1984). The dunes were sampled at 2 km intervals between km 2 and 116 providing 53 samples. van Bemmelen (1988) studied the beach sands at high and low water, also at 2 km intervals providing 112 samples. Surf zone sediments were sampled by van Alphen (1987) at 35 locations between km 37 and 110 at approximately 2 km intervals. At each location 4 to 5 samples were obtained at 100, 200, 400, 600, 800 and 1000 m seaward of the shoreline generating 179 samples. In total data from 344 samples were available. This study utilized the following sediment characteristics from all these samples: median grain size (D50um) and standard deviation, sorting and standard deviation, and for the surf samples the percentage of calcium carbonate and mud. The median grain size was also converted to mean fall velocity (Ws). The results are discussed in section 3.

2.5 Beach and nearshore profiles

Beach profiles, usually extending 1 000 m seaward, are surveyed annually every 250 m by Rijkswaterstaat. From this data set 118 cross-shore profile envelopes were plotted for each kilometre beach pole (km 1-118) from 1976 to 1985. The plotting was performed by Rijkswaterstaat. From each of the 118 profile envelopes a number of morphometric variables were then measured. The results are presented in section 6.

Nearshore profiles extending several kilometres seaward are surveyed periodically by Rijkswaterstaat. They are published as individual survey lines and as bathymetric charts. Twenty three profiles spaced at approximately 5 km intervals between km 5 and 118, and 49 profiles at 1 km intervals between km 70 and 119 were obtained from Rijkswaterstaat. These profiles were used to measure the nearshore gradient out to the break in slope, and the distance and depth of the break in slope. The results are also discussed in section 6.

2.6 Waves

Wave parameters are recorded at eight deepwater stations in the Netherlands sector of the North Sea (Fig. 2.3). Daily summaries were obtained from Rijkswaterstaat for the four stations closest to the coast (LEG, MPN, YM6, ELD) for the period 1.1.79 to 31.12.86. Records from 1.1.87 to 31.12.88 for all records (usually 3 hourly and 8 per day) were obtained for MPN and YMG from the Royal Netherlands Meteorological Institute (KNMI), Division of Oceanographic Research. The latter data was summarized into daily averages of wave height and period.
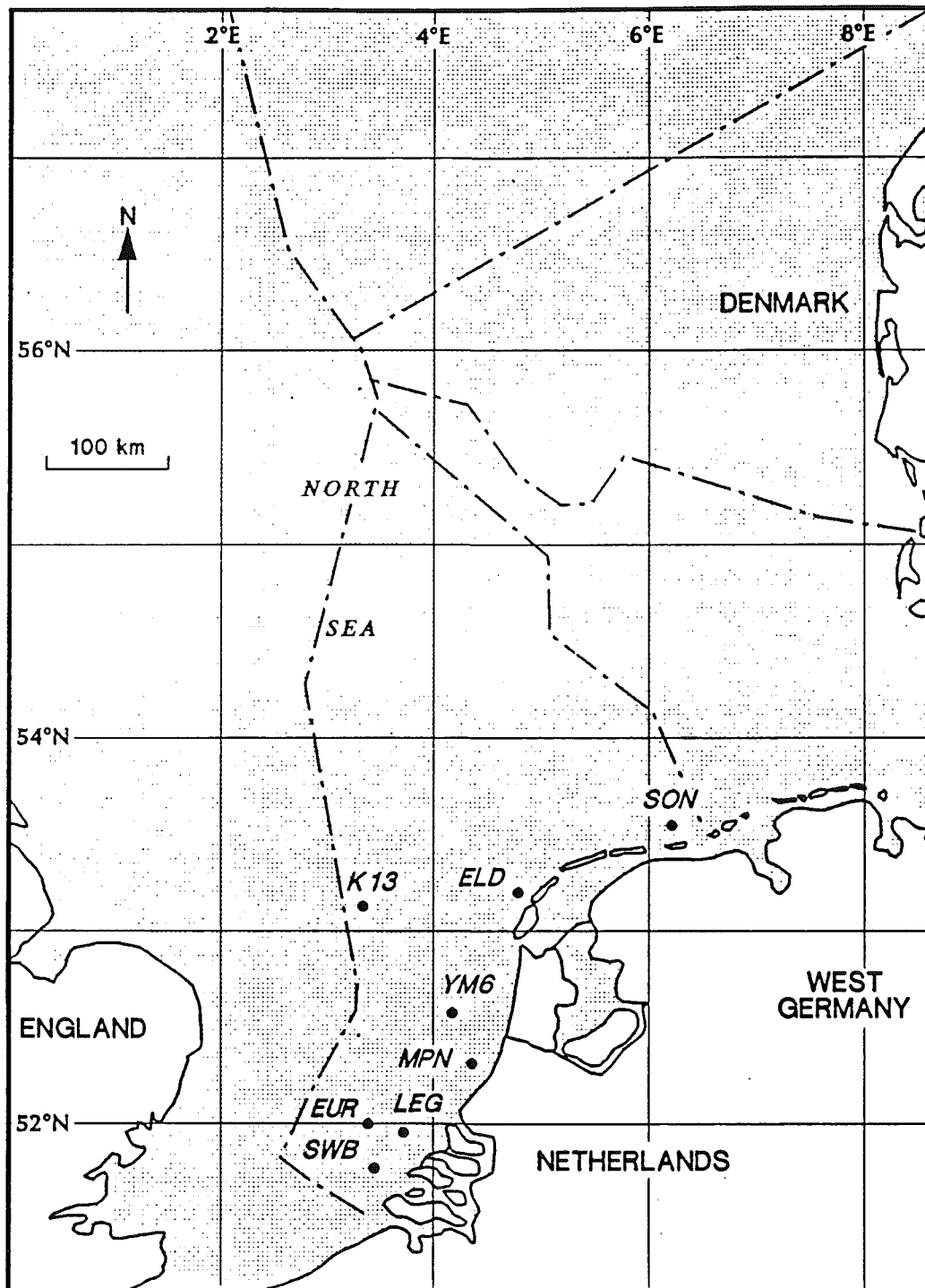
Figure 2.3   Location of the eight wave measurement stations (dots) in the Netherlands sector of the North Sea. Source: Roskam, 1988.

The entire data set was organized to provide two continuous daily records of wave height (Ho) and period (To) for MPN and YM6, the two stations closest to the central coast (Fig. 2.3). When daily data was missing from these stations, it was obtained from one of the other stations (LEG or ELD).

The records were analyzed for two purposes. First, to provide daily wave conditions leading up to the date of each aerial photograph (Table 2.2), and second, to permit an assessment of the monthly and annual wave climate. To achieve the latter A.P. Roskam (Rijkswaterstaat, Tidal Waters Division) provided monthly and annual summaries for the stations for 1979 to 1986. The summaries for 1987 and 1988 were obtained from the KNMI data.

Wave direction is important for determining longshore sediment transport and for the orientation of beach morphology and dynamics. In the North Sea the direction is closely related to wind direction owing to the limited fetch and prevalence of seas. A summary of wave directions for the LEG station was extracted from Roskam (1988). All wave results are presented in section 4.

2.7 Other coastal processes

Tides, tidal currents, wind, wind generated currents and storm surges, all made substantial contributions to coastal processes along the Netherlands coast. However, given the nature of this study, these processes are considered secondary to waves in controlling beach morphodynamics, and in particular contributing to spatial and temporal change.

Tides do make an important contribution to beach morphodynamic processes and type, as found in studies by Wright et al. (1982, 1986, 1987) and Short (in press). Along the central coast the tide is micro-tidal and relatively uniform longshore ranging from 1.4 m at Den Helder to 1.7 m at Hoek van Holland (Fig. 2.4). Therefore the range itself is not considered important in contributing to temporal or spatial variation in beach morphodynamics. This however, would not be the case in the Wadden Sea and the Delta coasts, where increasing tide range (Fig. 2.4) is expected to increase its impact on beach morphodynamics.

Tidal currents are also prominent along the central coast. The tide floods to the north with a maximum surface flow of between 0.6 to 1.0 m/sec and ebbs to the south with a lower velocity resulting in a residual of about 0.05 m/sec (Wiersma and van Alphen, 1988). While these currents will imprint themselves on the surf zone current regime, and can be measured at the shoreline in calm conditions, they are considered secondary to waves in producing beach changes and are therefore not considered in this report. They are considered important however, in producing a seaward coarsening of sediment in the outer surf zone (Wiersma and van Alphen, 1988), and interact with, and may influence the morphology of the inner shelf shoreface connected sand ridges. Likewise wind generated littoral currents are no doubt important in surf zone processes, particularly when accompanying wind generated waves. Following winds are likely to enhance the impact of oblique waves on beach morphology and currents, particularly rip skewing. Unfortunately no data on these currents exits and their impact cannot be assessed in this study.

13
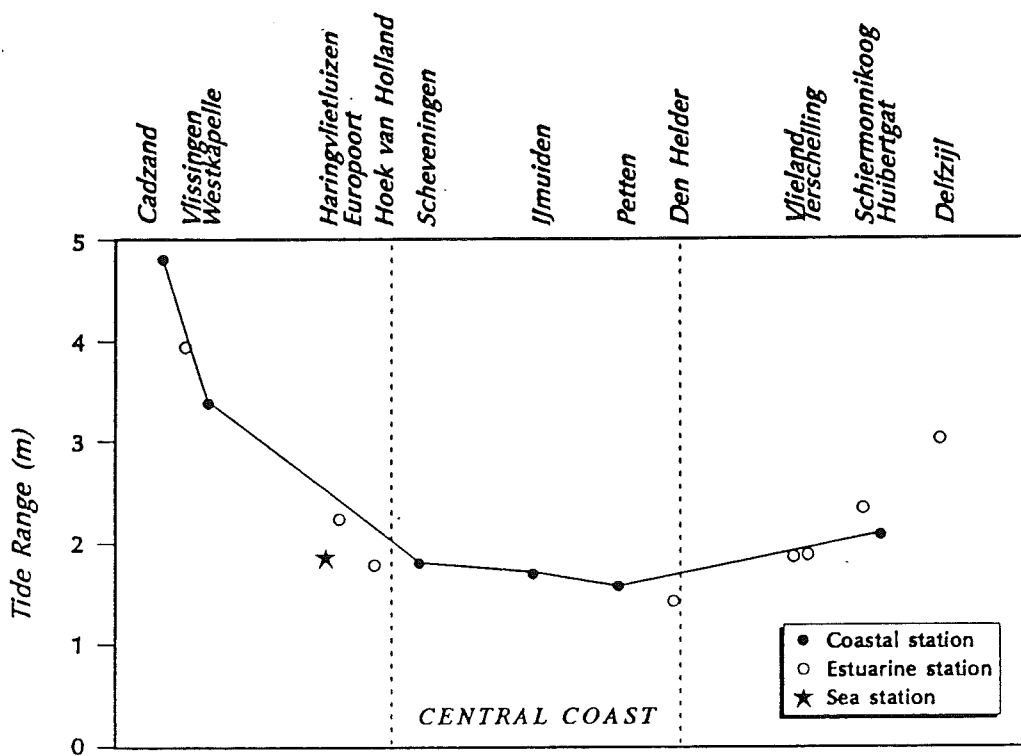
Figure 2.4   Mean tide range along the Netherlands coast. Modified from: Stolk, 1989.

The wind climate of the North Sea generates most of the waves that arrive at the Netherlands coast. The wind is therefore considered in the assessment of the wave climate and in the summary of wave directions. Further summaries of the coastal wind regime are provided by Stolk (1989).

Finally, storm surges are a major threat to all beaches and low lying sections of the North Sea coast. Their occurrence has resulted in major man made changes to the coast particularly in the Netherlands and Germany. Coastal processes and beach change will be most intense during the high seas and winds that produce a storm surge. The storm surge will therefore have a temporal impact on beach type leading to more dissipative conditions during high sea-surge conditions. Unfortunately, while storm surges can be expected to produce beach erosion and more dissipative beach conditions, the morphological data base (the aerial photographs) do not include the coast immediately following a storm surge. Therefore this high energy end of the wave-surge spectrum can only be inferred from models of beach behaviour and the literature rather than the existing data base. These models will be used to predict such extreme beach response in section 7.

14

2.8 Data Management

All data analysis was performed on an Hewlett Packard Vectra ES/12, an IBM compatible PC. The data was stored using DBase 3 plus and most analysis and plotting performed using Statgraphics software. All reduced data is available on floppy disc from the Department of Physical Geography, University of Utrecht.

3. SEDIMENTS

3.1 Origin

The Holocene evolution of the Netherlands coast, including nature and origin of the coastal sediments has been well documented in a number of studies. Eisma (1968) provides the most detailed study of the coastal sands, while van Straaten (1965), Jelgersma et al., (1970), Roep (1984) and Zagwijn (1984) have reported on aspects of the Holocene evolution of the central Netherlands coast.

Barrier progradation commenced along the central coast as the sea-level rise diminished, beginning about 5500 years BP and continuing at varying rates up to Roman times. Contemporaneous with barrier progradation was the aeolian reworking of their crests to form 'Older Dune Sands' (Jelgersma et al., 1970). The next major change in coastal development was the formation of the 'Younger Dune Sands' between 1000 to 1900 AD. These shell rich sands were derived from the adjacent sea floor leading to a steepening of the nearshore gradient from 1:200 to 1:100 between 0 and 5 m water depth (Roep, 1984). These latter changes have an important bearing on the present beach systems as most of the beach sands are composed of reworked nearshore sands, resulting in relative uniformity alongshore. Furthermore the steepening of the nearshore gradient should produce less wave attenuation, higher breaker waves and possibly more dissipative beach conditions. Wiersma and van Alphen (1988) suggest this scenario may be responsible for the well developed multi-bar system along the steeper central section of the study area. These interactions will be assessed in section 7.

During the past three hundred years the coastal sediment budget can be divided into three zones. Coastal erosion north of Egmond aan Zee (-0.92 m/yr) and south of Scheveningen, (-0.35 m/yr) with accretion in the central region (+0.25 m/yr) (Dillingh and Stolk, 1989). More recently the coast continues to erode near Den Helder (-0.5 to -1.5 m/yr) with erosion decreasing toward Egmond aan Zee. The coast is fairly stable to accretionary from Egmond to Scheveningen (km 33-100) while from Scheveningen to Hoek van Holland (km 100-120) groynes may have stabilised the coast (Dillingh and Stolk, 1989). Local accretion is also occurring adjacent to breakwaters at IJmuiden (Fig. 1.5) and Hoek van Holland as the coast readjusts to the structures.

3.2 Sediment characteristics

Eisma (1968) confirmed Baak (1936) earlier observations that the central coastal sands consist of two mineralogical types. North of Bergen (km 0-33) are reworked Saalian glacial sand, Meuse sands and Rhine sands, while south of Bergen (km 34-120) the sands are mainly reworked Rhine sands. In terms of grain size Eisma distinguished two major provinces, fine sands south of IJmuiden (km 56-120) and coarser sands to the north. The dune sands also followed the same trend but with more fine grains (<350 um). He was unable however, to distinguish statistically between the beach and dune sands.

16

In order to characterize the dune, beach and surf sediments this study used the results of three recent reports. The spatial variation in mean grain size along the central coast is illustrated in Figure 3.1 and Table 3.1. The dune sands are relatively uniform alongshore with an overall mean of 226 um (sd = 21 um). The slight trends which do occur, particularly the coarsening around km 12, 18, 44 and 60 are paralleled by similar trends in the MHW beach sands. The MLW beach sands are the coarsest (mean D50 = 286 um, sd = 48 um) with a high degree of longshore variation. Comparing the three populations (dune, MHW, MLW) the dune sands remain consistently fine (<280 um) and uniform (sd = 21 um), while the beach sands are more variable. The MHW and MLW sands display both parallel trends (km 70-120) as well as opposing trends (km 0-70) suggesting a more uniform population in the south. The most significant trends are however related to the shoreward decrease in grain size from MLW to MHW to the dunes.

Table 3.1 Summary of dune, beach and surf zone, sediment characteristics of the central Netherlands coast

	n	D50 (um)	D50 (sd)	Min (um)	Max (um)	Sort	%CaCO₃	%mud
Dune[1]	53	226	21	180	277	-	-	-
Beach[2]								
MH	56	262	38	195	380	-	-	-
MLW	56	286	48	185	420	-	-	
Mean		215	46					
Total	112							
Surf[3]								
200 m	29	229	61	174	431	0.42	10.2	0.9
400 m	35	189	41	151	382	0.40	11.6	2.6
600 m	36	185	60	150	489	0.39	12.1	1.9
800 m	34	201	78	147	466	0.43	13.9	2.3
1000 m	35	212	109	133	615	0 47	13.7	4.6
Mean		204	73					
Total	179							

1 Kohsiek (1984)
2 Van Bemmelen (1988)
3 Van Alphen (1987)

See Appendix 12.1 for more details

In the surf zone-nearshore the results of van Alphen (1987) are shown in Figure 3.2 and Table 3.1 with details in Appendix 12.1. Sediments are coarsest at 200 m (229 um), fine seaward to 400 and 800 m (189 and 185 um) then coarsen to 800 and 1000 m (201 and 212 um). This trend was also observed south of Bergen (km 35) by Wiersma and van Alphen (1988). This pattern suggests they represent three dynamic regimes associated with: 1. high energy surf zone and beach unit; 2. seaward fining across the mid surf zone (400-600 m); and 3. coarsening beyond 800 m possibly due to increasing flood tide velocities.
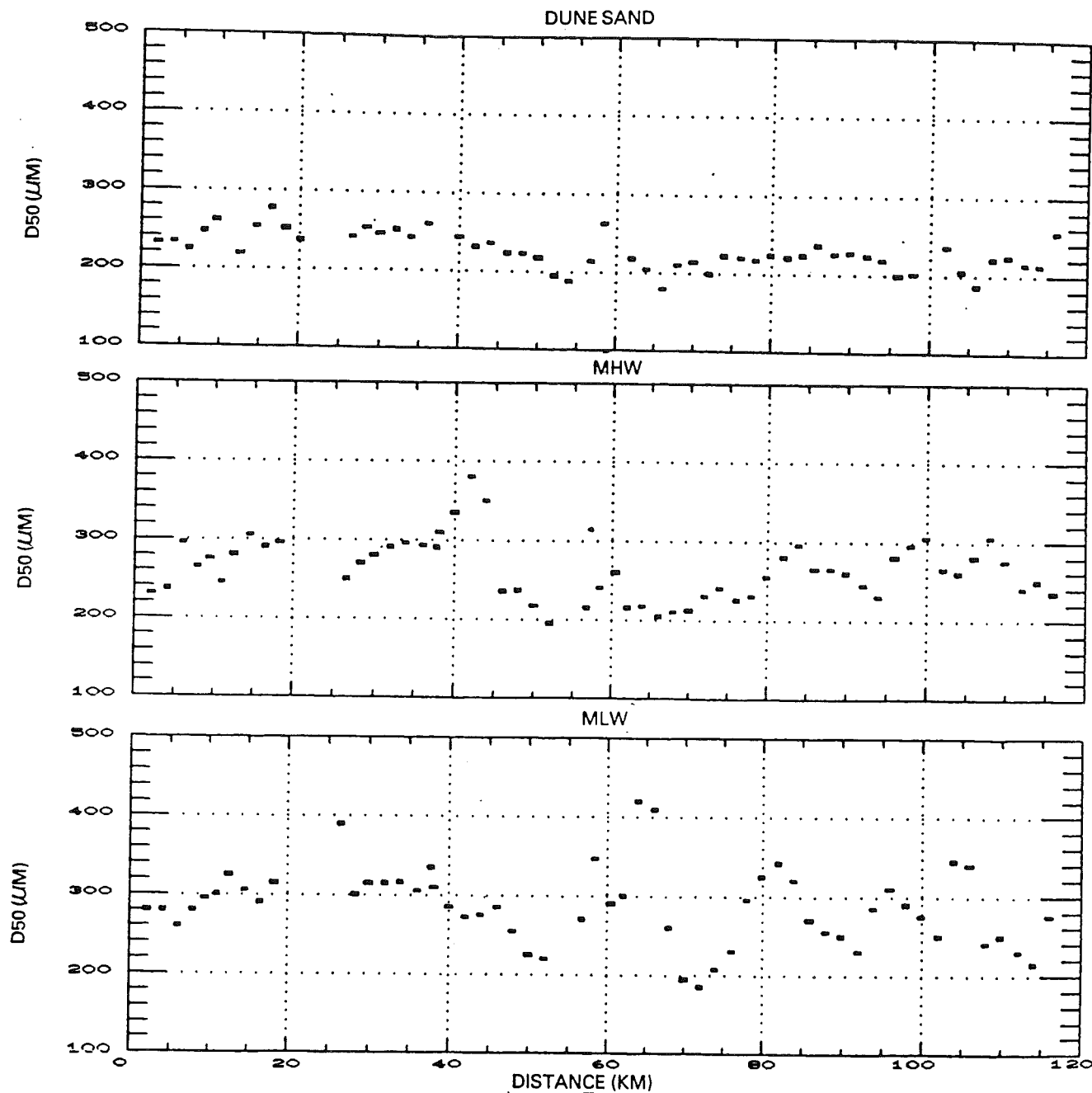
Figure 3.1   Dune and beach mean grain size along the central Netherlands coast. Shown are dune sands (a) (from Kohsiek, 1984) and beach sands (mean highwater (b) and mean low water (c) from van Bemmelen, 1988). Distance refers to kilometer beach pole locations shown in Figure 2.1.

Given the aims of the sediment analysis were to assess longshore trends in grain size and select representative grain size characteristics the following conclusions were made:

1.   No longshore trends were coherent across all sediment populations (dune, beach, surf zone), a conclusion reached by Wiersma and van Alphen (1988) and Stolk (1989). The former consider subsoil inheritance to partially explain the present patterns.

18
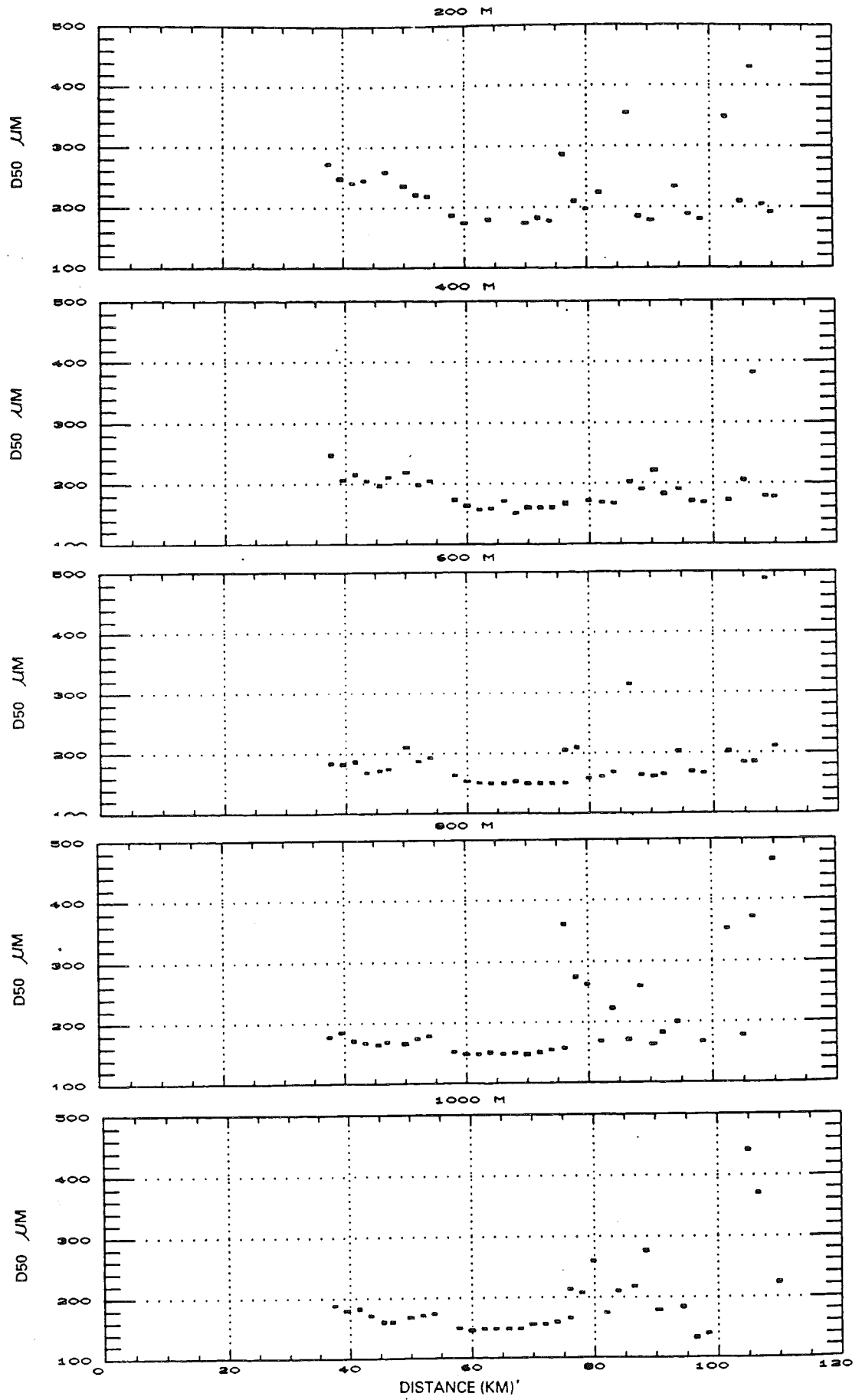
Figure 3.2 Surf zone and nearshore mean grain size along the central Netherlands coast. Shown are the grain size at 200 m (a), 400 m (b), 600 m (c), 800 m (d) and 1000 m (e) distance from the shoreline. Source: van Alphen, 1987. Distance refers to kilometer beach pole locations shown in Figure 2.1.

19

2. For the purpose of this study of beach morphodynamics, the inner surf zone sediments were selected for more detailed trend assessment and for use in equations requiring grain size characteristics.

3. The inner surf zone sands (200 to 400 m) display a weak trend with coarser sands north of IJmuiden (km 0-56) and finer sands to the south (Fig. 3.2d, e). Based on this the values of mean grain diameter of 240 um and 200 um were adopted for locations north and south of km 56 respectively.

4. WAVES

4.1 Background

Waves arriving at the Netherlands coast are generated by wind blowing over the North Sea, together with occasional low northerly swell arriving from the north Atlantic. The strongest wind and largest waves are associated with west to east tracking subpolar low pressure systems. These produce a predominantly westerly flow of air and are the major source of wave generation for the coast. The wave climate is however highly variable as it depends not only on the frequency and track of the cyclones, but also their regional wind direction, velocity and duration. The wave generating forces act across a sea with a highly variable fetch, with a relatively shallow shelf, including the shoal areas of the Dogger and Bruine Banks (Figure 1.2) together with the numerous ridges off the Netherlands coast. The banks produce both wave attenuation and refraction of northerly swell which further complicates the wave regime. Near the coast relatively low nearshore gradients, shore face connected ridges and ebb tide deltas (Fig. 2.1) further effect breaker conditions. Finally, within the surf zone the location and elevation of the shore parallel bars induces further cross shore breaker wave transformation.

The nature of the breaker wave climate along the central coast is critical to any understanding of the beach morphodynamics and its variation in time and space. In order to assess the nature of the waves the report of Roskam (1988) and the wave data supplied by Rijkswaterstaat and KNMI (see section 2.6 and Table 2.1) was utilised to compile both time series of daily changes in deepwater wave height and related parameters, as well as, a summary of the monthly and annual wave climate.

No data is however available for the breaker wave conditions or their longshore variation. Further it was outside the scope of this study to use the wave refraction and attenuation programs necessary to calculate breaker wave heights from deepwater waves, and to accurately calculate the reduction in breaking height across the surf zone bar systems. The deepwater values for MPN and YM6 do however provide accurate information on daily changes in nearshore wave conditions, together with wave summaries. These changes, whilst of a slightly higher magnitude than breaker waves, will possess the same frequency characteristics and therefore will provide a very good approximation of temporal changes in breaker wave height and corresponding beach change.

4.2 Wave climate of the central Netherlands coast

The wave climate of the Netherlands coast was recently published by Roskam (1988). This report summarizes data for the eight deepwater stations (Fig. 2.3) for the period 1979-1986. The report presents tables for wave height versus period, low frequency (10-20 sec) wave heights versus wave period, wave exceedence curves for all eight stations, and wave height versus period for 30° directional sectors for the LEG station. The wave exceedence curves are reproduced in Figure 4.1 and the wave directional tables reformatted in Figure 4.2 and Roskam's height and period matrices given in Appendix 12.2.1.

21
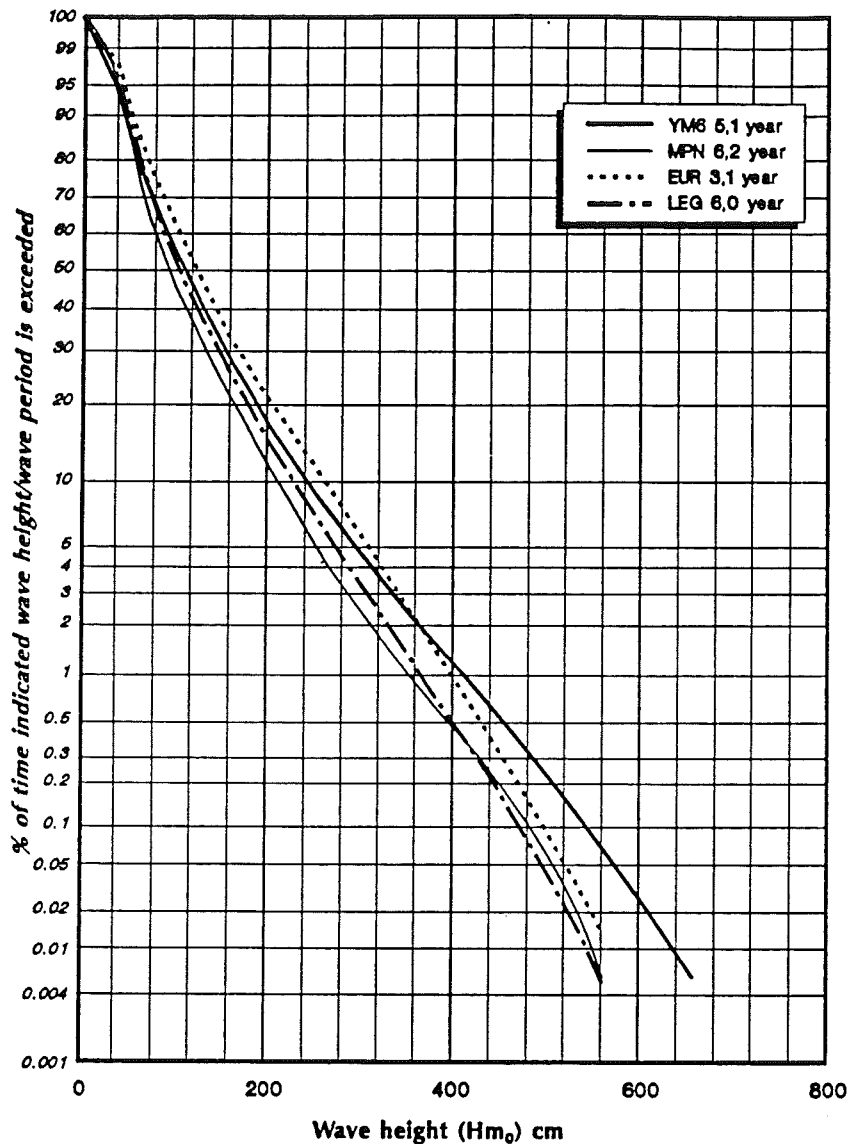
**Exceedance curves wave height
Stations: YM6, MPN, EUR, LEG
Period: 1976-1986**

Figure 4.1   Wave exceedence curve for YM6, MPN, EUR and LEG wave stations. Modified from:
Roskam, 1988. See Figure 2.3 for locations.

The highest waves in the Netherlands sector of the North Sea are recorded at the
K13 station located 110 km off Texel (Fig. 2.3). The lowest waves are recorded on
MPN located 10 km off Noordwijk in 18 m water depth. At the coast waves will not
only be slightly lower but also only arrive from offshore directions as all winds
between 30° and 210° will blow offshore (Fig. 4.2) and produce calms at the shore.

At K13 mean wave height is 1.5 m with a period of 5.1 seconds, this reduces near the
coast to 1.27 m and 4.8 sec. at YM6 and 1.06 m 4.7 sec. at MPN with the lowest
mean wave height. Likewise waves exceed 3 m at K13 7.5%, YM6 4.5% and MPN
only 2% of the time.
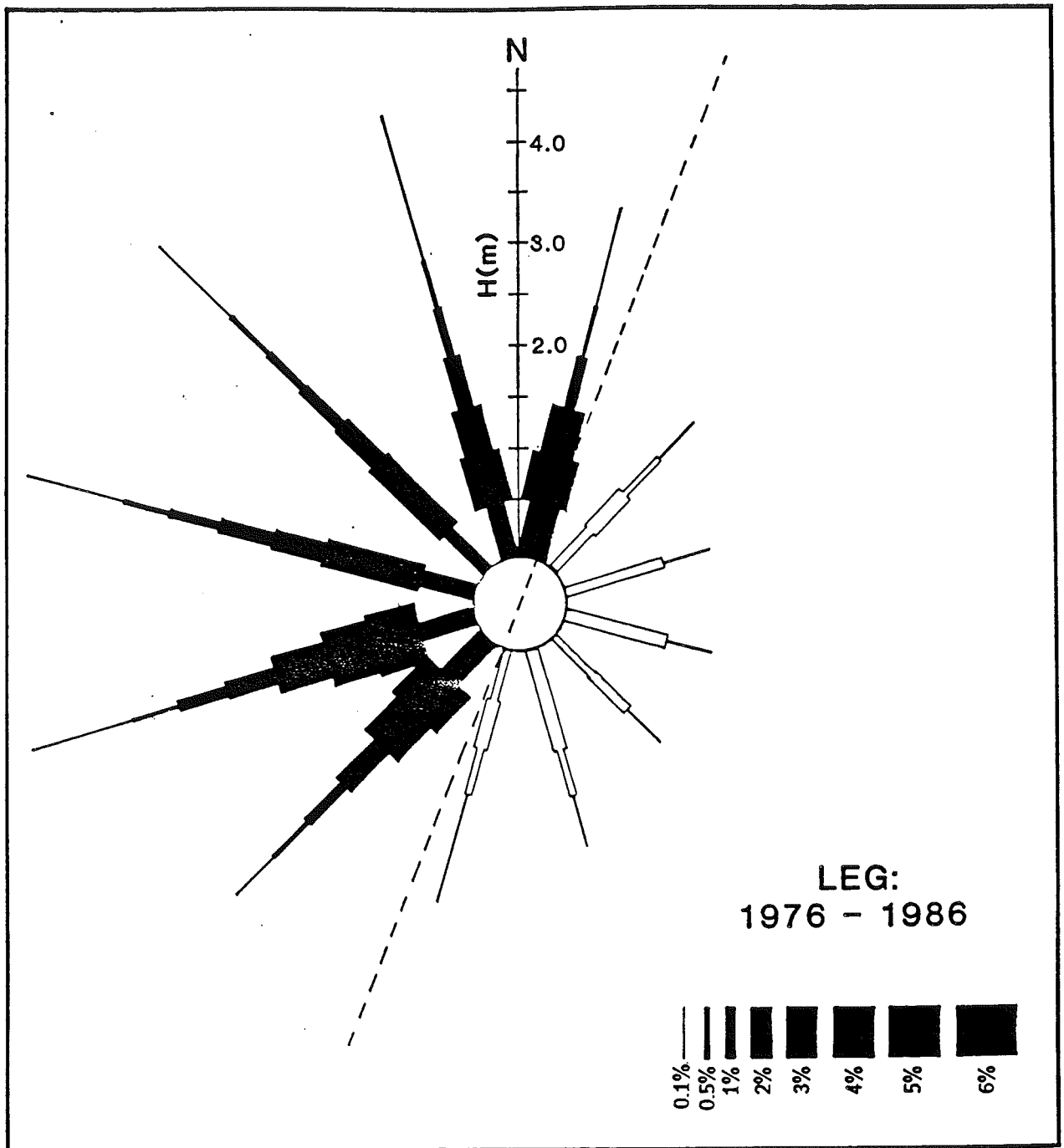
Figure 4.2 Wave rose for LEG station (see Fig. 2.3 for location) based on data from Roskam, 1988.
The rose includes wave direction, height and frequency of occurrence. The dashed line
indicates the alignnment of the central Netherlands coast. The shaded directions produce
waves at the coast, while open roses should result in waves moving offshore and calms at the
shoreline.

These results indicate that in the south eastern North Sea the breaker wave climate
is dominated by waves of a moderate height (~ 1.5 m) and short period (~ 5 sec.).
The height is further reduced as it approaches the shore resulting in still lower mean
values (~ 1 m).

23

4.2.1 Wave direction

Wave direction versus wave height for the LEG station is illustrated in Figure 4.2 and the frequency of wind direction for all stations is given in Appendix 12.2.2.. The wave rose shows a dominance of southwest through north waves with the largest waves arriving from the west through north quadrants. The dominance of south through west winds is reflected in the higher frequency of lower waves from this quadrant. The dominance of higher waves from the north reflects the occurrence of lower frequency but high velocity winds from these directions, coupled with the longer fetches in these quadrants.

In conclusion waves on the central Netherlands coast arrive from all offshore directions. They arrive at the coast between 75 to 85% of the year, with a modal wave of 1 m and 5 sec. Waves exceed 2 m approximaterly 10% of the time, 3 m 2%, 4 m 0.5% and 5 m 0.05%. Most waves arrive from the W-WSW though they are spread across the SSW to NNE sectors. The highest waves however arrive from the W to N sectors.

4.2.2 Temporal variation

The temporal variation in wave conditions drives beach change and is therefore essential for any assessment of beach morphodynamics. Temporal variation for the central coast is based on the daily, monthly and annual wave characterists for YM6 and MPN stations.

The daily wave summaries for YM6 stations are plotted in Figure 4.3 for 1987 and 1988. 1987 represents a low energy year (Hmo = 1.21 m, T =5.3 sec), while 1988 is the highest energy year recorded (Hmo = 1.49 m, T = 5.6 sec) (Appendix 12.2.3). An interesting aspect of both years however, is the frequency of higher wave events. Waves exceed 1-1.5 m approximately 5 to 6 times per month. These peaks are superimposed on periods of higher and lower waves which roughly follow the seasonal trends discussed in next section. A periodogram (or spectral analysis) of the two time series reveals however more confusion than clarity (Appendix 12.2.4). In 1987 most energy peaked at 40 days followed by 60, 364, 16 and 12 days. In 1988 the peaks were at 366, 33, 91, 26, 16 and 12. Interestingly, neglecting the annual peak (365), the recurrence of the 16 and 12 day peak may correlate with the passage of cyclonic depressions and cyclone generated seas. These could correlate with the approximately 30 peaks above 1.5 m wave height in 1987 (average of 1 every 12 days) and 37 peaks in 1988 averaging 10 days apart. However such periodicities are not confirmed by meteorological data.

The main point is that wave height is highly variable in height and frequency, oscillating between extremes on a period of several days, with the actual extreme height varying considerably between storms, seasons and years. The longterm (decadal) trends are presently the subject of debate (Carter and Draper, 1988), with the Netherlands data providing the clearest picture of longterm cycles in the North Sea wave climate (Hoozemans and Wiersma, in press).

24

WAVE HEIGHT 1987
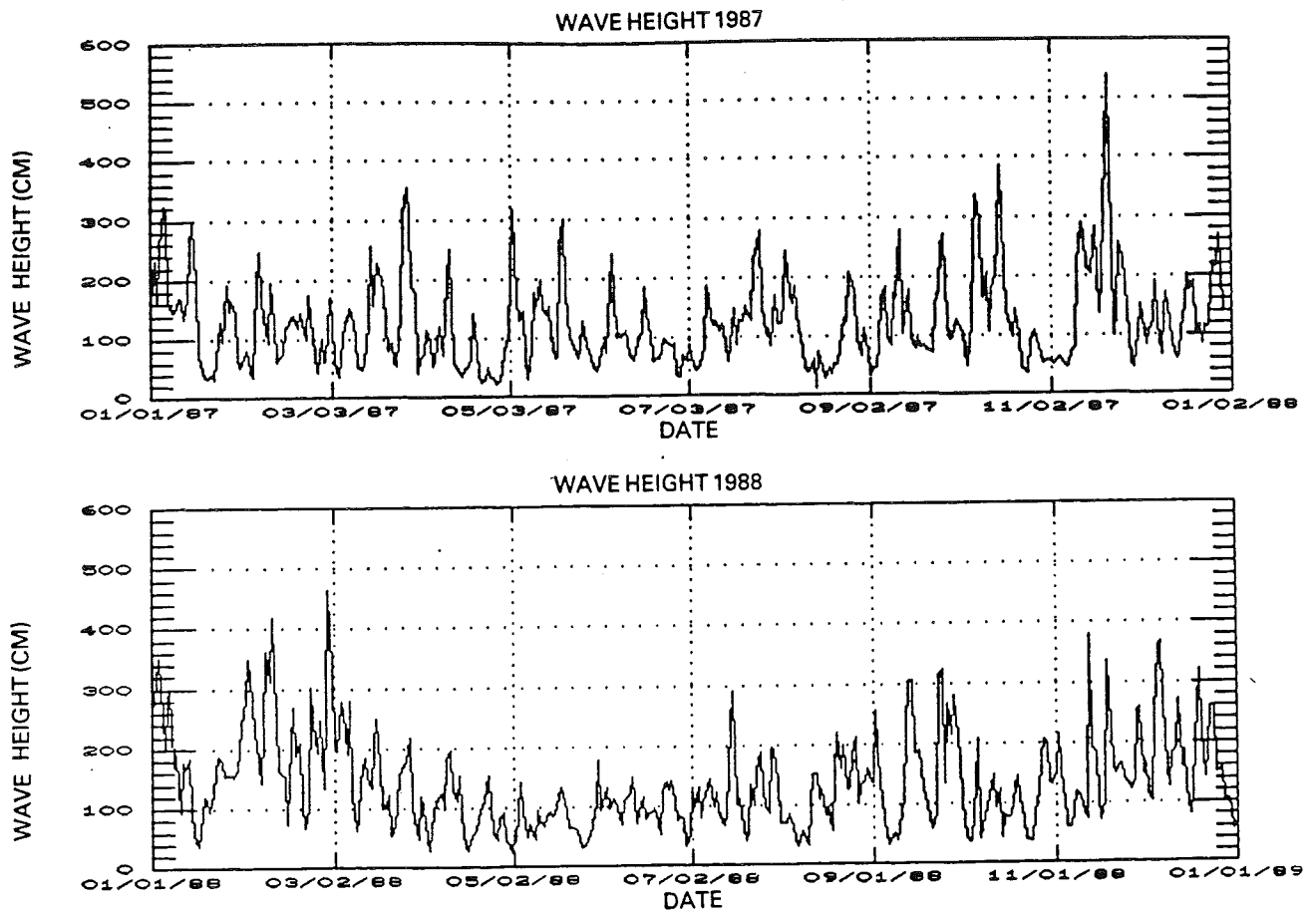
WAVE HEIGHT 1988

Figure 4.3 Daily mean wave height for YM6 station, 1987 and 1988 (see Fig. 12.3 for location). Based on data supplied by KNMI, Divison of Oceanographic Research. Note: date = month/day/year.

The monthly and annual wave height summaries for YM6 and MPN are listed in Appendix 12.2.3 and illustrated in Figure 4.4. Both stations show the same trend which consists of the following four wave 'seasons'.

Summer (April, May, June, July, August) is the period of lowest waves (0.93-1.08 m mean height) with low variance (sd = 0.17-0.24 m). For all years the highest summer monthly mean was 1.57 m (T = 7.8 sec), the lowest 0.59 m (T = 4.84 sec). Summer is a period of low and consistently low waves, with few major storms as illustrated by the low variance in Figure 4.4.

Fall (September, October) is a shoulder or a transition period between summer and winter. It is characterised by increasing wave height and variance the latter produced by the occurrence of higher waves.

The winter period (November, December, January) contains the highest waves increasing in size each month to peak in January (Ho = 1.86 m). While November and December have relatively low variance (sd = 0.26 m), January has the highest

25

variance (sd = 0.71 m) with some years of extreme storminess and high waves such as 1984 (Ho = 3.23 m) but also occasional calm years such as 1982 (Ho = 0.71 m). The extreme January waves are followed by a marked drop in wave height in the spring period (February, March). Mean wave height drops dramatically to 1.26 m in February and continues in March, before the next drop to the April summer conditions. The February variance is relatively high (sd = 0.41m). Large storms can occur such as in 1988. However, usually it is a substantially quieter month than January, probably a result of high pressure systems stabilising over the North Sea.
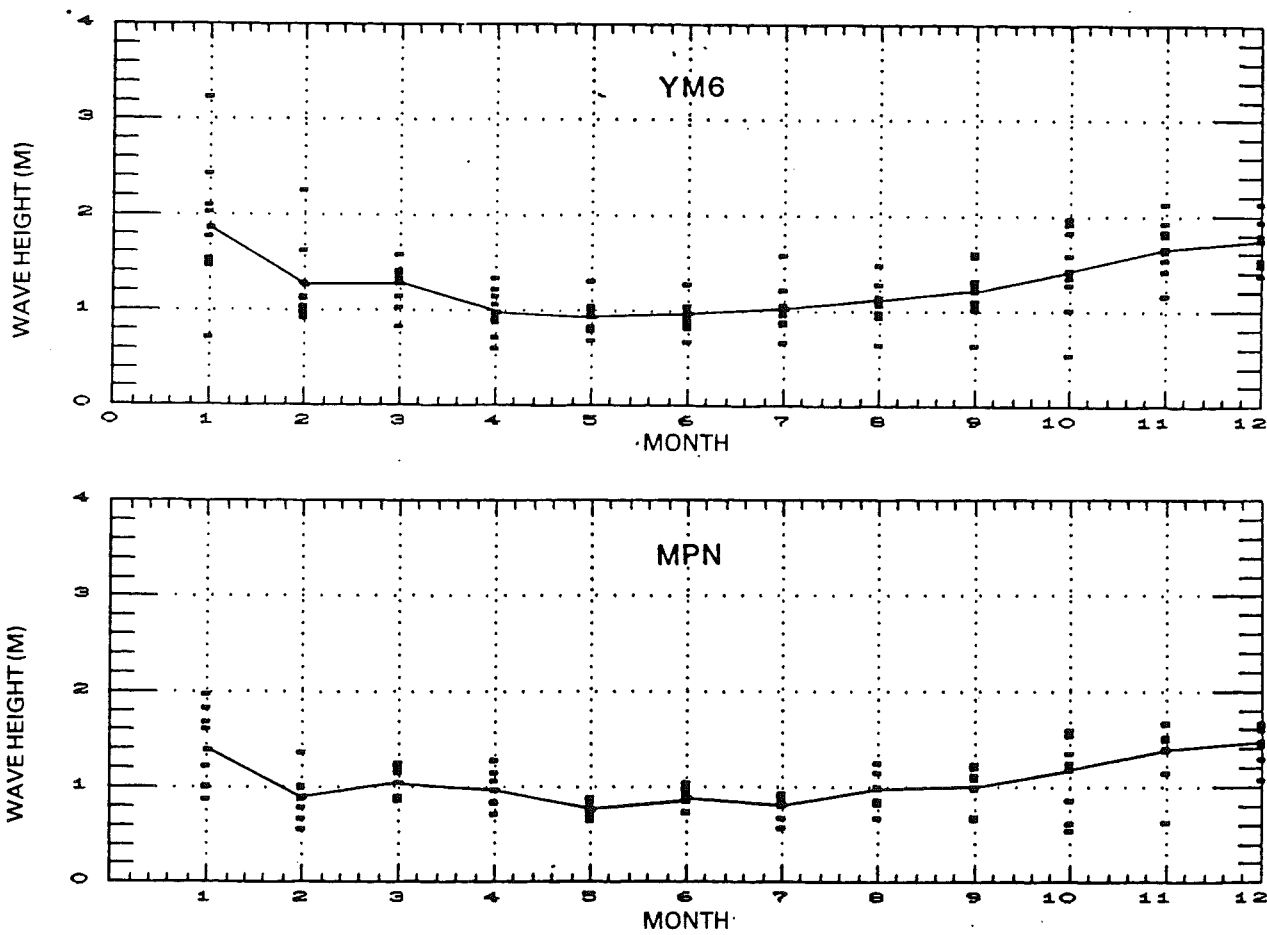
Figure 4.4 Mean monthly wave height at YM6 and MPN stations for period 1979 to 1988. Line indicates monthly mean for the 10 years and points each year. See Appendix 12.2.3 for actual values for each month and year.

Wave period averages 4.9 sec. (sd = 0.3 sec.) and varies little from month to month. There is however a consistent trend of slightly longer wave periods during winter compared to summer (Fig. 4.5) The most important variation in wave period however is associated with wave height. Appendix 12.2.1 clearly shows that as mean wave

height increases so too does mean wave period. Modal wave period is 3-5 sec. for waves less than 1.5m, but increases to 5-7 sec. for waves 1.5 to 4 m, and 7-9 sec. for waves greater than 4 m.
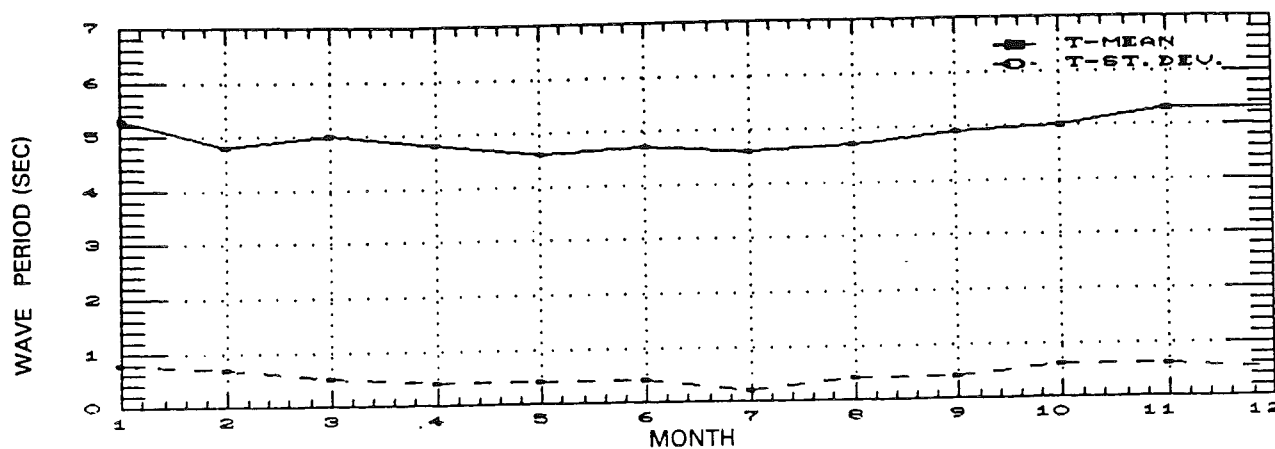
Figure 4.5   Mean-monthly wave period and standard deviation for MPN station for 1979-1988. See Appendix 12.2.3b for actual values.

5. BEACH MORPHOLOGY

The beach system of the central Netherlands coast runs essentially continuously for 119 km (Fig. 1.2). It consists of a subaerial beach containing a usually attached first bar (or ridge) and two outer bars (bars 2 and 3). South of km 85 only one outer bar (bar 2) is present (Fig. 5.1).
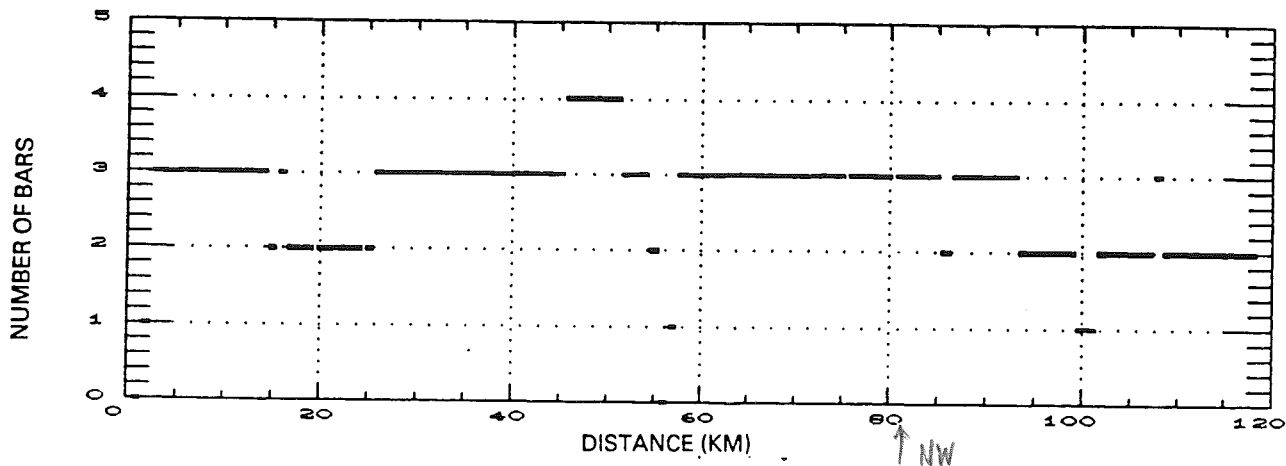
Figure 5.1   The number of bars (1 to 4) present along the central Netherlands coast. Based on Rijkswaterstaat 1 km beach profile surveys 1976-1985.

This description of the beaches is based on four sources. First, ten sets of beach profiles made annually from 1976 to 1985 at each of the 118 beach poles; second, seven sets of aerial photographs taken annually from 1982 to 1988 together with four air photo mosaics taken between 1966 and 1971 (Table 3.2); third, literature and publications on the central coast; and fourth, several field visits made during April to July 1989, including aerial reconnaissance from IJmuiden to Den Helder on 13.07.89.

Table 5.1   Some characteristics of surfzone bars estimated from 3-D time plots. From de Vroeg, 1987

Profile number (km)	L (m)	C (m/year)	Per (year)
9.94	400	nearly 0	very large
20.15	400	nearly 0	very large
30.00	300	20	15
30.00	300	26	19
50.00	350	13	27
60.00	200	70	3
70.00	240	50	5
80.00	200	50	4
90.00	240	45	5
101.00	-	-	-
109.00	-	-	-
116.62	-	-	-

28

The beach profiles provide an accurate cross-sectional picture of the entire beach system. An identical data set over the period 1970-1985 was analyzed by de Vroeg (1987) to beautifully illustrate and calculate the overall bar location, longshore shape and direction and rates of migration. He found two outer bars (bars 2 and 3) are present between Petten and Katwijk (km 30-86) with only one outer bar (bar 2) present south of Katwijk (km 86-119) (Fig. 5.2). North of Petten (km 0-20) a more complicated pattern is probably induced by the Den Helder tidal delta (Fig. 1.2). The bars, particularly between Petten and Katwijk are eneschelon to the shore, beginning as an attached bar 2, then detaching southwards to move offshore and eventually disappear into the nearshore zone. The bars or bar forms also migrates longshore at rates ranging between 0 and 70 m/yr and seaward at rates between 0 and 80 m/yr (Table 5.1, Appendix 12.3).

The 1976-85 beach profile sets were analyzed to provide morphometric data on beach gradients, beach and bar locations and mobility. An example from five profile locations is presented in Figure 5.3. A summary of the variables obtained from the profiles is given in Table 5.2.

Table 5.2   Summary statistics of beach profile variables

Variable	tanβ	NOBARS	NETSHORE	NETAMP	WIDSWEEP	AMPBAR2
Sample size	116	118	117	112	117	114
Average	0.0128621	2.64407	42.6923	1.35625	691.966	1.97807
Median	0.011	3	35	1.5	800	2
Mode	0.01	3	30	1	800	2
Standard dev.	4.41715E-3	0.710428	29.1883	0.482258	164.171	0.562038
Minimum	5E-3	0	0	0.5	190	1
Maximum	0.04	4	240	3	850	4
Range	0.035	4	240	2.5	660	3

Variable	BAR1MIG	BAR2MIG	BAR3MIG	AREASWEEP	AREA10YR
Sample size	110	112	82	114	110
Average	59.3636	112.589	174.878	1419.91	82.5091
Median	60	110	180	1600	75
Mode	60	100	200	1600	60
Standard dev.	23.4727	45.2569	63.9684	575.713	49.356
Minimum	10	10	20	200	5
Maximum	150	200	300	3200	300
Range	140	190	280	2980	295

tan β - slope;
NOBARS - number of bars;
NETSHORE - net shoreline width;
NETAMP - net amplitude of shoreline changes;
WIDSWEEP - width of swept prism;
AMPBAR2 - net amplitude of bar 2 changes;
BAR1MIG - net shoreline movement;
BAR2MIG - net movement of bar 2;
BAR3MIG - net movement of bar 3;
AREASWEEP = AMPBAR2 x WDSWEEP; AREA10YR = NETAMP x BAR2MIG.
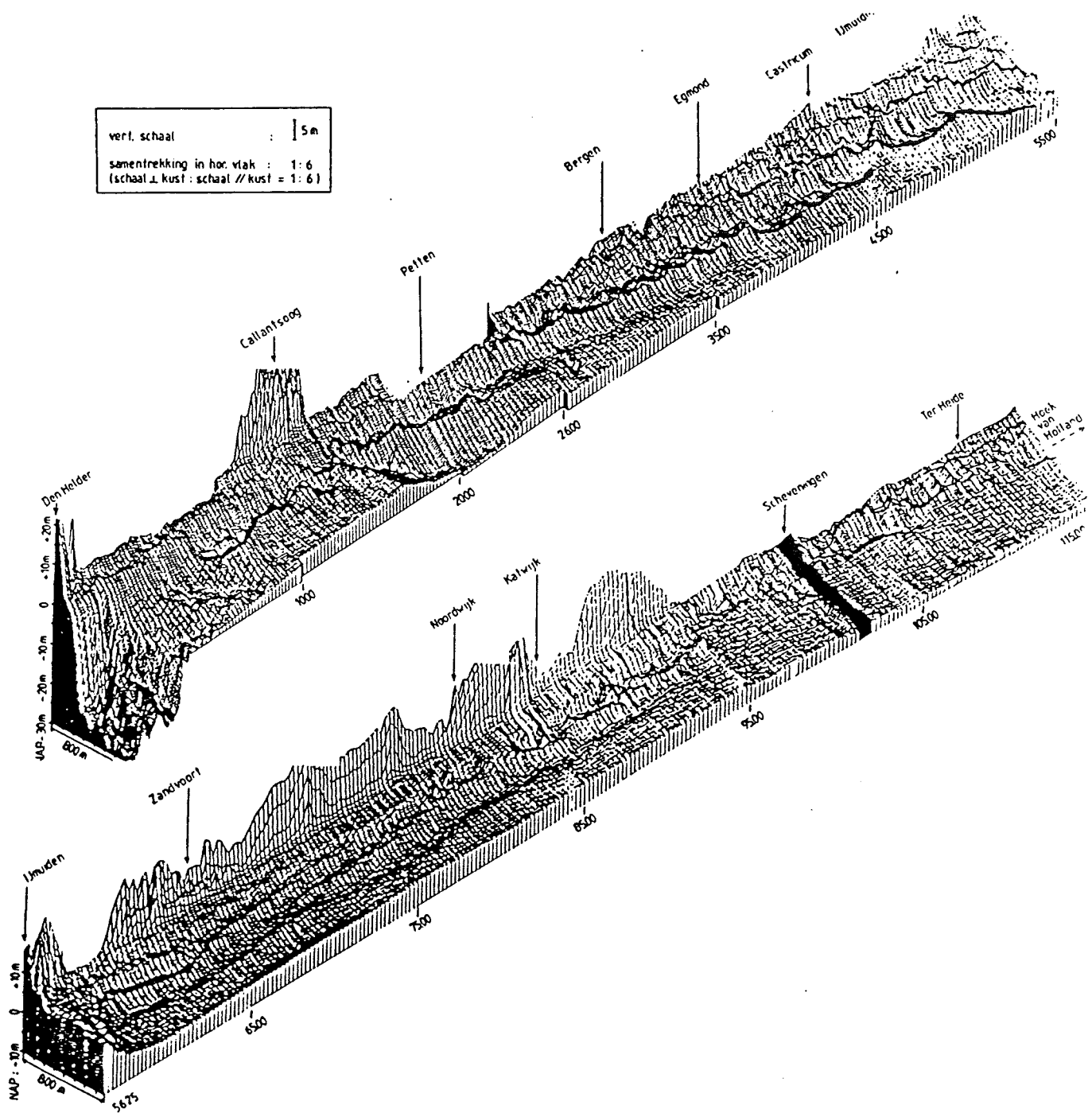
Figure 5.2   Three dimensional morphology of the central Netherlands coast from Den Helder to IJmuiden (upper) and Ijmuiden to Hoek van Holland (lower). Source: de Vroeg, 1987.
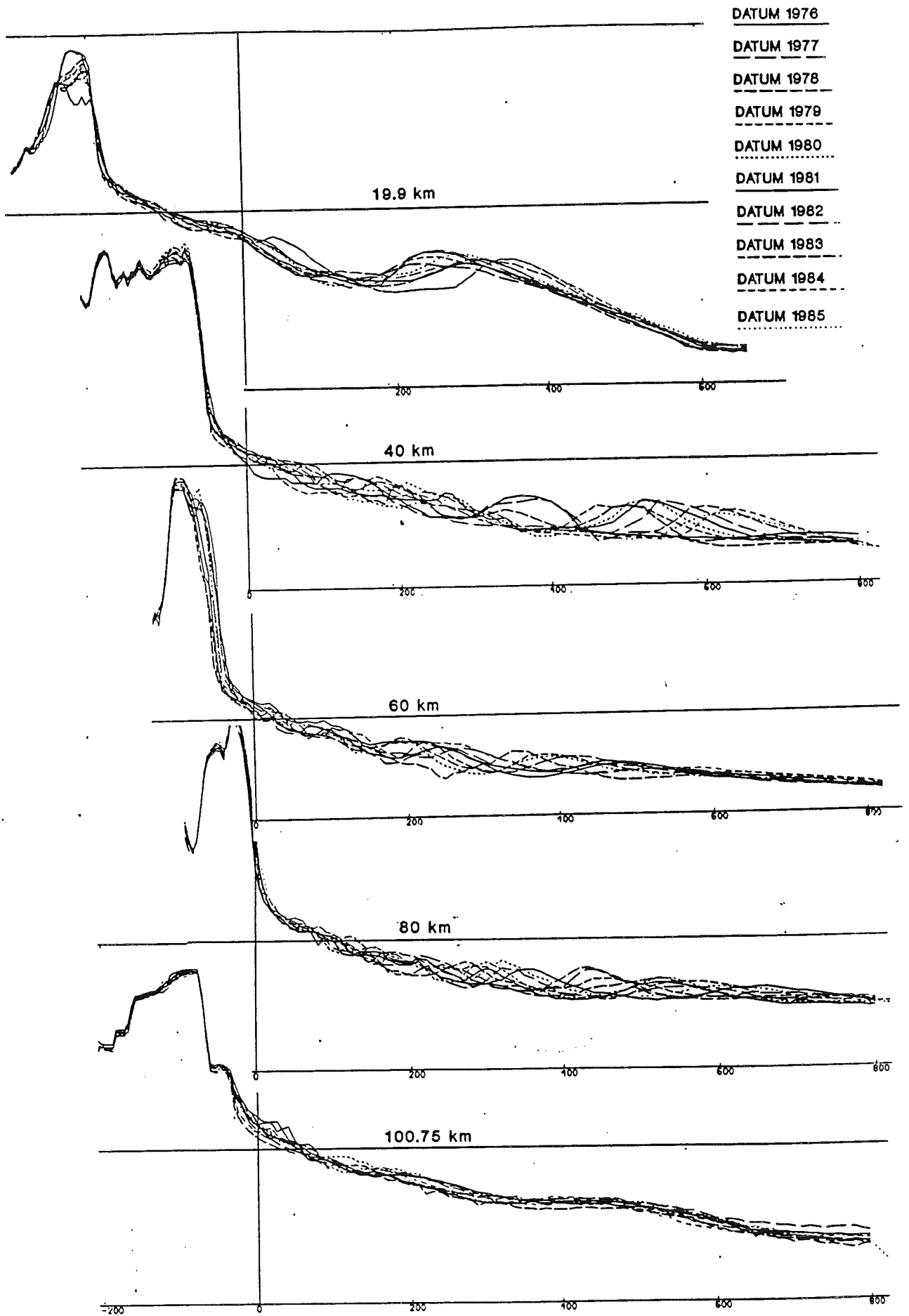
Figure 5.3　An example of beach profiles along the coast at km 19.9, 40, 60, 80 and 100.75. Source: Rijkswaterstaat, Tidal Waters Division.

31
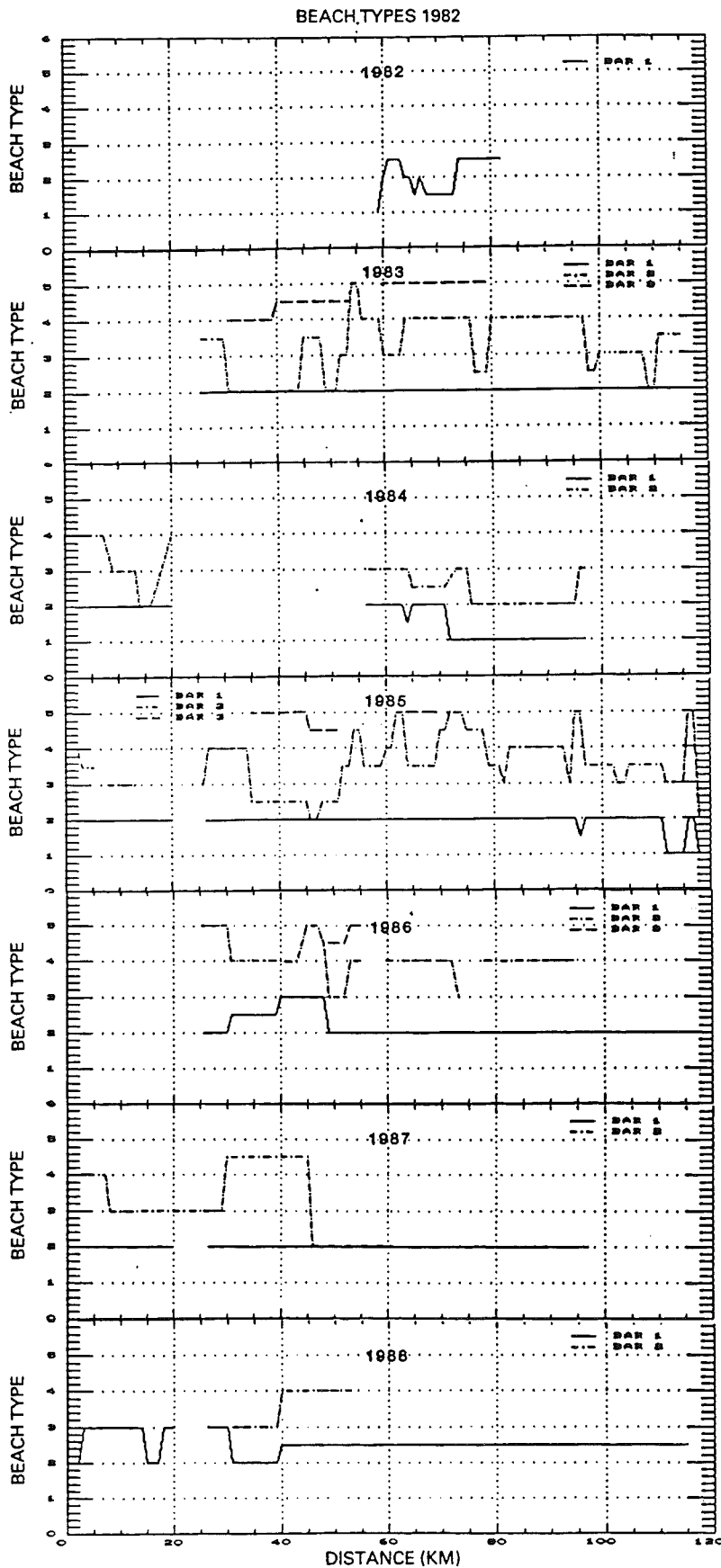
Figure 5.4   Beach types for beach/bar 1, bar 2 and bar 3 observed on aerial photographs 1982-1988. No data for bar 1 indicates no aerial photograph coverage. Missing data for bar 2 and/or 3 indicates no photograph or bar not visible on the photograph. Bar 3 in particular was often off the photograph or not visible due to water turbidity and/or lack of breaking waves. See Table 2.2 for actual date and extent of photo coverage.

32

The aerial photographs were however, the major source of information on beach morphology and beach type. It is these data which will be used as a basis of this assessment coupled with the profile data and the literature. The beach types were interpreted from the aerial photographs for beach/bar 1, bar 2 and bar 3 for each year. The model of Wright and Short (1984) (Fig. 2.2) was used to visually determine type and the results coded using the system shown in Table 2.3. The results are shown in Figure 5.4 and summarised in Table 5.3.

An assessment of the morphology of each of the three bars is now presented, followed by the results of the rip measurements, and the impact of structures (breakwaters, dykes and groynes). Finally an overview of the entire beach morphology is presented.

Table 5.3   Summary statistics of beach type observations for beach/bar 1, bar 2 and bar 3 based on 1982-1988 aerial photographs

|	1982	1983	1984	1985	1986	1987	1988	
BEACH TYPE BAR 1	n	n	n	n	n	n	n	Frequency
Reflective (1)	8	0	27	6	0	0	0	0.07
RR/LTT (2)	16	93	35	107	81	91	90	0.87
TBR (3)	0	0	0	0	9	0	25	0.06
n total	24	93	62	113	90	91	115	588
mean beach type	1.66	2.00	1.57	1.95	2.15	2.00	2.55	2.08 (SD = 0.38)
BAR TYPE BAR 1	n	n	n	n	n	n	n	Frequency
HC (1)	0	0	26	0	0	0	0	0.05
RR (2)	3	0	30	27	60	78	71	0.51
RR + LT (2)	10	31	5	14	0	0	0	0.11
LTT (2)	10	62	1	67	18	13	0	0.33
n total	23	93	62	108	78	91	71	526
mean beach type	1.9	2.0	1.6	2.0	2.0	2.0	2.0	1.95 (SD = 0.22)
BEACH TYPE BAR 2	n	n	n	n	n	n	n	Frequency
Reflective (1)	0	0	3	0	0	0	0	0.01
RR/LTT (2)	0	24	31	18	0	16	0	0.22
TBR (3)	0	26	21	46	5	22	9	0.32
RBB (4)	0	35	5	34	48	23	14	0.40
LBT (5)	0	2	0	9	8	0	0	0.05
n total	0	87	60	107	61	61	23	399
mean beach type	-	3.28	2.55	3.57	4.07	3.25	3.61	3.38 (SD = 0.87)
BEACH TYPE BAR 3	n	n	n	n	n	n	n	Frequency
RBB (4)	0	23	0	6	4	0	0	0.44
LBT (5)	0	20	0	19	3	0	0	0.56
n total	0	43	0	25	7	0	0	75
mean beach type	-	4.63	-	4.88	4.71	-	-	4.72 (SD = 0.35)

5.1 Beach/Bar 1

The subaerial beach and bar 1 extend from the foot of the vegetated dune out to low water. It runs the entire length of the coast except along the Hondsbossche Dyke (km 20-26) and in the harbour moles at IJmuiden and Scheveningen. It averages 43 m in width (sd = 29 m) on increasing substantially in width (max = 240 m) adjacent to the IJmuiden breakwater which has produced recent shoreline progradation.

Figure 5.5   Three aerial photographs illustrating the beach with a. low tide terrace at km 68.5, 4.4.82; b. single ridge and runnel with drains at km 94, 15.4.83; and c. double ridge and runnel at km 79, 30.4.86. Source: Rijkswaterstaat, Mapping and Survey Division.
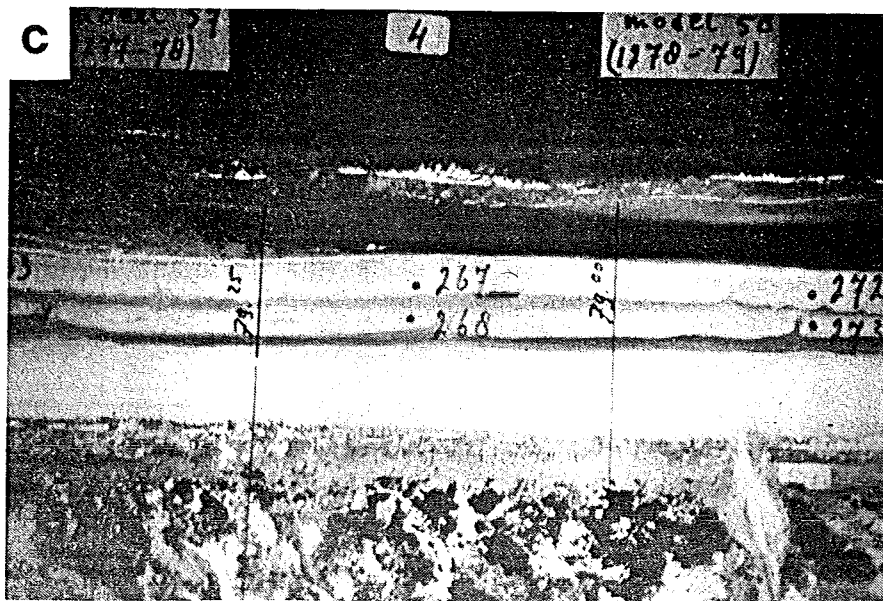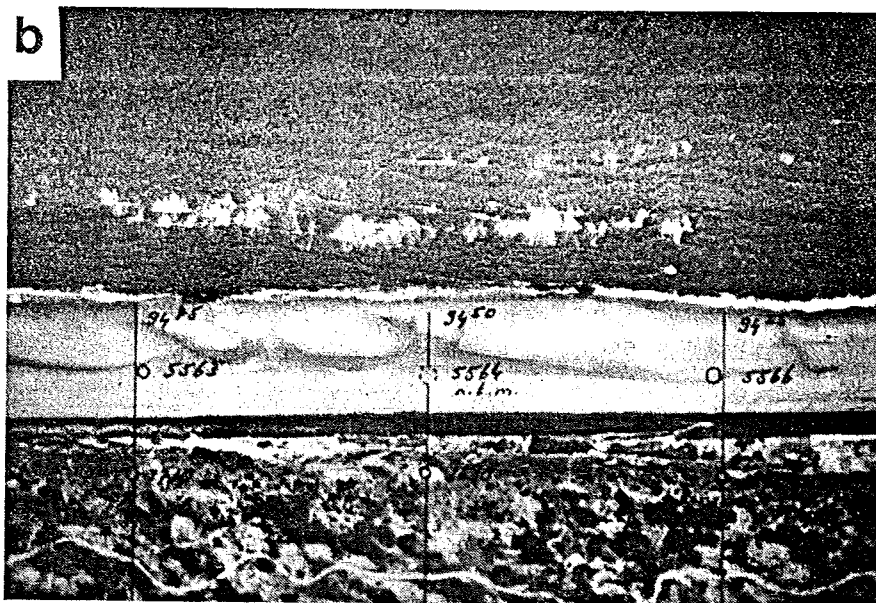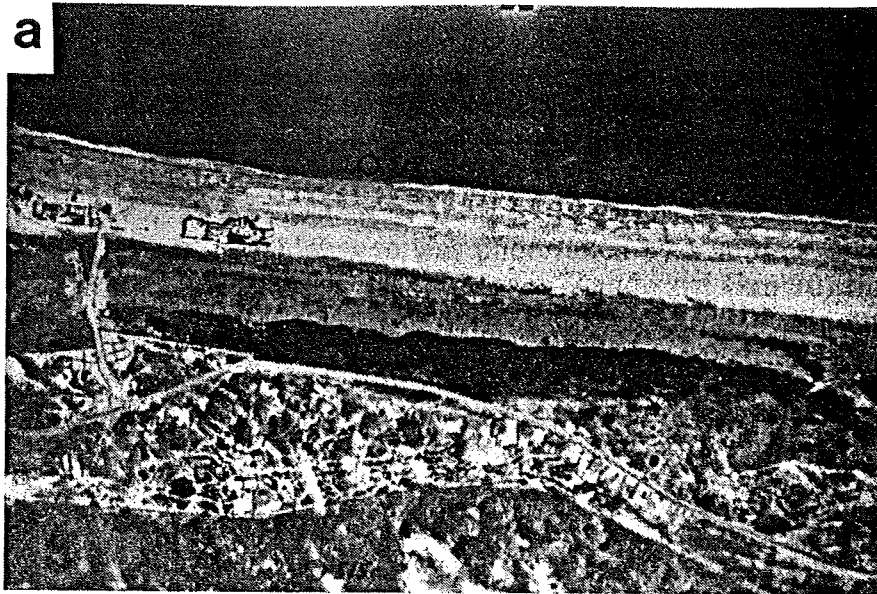
The beach consists of a usually dry backshore which slopes at about 1:15 and is only awash during severe storms and storm surges.

The intertidal beach may consist of a flat post-storm profile or lowtide terrace (Doeglas, 1954) or more often a welded bar 1 or ridge usually backed by a runnel. At times two ridges bar 1 and bar 2 may attach to the beach. Figure 5.5 illustrates the beach with a LTT (a), a ridge and runnel (b) and double ridge and runnel (c).

The most detailed study of beach change was undertaken by Van den Berg (1977). He found in an eight year survey of monthly beach changes at Zandvoort (km 70) that the post storm profile (= low tide terrace, LTT) occurred only 7.2% of the time, while one or two ridges (average 1.2 ridges) dominated 71.2% and a steep reflective beach 21.7%. Further, he found "that storms have to be rather severe and of long duration to produce the characteristic post storm profile on this beach" (ie. LTT).

Doeglas (1954) recorded similar results from a two month survey at beach pole 67. In particular his daily surveys showed that following storm erosion and formation of the LTT, the beach recovered quickly with a new ridge accreting within two weeks. This would explain the low frequencey of LTT observed by Van den Berg (1977).

Table 5.4   Beach/bar 1   Beach types (Percent observed)

	Van den Berg 1977	This study
TBR	not noted	6
LTT	7.2	29
LTT & RR	} 71.2	20 } 54
RR		34
R	21.7	11

The aerial photographs both confirm these results as well as illustrate the extent of these systems along the coast and their variability on a scale of years. Figure 5.4 shows the beach/bar 1 type ranged between 1 (reflective) and 3 (TBR) and was modally 2 (RR or LTT). Figure 5.6 shows that while LTT dominated in 1983 and 1985, ridges were present most years. Table 5.3 shows that reflective conditions were observed 11%, RR 54%, LTT 29% and TBR 6%. These figures compare favourably to Van den Berg's results (Table 5.4), despite the very different temporal and spatial scale of each data base. Examination of the four air photo mosaics (Table 5.5) which cover the coast between Katwijk and Hoek van Holland (km 86-119) also confirms these results. The beach/bar 1 was either LTT and/or RR and on one occasion also contained high tide cusps behind the LTT.

A. Kroon (pers. comm.) reported that during the 1989 summer a reflective beach (bar 1) with cusps was a dominant feature of the beach at Egmond aan Zee (km 38-40). It is probable that cusps were undetected on some aerial photographs and that the 5% occurrence indicated in Table 5.3 is too low.

The resulting modal beach state for the beach/bar 1 is therefore a ridge and runnel (see e.g. Fig. 5.5.b) (mean BS = 2.08, sd = 0.39). This relatively narrow range is accounted for by the infrequent erosion as noted by Van den Berg (1977) together with rapid ridge recovery as
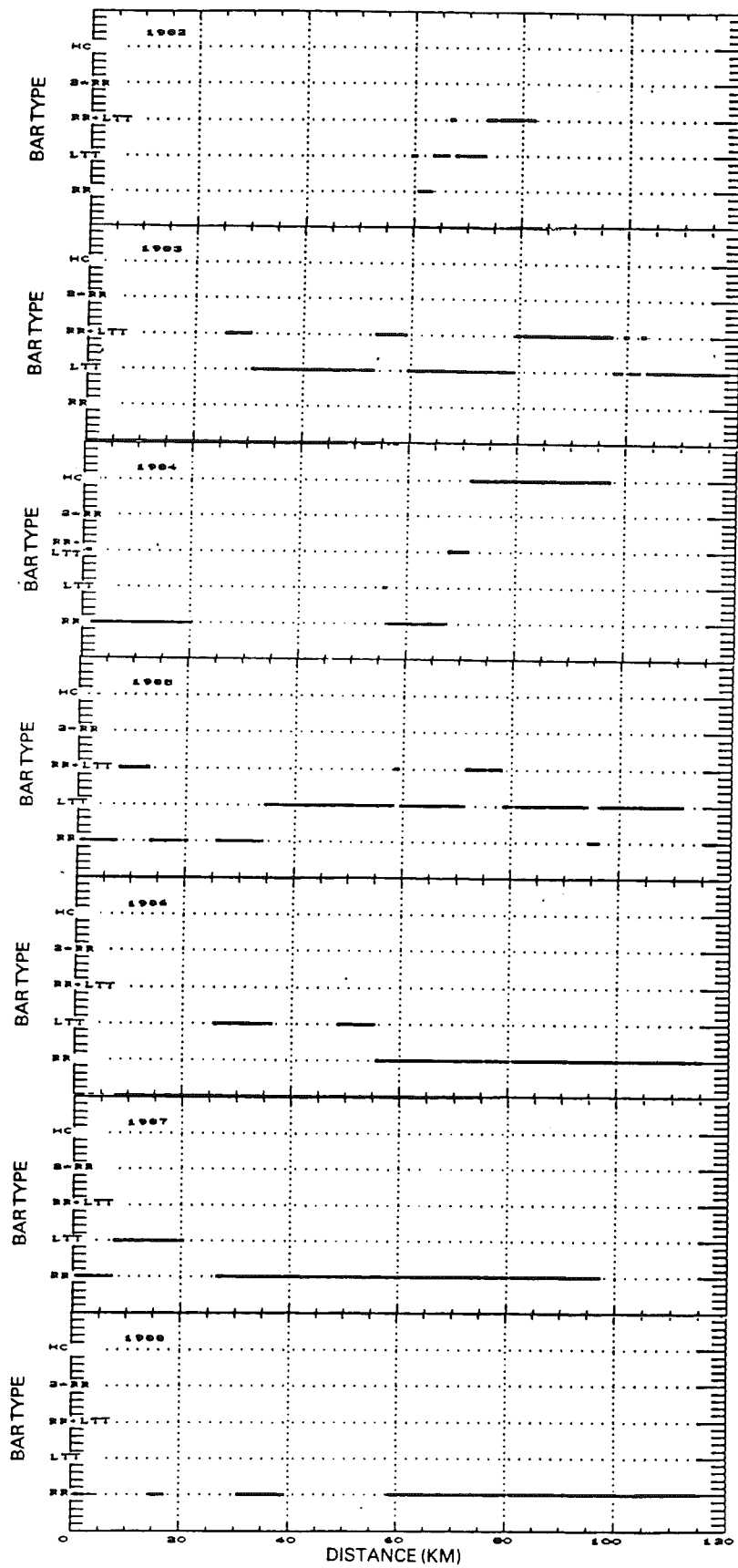
35

Figure 5.6 Beach type observed on the beach/bar 1 from aerial photographs 1982-88. HC = high tide cusps; 2RR = double ridge and runnel; RR = ridge and runnel; LTT = low tide terrace.

36

noted by Doeglas (1954), both of which are a characteristic of this beach type (Short, 1980). It is also confirmed by the profile data which reveal a mean net shoreline oscillation of 59 m (sd = 23 m, BAR1MIG Table 5.2). This oscillation is not only greater than the mean beach width of 43 m (sd = 29 m) but is relatively uniform alongshore (Fig. 5.7c). This mobility represents two processes. Firstly, beach erosion (LTT) and recovery (RR) which in Van den Berg's (1977) three survey lines resulted in beach change of 17, 39 and 42 m (mean = 33 m); and second, longshore (northward) migration of points of bar attachment.

Table 5.5   Beach morphology based on air photo mosaics[1]

Date	Coverage	Beach type		
		Beach/Bar 1	Bar 2	Bar 3
28/2/66	108-199	LTT (+ HC)	-	-
16/3/68	86-103	LTT + RR	LBT	-
17/6/70	86- 97	RR	RBB	-
	97-119	LTT (groynes)	RBB	-
14/7/71	86- 97	LTT	LBT	-
	97-119	LTT (groynes)	TBR (groynes)	-

1 Source: Rijkswaterstaat, North Sea Directorate
  See Table 2.3 for symbols

Bar attachment results in prominent shoreline protrusion as illustrated in Figure 5.8. This usually occurs as a result of bar 2 attachment at the shoreline (Fig. 5.8a, b) but can also occur when bar 3 attaches to bar 2 (Fig. 5.8c). The bar 2 attachments tend to migrate northwards at rates varying from 0 to 10 m/yr (de Vroeg, 1987) while bar 3 attachments are more episodic. The impact is to produce an increase in beach width and one which may be stationary or migratory. The end result is to contribute a low frequency shoreline oscillation. Such oscillations are impossible to detect on the beach profile data (Fig. 5.7) unless accompanied by simultaneous field or photograph observations. However, points of major bar attachment illustrated in Figure 5.2 may be roughly correlated with increased beach width (Fig. 5.7a) particularly between km 26 to 60 and at km 85. However, a closer analysis of both the profile data and aerial photographs is required to estimate the contribution of the bar migration to shoreline width and change.

Figure 5.7 also reveals three other interesting features of the beach/bar. First, structural impact on beach width is apparent at the Hondsbossche Dyke (km 21-26) with no beach; and at IJmuiden and toward Hoek van Holland where substantial shoreline accretion has followed breakwater construction. The minor Scheveningen breakwaters and the groyne fields (km 0-31 and 97-115) have no apparent impact on beach width. Second, the uniformity in shoreline oscillation, both lateral (BAR1MIG) and vertical (NETAMP Fig. 5.7) relative to the regional variation in shoreline width suggests that high frequency shoreline processes and beach types are relatively uniform alongshore, a fact confirmed by the air photo data (Fig. 5.4 bar 1). These oscillations are superimposed on the lower frequency changes in shoreline width induced by bar protrusion migration and by structural impact. Third, the volume of shoreline change (AREABAR1, Fig. 5.7d) is small (mean = 83 m^3, sd = 49 m^3, Table 5.2) relative to the volume of change across the surf zone as will be seen in the next section.
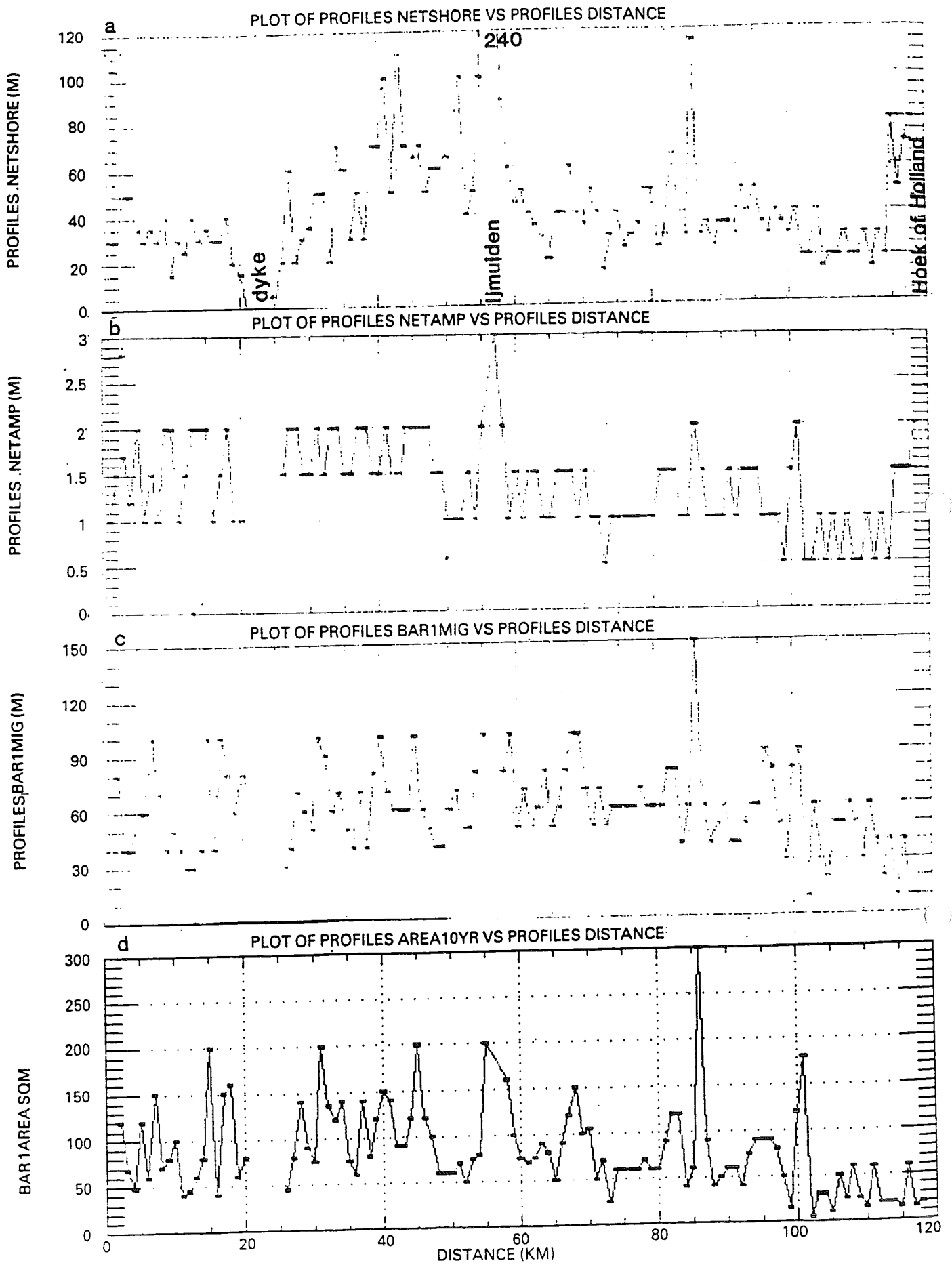
Figure 5.7 Plot of longshore variations in beach width (NETSHORE, a) net beach amplitude (NETAMP, b), shoreline mobility (BAR1MIG, c) and of shoreline change (AREA10YR, d). Based on annual Rijkswaterstaat beach profiles 1976-1985.

38

Figure 3.8   Three aerial photographs illustrating bar attachment and beach or shoreline protusions.
a. bar 2 attachment at km 72-73, 14.4.83;
b. bar 2 attachment at km 78, 11.4.84, and
c. bar 2 attachment with major shoreline protusion, together with bar 3 RBB producing a rhythmic and 'protuding' bar 2 at km 34, 1.6.85. Source: Rijkswaterstaat, Mapping and Survey Division.
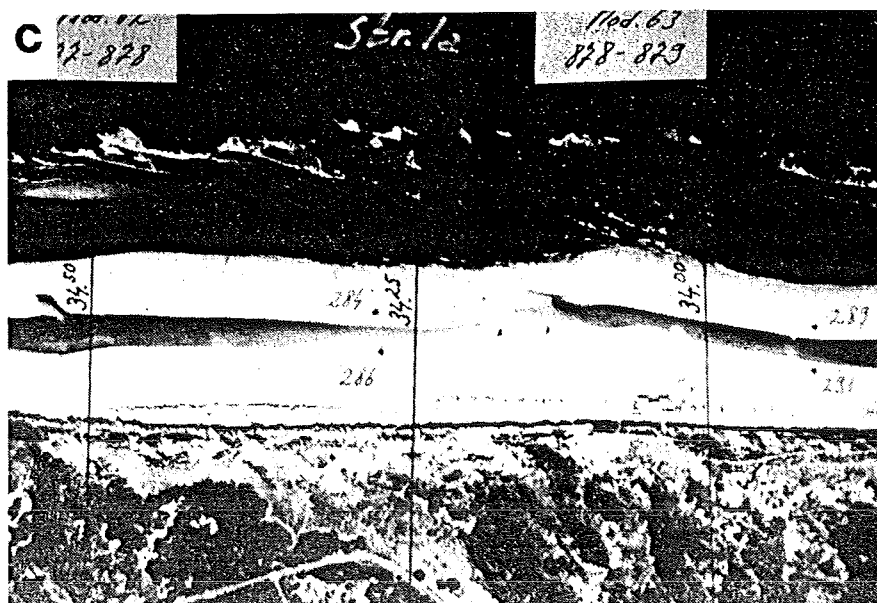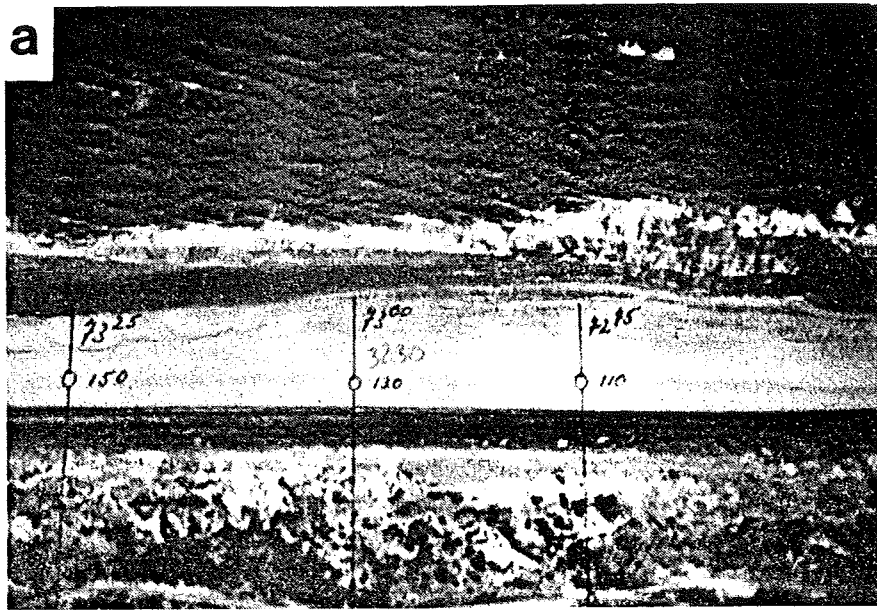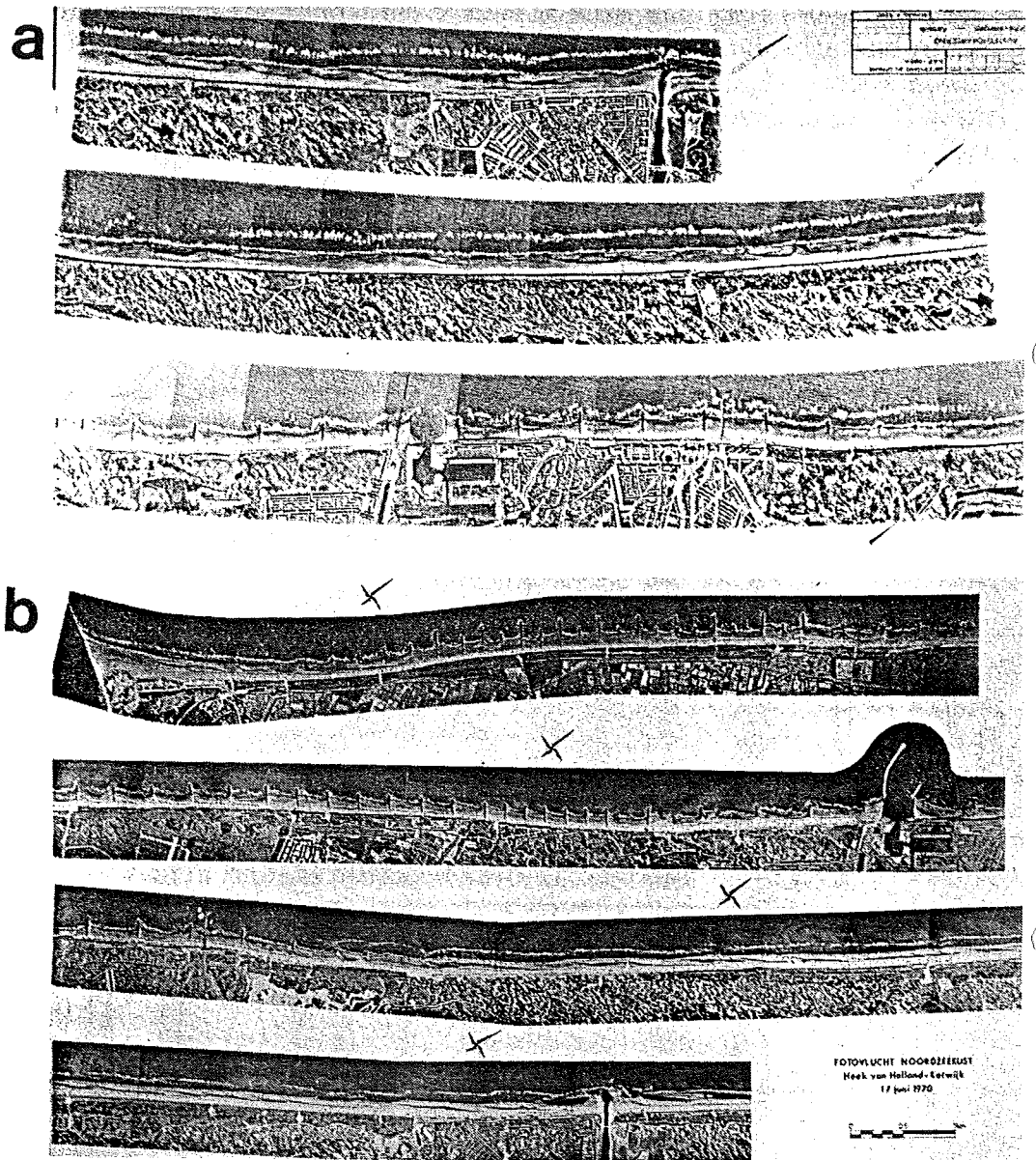
Figure 5.9   Aerial photo moasics of the coast between Scheveningen and Katwijk on 16.3.68 (a), and between Hock van Holland and Katwijk on 17.6.70 (b). The shore parallel longshore bar and trough of bar 2 is clearly evident between the groynes and Katwijk. Source: Rijkwaterstaat, North Sea Directorate.

5.2 Bar 2

A second bar is present along the entire coast. This is apparent in Fig. 5.1 and 5.2. Figure 5.2 shows how this bar usually begins as a shoreline attachment and gradually moves seaward to eventually become the third bar and finally merge with the nearshore zone. The outer bars migrate longshore at rates ranging from 0 toward Den Helder to a maximum of 70 m/yr near IJmuiden (Table 5.1). The bar usually lies between 0 and 300 m from the shoreline, averaging about 200 m).

Based on the aerial photographs the modal bar 2 state is RBB and TBR (40% and 32% respectively Table 5.3). At times the bar welds to the beach as a second ridge and runnel (22%, Fig. 5.8c) and very rarely may even be reflective (1%). Under higher waves however, the bar detaches and straightens to form a LBT (5%, Fig. 5.9). These values are however tentative as they are based on a limited spatial and temporal sample, as indicated in Figure 5.4. The air photo mosaics (Table 5.5) also recorded bar 2 ranging from TBR to LBT. The prevelance of rips in bar 2 is a characteristic of all its beach types (RR, TBR, RBB and LBT). The common occurrence of surf zone rips along the central coast has been noted by Ten Hoopen and Van Driel (1979) and Gerritsen and van Heteren (1984). The details of the bar 1 and bar 2 rips will be dealt with in section 5.7.
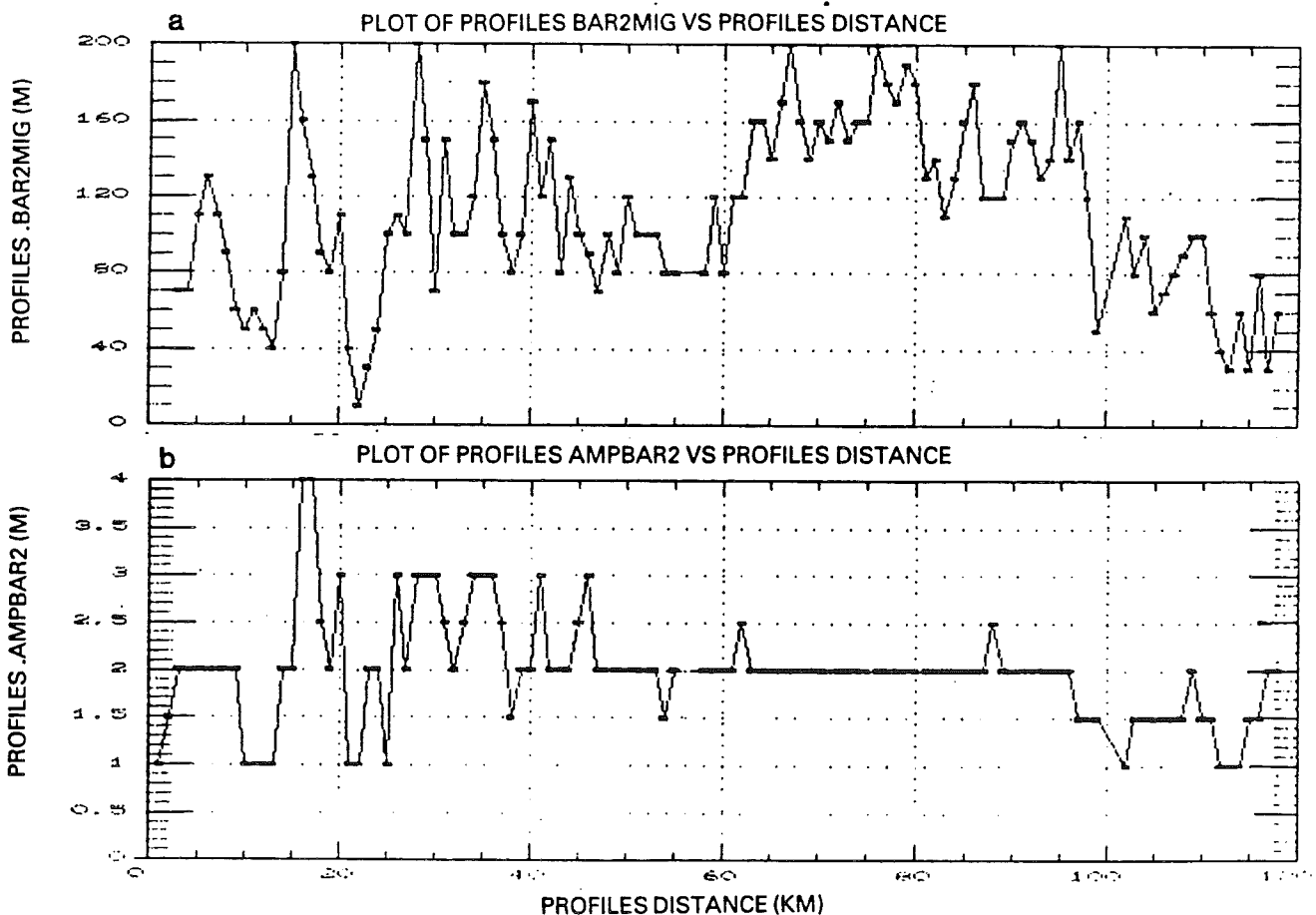
Figure 5.10 Plot of longshore variation in the mobility of bar 2 crest (BAR2MIG, a) and the change in amplitude of the bar 2 crest (AMPBAR2, b). Based on annual Rijkswaterstaat beach profile survey 1976-1985.

41

Bar 2 is highly mobile with a mean shore normal oscillation of 113m (sd = 45m, Table 5.2). The oscillation is also highly variable longshore (Fig. 5.10a). The oscillation in bar crest can be accounted for by two scales of bar change. First, high frequency on-offshore bar migration in response to periods of low and high waves, as reflected also in the shift in beach types from attached (RR and TBR) to detached (RBB and LBT) bar. Second, to the lateral bar migration recorded by de Vroeg (1987), which also results in net offshore bar migration. The offshore migration ranges from zero north of km 20 and south of km 100 to a maximum of about 45 m/yr at IJmuiden (km 70, Appendix 12.3). In order to resolve the high versus low frequency contribution to bar migration high frequency surveys would be required. As these are not available their relative contribution of the high frequency change cannot be obtained from these data. An indication of the relative contribution of each can be gauged from the fact that when the bar was in a LBT state it was separated from the beach by a trough up to 50 m wide. This value provides an approximation of the magnitude of bar 2 high frequency lateral migration. Given this the overall mean value of 113 m would suggest a substantial amount is due to net offshore migrations (i.e. ~ 60 m). This fact is further supported by a decrease in lateral bar oscillation in zones of low offshore bar migration, particularly south of km 98, where overall lateral mobility ranges between 40 and 80 m.
The amplitude of bar crest oscillation is relatively uniform alongshore averaging 2 m (sd = 0.6 m) (Table 5.2, Fig. 5.10b)

5.3 Bar 3

The aerial photograph observations of bar 3 are limited owing to the problems outlined earlier. They are restricted to a few observations in 1983, 1985 and 1986, when it was modally LBT (56%) and RBB (44%) (Table 5.2 and Fig. 5.4). It was not visible on any of the air photo mosaics as these were taken in the two bar section of coast (Table 5.5). However, its presence is clearly verified by de Vroeg (1987) and the profile data (Fig. 5.1). It is present continously between Den Helder and km 95 but not present between km 95 and 119. It is also present off the Hondsbosse dyke where only two bars are shown in Fig. 5.1, here the missing bar is bar 1 and not bar 3.
Bar 3 is the most dynamic of the three bars experiencing predominantly offshore migration with rates similar to bar 2 (Table 5.1). The average on-offshore movement of the bar is 175 m over a 10 year period (sd = 64 m, Table 5.2) suggesting on-offshore plus net offshore movement contribute to bar crest mobility. This fact, like bar 2, is also supported by the decrease in bar mobility in the areas of more stable bar forms north of km 25 and south of km 85 (Fig. 5.11).
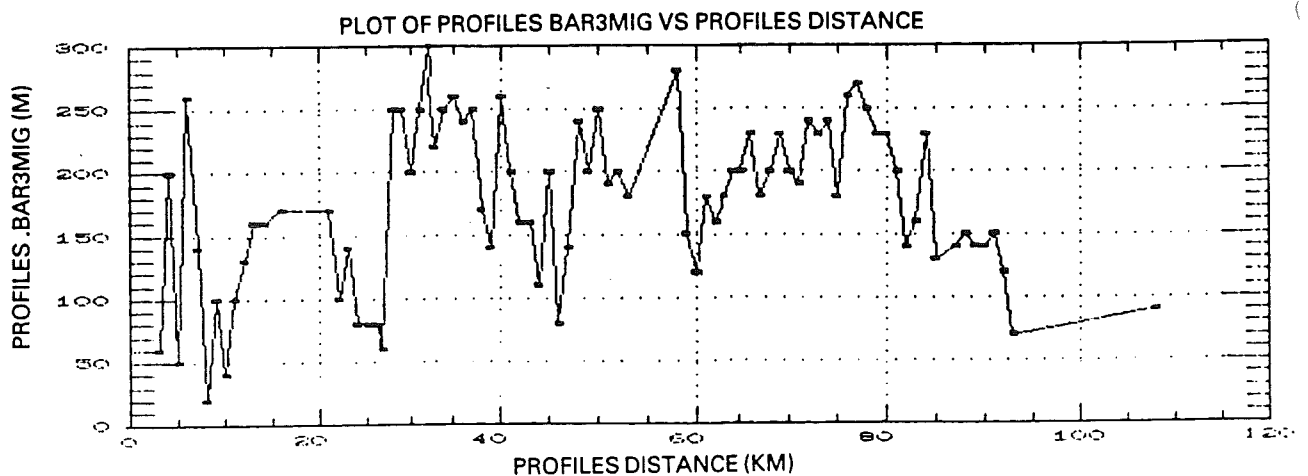

Figure 5.11 Plot of longshore variation in the mobility of bar 3 crest. Based on annual Rijkswaterstaat beach profiles 1976-1985.

5.4 Beach and bar mobility

The overall beach mobility and particularly the impact on potential sediment transport can be assessed from Fig. 5.12. It illustrates the mobility of the three bars, the width of the active sweep zone and volume of shoreline and surf zone change. Bar mobility over the period 1976-1985 increases dramatically offshore from a mean of 60 m at bar 1 to 113 m at bar 2 and 175 m at bar 3 (Table 5.2). Laterally mobility is greatest in areas of offshore migration (km 25-90) while decreasing south of km 90. The active sweep zone averages 692 m in width with a distinct 800 m wide modal range which like beach mobility decreases north of km 25 and south of km 80. The area or volume (area x m) of sediment mobility increases dramatically offshore. The shoreline changes average 82 m^3 (sd = 49 m^3) while the outer bars average 1420 m^3 (sd = 576 m^3) 17 times greater. These figures illustrate the dominance of surf zone versus shoreline processes in contributing to sediment mobility and transport. While these results and the findings of de Vroeg (1987) indicate both regional variation in sediment mobility together with maximum mobility in the surf zone, they cannot be used to infer either the direction of sediment transport nor the net sediment balance. It does however illustrate the dominance of surf zone processes in contributing to sediment transport.

5.5 The beach system - what type?

The previous sections have shown the central Netherlands beach system to consist of 2 to 3 bars set in a hierarchy of increasingly higher beach types. These are summarized in Figure 5.13 which plots the mean beach type for the three bars based on the aerial photographs. The model used to type this system (Fig. 2.2) consists of one (LTT, TBR, RBB, LBT) and at most two bars (LBT and D). Therefore if the present system is to have a single beach classification a new or expanded model applicable to multi-bar beaches is required. This will be discussed and resolved in section 8.4.

5.6 Structural Impacts

5.6.1 Breakwaters

The numerous man made structures along the central coast (Fig. 2.1) influence beach morphology in two ways. Firstly, the larger harbour breakwaters or moles at Den Helder, IJmuiden and Hoek van Holland together with Den Helder's ebb tide delta all induce lower nearshore gradients and substantial reduction in breaker height toward the breakwaters. This has produced four wave shadow zones with breaker height approaching zero, particularly toward Den Helder and the IJmuiden moles. At IJmuiden and Hoek van Holland it has also resulted in substantial shoreline progradation though the latter has also been aided by beach sand nourishment (Fig. 5.6a). The net result is a wide low gradient beach, fronted by a wide low gradient surf zone-nearshore zone, with the adjacent bars merging with the ebb tide delta (Fig. 5.2).

The beach type in all cases shifts to a lower and/or inactive type, inactive here meaning remains unchanged following higher waves or storm erosion. The inactive morphology is particularly noticable in the beach-groyne field toward Den Helder which will be discussed in 5.6.3.
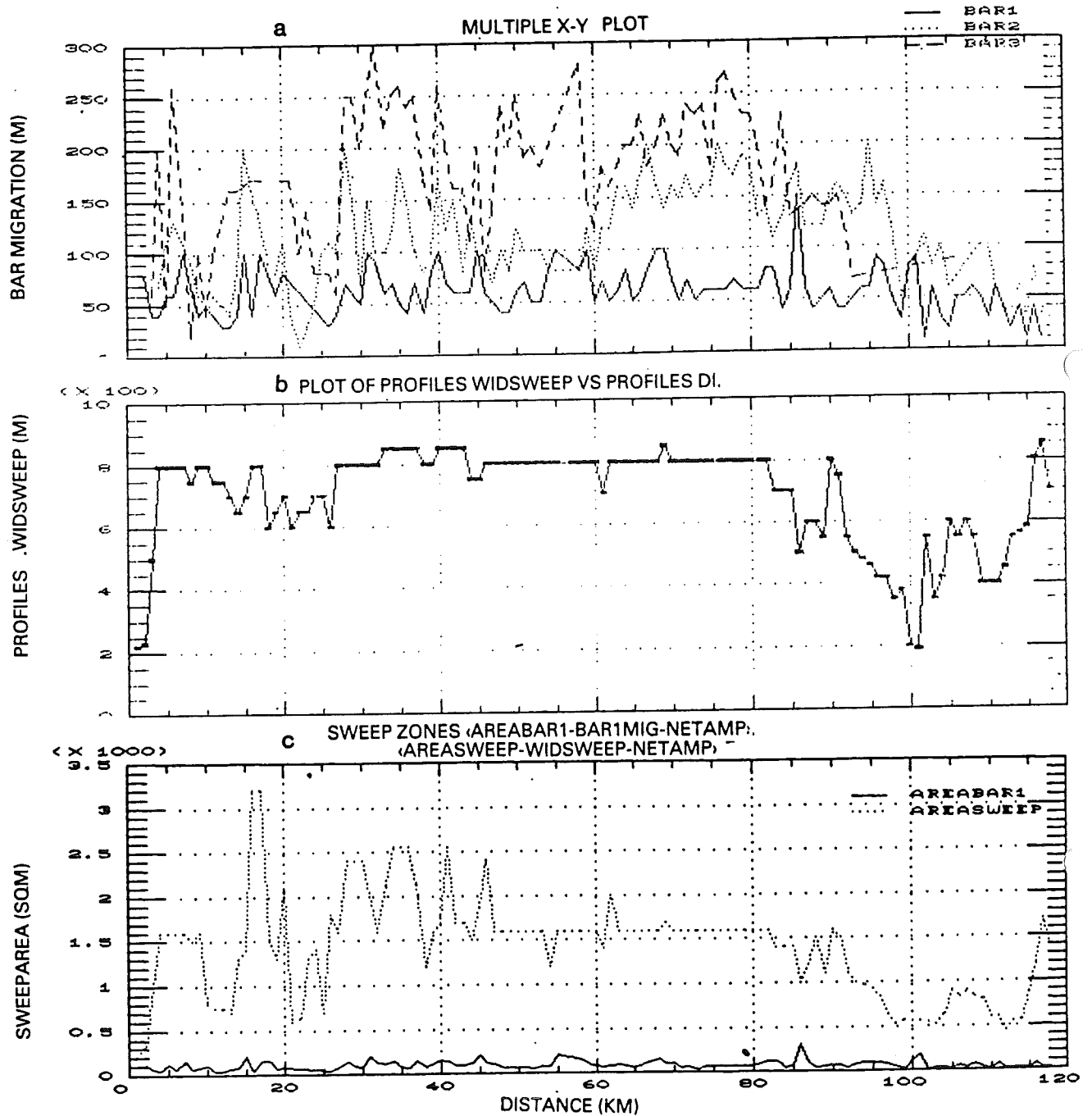
Figure 5.12 Plot of
   a. longshore variation in a maximum shore normal mobility of the shoreline (bar 1) and crests of bars 2 and 3;
   b. width of the active sweep zone; and
   c. area of shoreline change (AREA BAR 1) and surf zone change (AREASWEEP).
      Based on annual Rijkswaterstaat beach profile surveys 1976-1985.

The long term impact on beach morphology is partially illustrated in Figure 5.13, which shows the mean beach type. At both Den Helder (km 0) and Hoek van Holland (km 120) there is a shift in bar 1 toward lower energy more reflective conditions (2 --> 1) and bar 2 toward more dissipative, the latter suggesting an inactive 'storm' bar form.
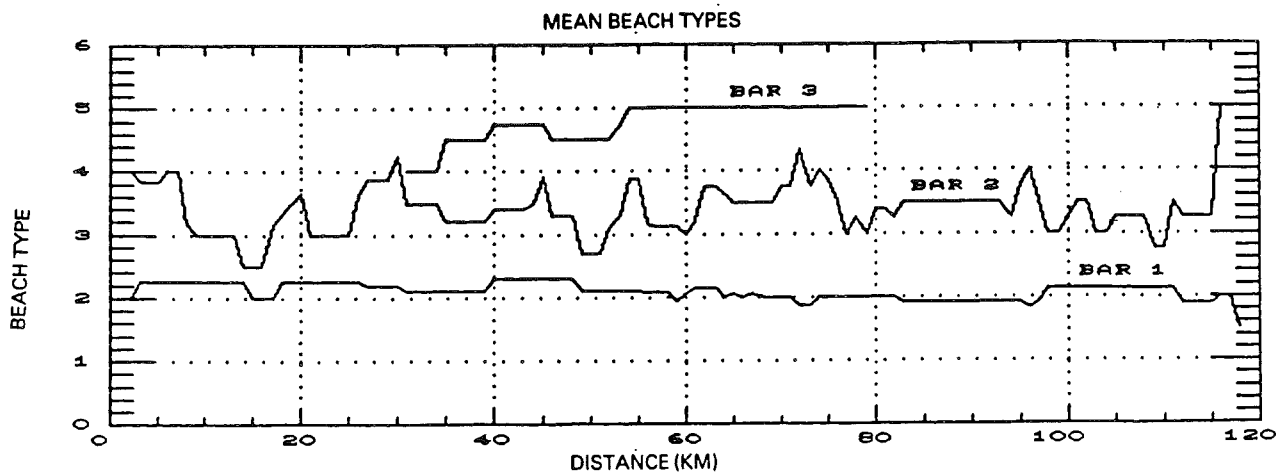
Figure 5.13 Longshore variation in mean beach type for beach/bar 1, bar 2 and bar 3, based on annual aerial photographs 1982-1988. See Figure 5.4 for annual beach type.

5.6.2 Hondsbossche dyke

The Hondsbosse dyke was constructed in its present location in 1823 to seal the former estuary. The dyke was built in line with the 1823 beach. Since then over 100 m of shoreline retreat has left it seaward of the present shoreline. As a result it replaces the beach along this 4.5 km section of coast (Fig 5.14). It is interesting to note however, that the outer bars 2 and 3 appear to continue their migration past Hondsbosse uneffected by the dyke (Fig. 5.2 and 5.10). Because of its seaward location the groyne field along the dyke is usually devoid of sand and therefore ineffective in directly influencing or containing sediment transport.

5.6.3 Groyne fields

Three groyne fields have been constructed along the coast (Fig. 2.1) with each having a considerable impact on the beach/bar 1 and bar 2 which they usually intersect. The major impact of groynes is to induce a topographically controlled variation in nearshore topography, wave breaking and refraction, surf zone circulation, and sediment transport and accumulation. All this is superimposed on the natural shoreline processes. The groyne fields and the adjacent non-groyned beaches provide a natural laboratory in which to assess their impact on the beach/bar 1 and bar 2 systems.

The structural characteristics of the groyne fields are illustrated in Fig. 5.15 and Table 5.6. The 90 groynes between km 0-20 (Fig. 5.16a) are usually 200 m apart, with some 300 m and others more random. The second field of km 25-30 (Fig 5.16b) has a range of spacings from 200 to 530 m. Likewise the southern field from km 97-115 (Fig. 5.9b) has three modes at 200, 300 and 500 m with others ranging from 50 to 550 m in spacing. The groynes usually extend between 100 and 200 m seaward of the beach and are awash at high tide.

Figure 5.14   Aerial view of the Hondsbossche dyke constructed in this location
in 1823. It has been stranded by continuing shoreline retreat.
Source: Rijkwatrstaat, North Sea Directorate.

Table 5.6   Groyne spacing for three groyne fields
            See also Appendix 12.4

Location	km 0-20	km 25-30	km 97-115
Number of groynes	90	11	57
Average (km)	0.218	0.370	0.314
Median	0.2	0.35	0.3
Mode	0.2	0.5	0.2
Standard Deviation	0.045	0.129	0.168
Minimum	0.1	0.2	0.05
Maximum	0.36	0.525	1.1
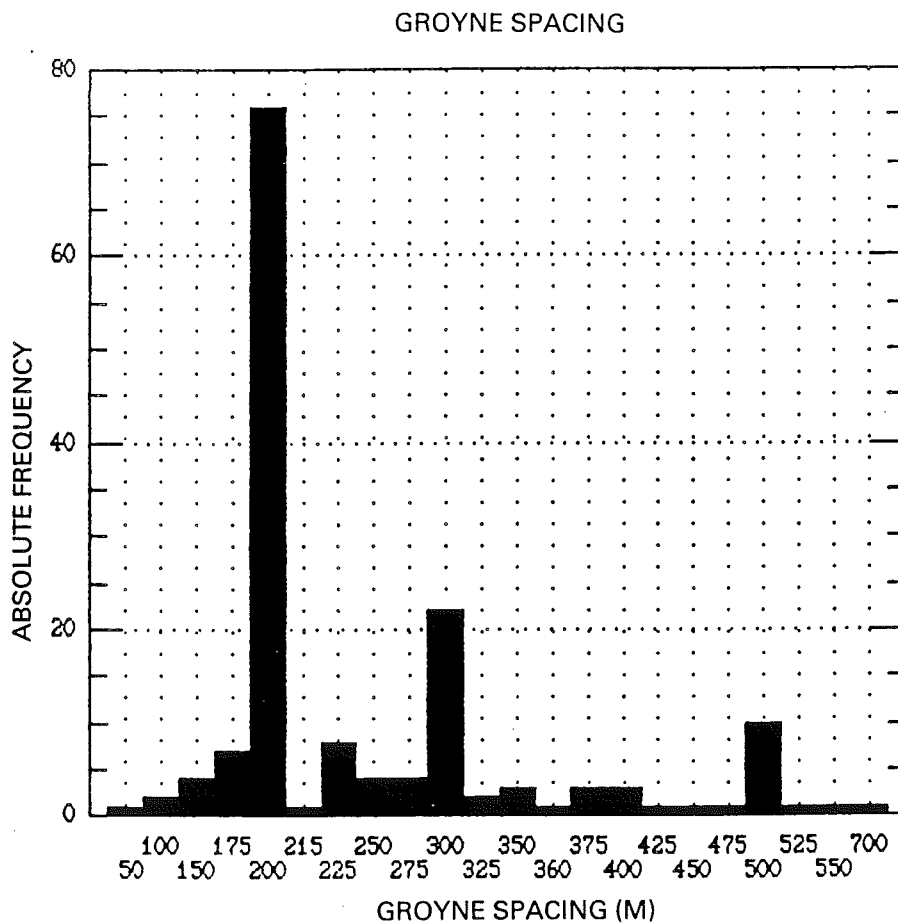
GROYNE SPACING

Figure 5.15 Frequency plot of groyne spacings for the central Netherlands coast. See Appendix 12.4 for frequency spacing for all three groyne fields.

Figure 5.16 Aerial view of a. the northern groyne field looking north toward Den Helder (km 0); and b. looking south with the Hondsbossche Dyke in the distance (km 15-21). Source: Rijkswaterstaat, North Sea Directorate.

The impact of the groynes on beach morphology can be assessed from the aerial photographs (e.g. Fig. 5.9) which clearly show both the beach type together with the location of groyne controlled features. This can best be illustrated using some of the morphological sketches shown in Figures 5.17, 5.18 and 5.19 and photographs in Figure 5.20.
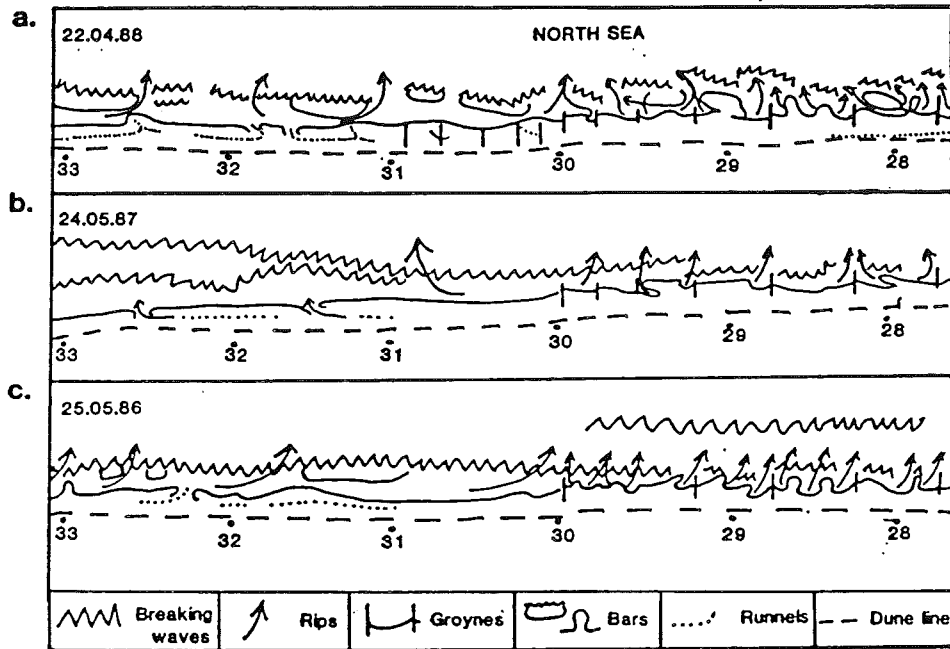
Figure 5.17 Morphological sketch of beach between km 28-33 based on aerial photographs. Dates indicated. Note the impact of groynes in producing more numerous groyne controlled rips.

The more obvious impact of the groynes is to produce more rips and locate them adjacent to one or both groynes. This is illustrated in Fig. 5.17 a and b (km 28-32 and km 96-99) which illustrate both natural and groyned section of coast exposed to the same wave conditions. Note that in Figure 5.17: 1. more rips are present in the groyne fields; 2. most rips are adjacent to groynes; 3. in more widely spaced groynes additional mid groyne rips occur; and 4. the beach/bar 1 while interupted by the groynes remains modally RR. In Fig. 5.17b and 5.18 under lower wave conditions the groynes interupted the RR to produce weak rip circulation at one or both groynes.
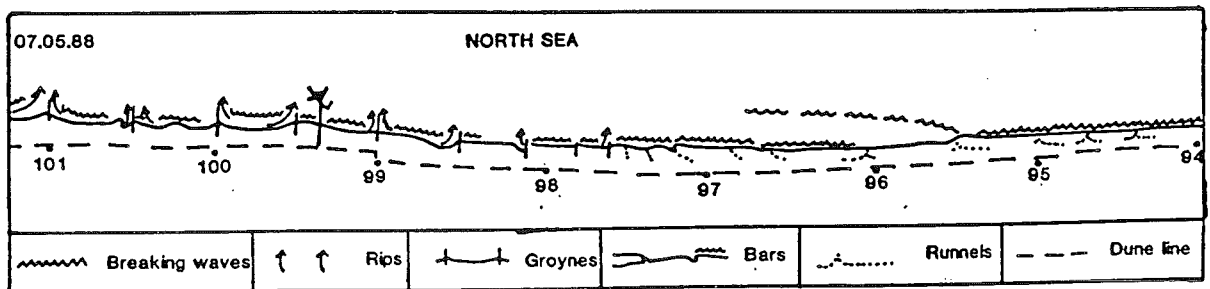
Figure 5.18 Morphological sketch of beach between km 94 and 101 based on aerial photograps. The groynes result in the beach type switching from a ridge and runnel to transverse bar and rip.

49
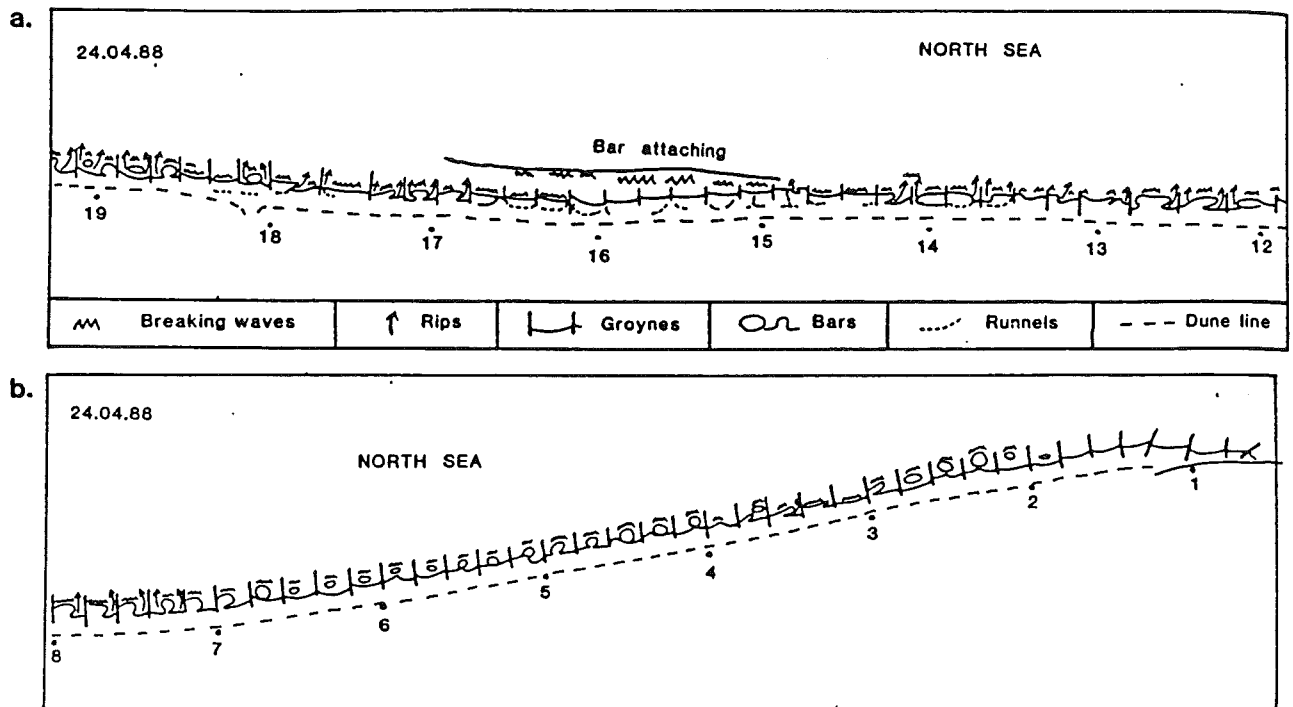
Figure 5.19 Morphological sketch of beach type in northern groyne fields based on aerial photographs. Date and location indicated.

Figure 5.19a and b illustrates two sections of the first groyne field on 24.4.88. In a. (km 18-13) bar 2 is attaching to shore between km 17 and 15, inducing a local decrease in breaker height in its lee. This permits the impact of variable breaker height to be assessed within the groyne field. In the zone of lower waves (km 17-15) the beach/bar 1 is RR with drains exiting at one or both groynes. As wave height increases past km 17 and 15 the bar 1 breaks up into TBR with groyne controlled rips at one or both ends.

This pattern is somewhat repeated in Figure 5.19b which shows the same field between km 1-7. Decreasing and variable wave height towards Den Helder (km 0) results in the beach type within the groyne field shifting between TBR (km 4-5), to RBB (km 2-3) to RR (km 1-2) and to R (km 0-1).

The air photo mosaics all cover the southern groyne field (km 97-116). The groynes have no apparent impact on 28.6.66 and 16.3.68 (Table 5.6). However, on 17.6.70 bar 1 shifts from RR to LTT in the groyne field (Fig. 5.6), while on 14.7.71 bar 2 shifts from LBT to TBR in the groynes, the latter resulting in numerous groyne controlled rips.

In summary the impact of the groynes is to:
1. interrupt the beach/bar 1 and bar 2 system: (Fig. 5.20);
2. the nature and scale of the interruption depends on the prevailing beach type and groyne spacing;
3. reflective beaches are uneffected apart from shoreline orientation;
4. ridge and runnels are largely uneffected apart from orientation and groyne controlled drainage channels, i.e. adjacent to groyne;
5. groyne controlled transverse bar and rip may replace RR with increasing wave height, and in a modal TBR beach the groynes will induce more rips both at groynes, and in more widely spaced groynes in mid groyne locations (Fig. 5.20c). As mean groyne spacing is 200-300 m and mean rip spacing is 400-500 m (see section 5.7) the groynes are inducing 50 to 100% more rips as well as controlling their location.

50

Figure 3.20 Examples of groyne controlled rips. a. Ridge and runner bar 1 with TBR bar 2 rip exit north and exiting against northern groyne, km 9-8, 14.4.84; b. RR bar 1 with TBR-RBB bar 2 with rips exiting against both groynes km 1-2, 13.5.84; c. LTT bar 1 with TBR bar 2 containing southerly skewed rips existing against groyne/s and in mid-groyne location, km 105-106, 15.4.83. Source: Rijkswaterstaat, Mapping and Survey Division.
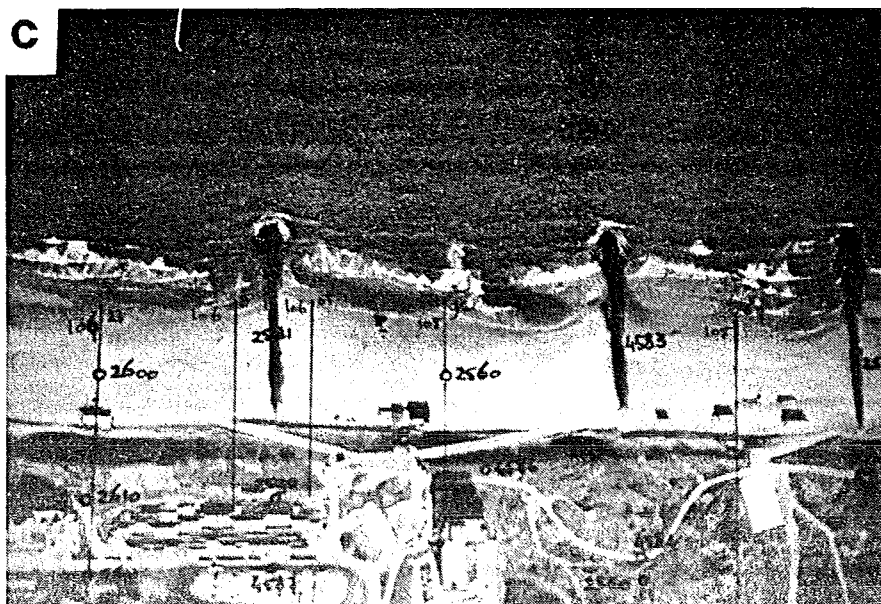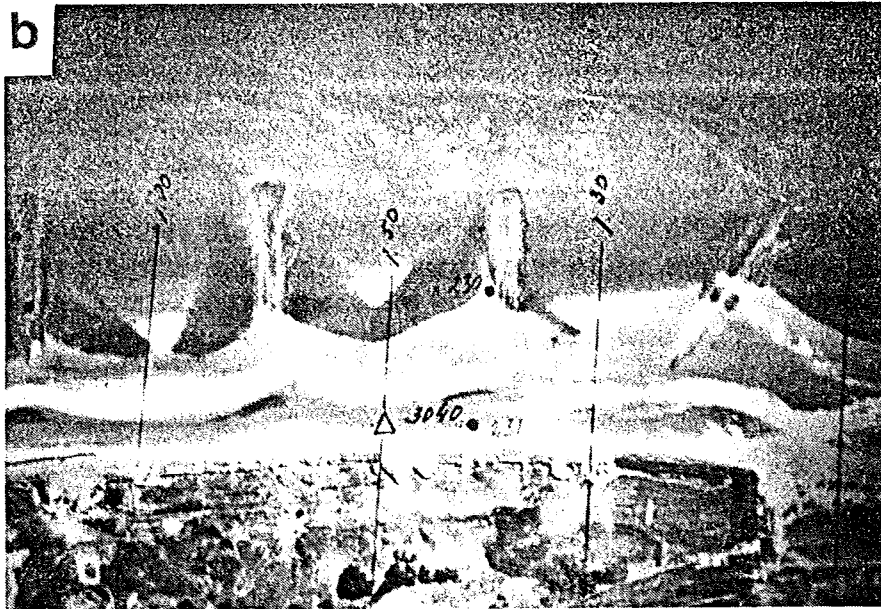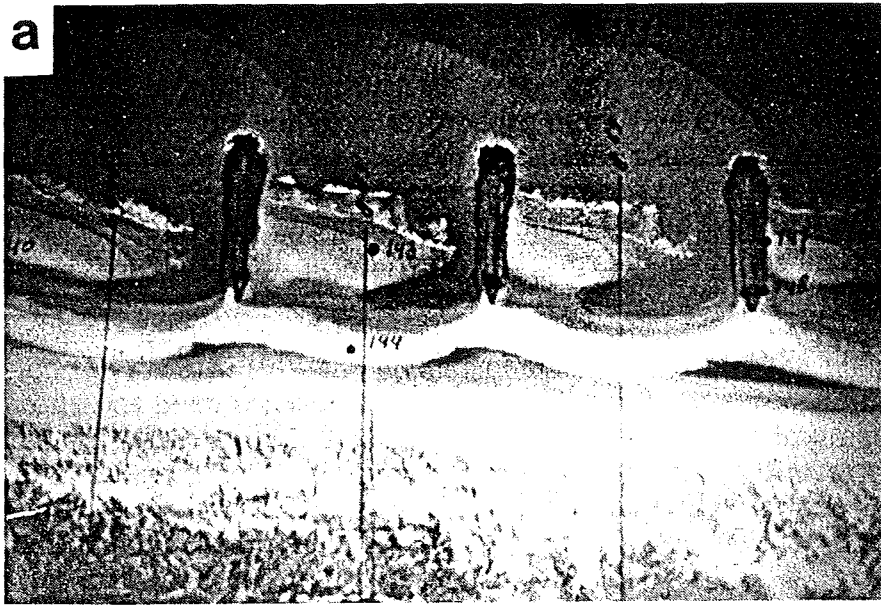
6. the TBR beach state is also more likely to shift into a RBB state, i.e. detached bar, in the presence of a groyne field.
7. the LBT state will however be broken up by the groynes into a lower RBB or TBR state.
8. In summary while groynes will tend to produce more rips and move the lower beaches/bar up and the higher states down as much as one beach state, they do not appear to determine the actual beach type or larger scale processes such as bar attachment and migration. This implies that the groynes are superimposed on the natural beach conditions and the actual conditions will prevail with the groynes serving as an irritant rather than determinant.

Furthermore, on the positive side, the greater number of rips and the higher beach type act as if the surf zone has been translated shoreward. Given the greater sediment mobility in the surf zone compared to the shoreline (Fig. 5.12c) this should result in greater sediment mobility within the groyne field and therefore greater potential sediment transport. If this is the case, the groynes may produce the opposite of their intended effect. One might also ask what criteria was used in determining the groyne spacing (Fig. 5.15) and lengths, none of which are sympathetic with the natural beach rhythms.

5.7   Rips

Rips are part of a three dimensional cellular surf zone circulation pattern consisting of zones of wave breaking and onshore flow, lateral flow along the shore in feeder channels which may converge to form a narrow, concentrated, higher velocity seaward moving rip current. Once the rip current penetrates the bar or surf zone it usually generates a series of pulsating vortices. Rips are an inherent, characteristic feature of the intermediate beach domain (Fig. 2.2; Short, 1987). Given the prevalence of intermediate beach types on the central coast, rips are a common feature along the coast being associated with all three bar systems. The nature, size and frequency of the rips vary considerably however between the bars, and in time and space.

In this section the rip characteristics of bar 1, 2 and 3 will be presented. The results are based on the aerial photographs, two previous publications and field observations during 1989. It should be stressed however, that on the Netherlands coast, the presence of rip channel topography does not necessarily imply occupation by a rip current. The presence of a rip current is dependent more on wave and tide conditions than on the topography. Due to the episodic nature of the wave climate, rip topography active during storms and high waves, often remains inactive or at least overfit during lower waves and calms. During these calmer periods low frequency tide and wind currents can be observed to move over and through the rip topography with no rip circulation. This section therefore reports on rip topography which may or may not have been occupied by a rip current at the time of the aerial photograph.

The rip data base is presented in Table 5.7 which contains summaries of their location, spacing, length and orientation. Rips were present in all years though in 1982 they were too few and too widely spaced to warrant measurement. Rips were also present when the 1968, 1970 and 1971 airphoto mosaics were taken (Table 5.5).

Table 5.7   Rip spacing and length based on aerial photographs 1982-198. Numbers indicate, mean rip spacing (m), standard deviation in brackets and number of rips (n) for each sector indicated by bars.
GCR = groyne controlled rips. The lower columns indicate dominant rip direction (orientation), the summaries of all rip spacing for the year (Ys) and all bar 1 and bar 2 rips, and where their length is heavily skewed.

BAR 1

	1983	1984	1985	1987	1988
		GCR			GCR
	444 (226) n=54	GCR	666 (349) n=9	450 (450) n=20	432 (231) n=21
				984 (453) n=13	646 (341) n=5
		416 (116) n=6		687 (180) n=3	413 (252) n=21
	558 (307) n=51	376 (213) n=13	341 (168) n=6		683 (323) n=25
		422 (208) n=52			407 (234) n=26
	358 (162) n=30	458 (352) n=6		414 (255) n=9	GCR

BAR 2

	1983	1985	1986	1988
		GCR		
	GCR 421 (269) n=7		GCR	567 (388) n=9
	555 (239) n=9	484 (317) n=47	909 (483) N=21	468 (223) n=39
		516 (420) n=25		
		355 (206) n=56		
	GCR	GCR		

BAR 3

	1985
	800 n=2
	1000 n=2

ORIENTATION	SOUTH	SOUTH	S/N/ NORMAL	SOUTH	NORMAL	ALL BAR 1	SOUTH	NORMAL	NORTH	NORMAL	ALL BAR 2	-
Ys	470 (260) n=135	410 (200) n=71	490 (330) n=21	610 (460) n=45	490 (290) n=98	494 (73) - n=235	550 (250) n=16	430 (310) n=128	909 (483) n=21	490 (260) n=48	595 (215) - n=213	900 (-) - n=4

| LENGTH | 499 (308) n=44 | 401 (167) n=64 | | Bar 1 Drains 523 - n=4 | Bar 1 Rips 502 - n=13 | | | | | | | |

- - - - - indicates limit of aerial photography
R   Rip
D   Drain

5.7.1   Bar 1 rips

Bar 1 is modally RR (53%) with LTT (29%) and TBR (6%). Two rip types were observed with bar 1. The first is the rip or 'drain' which discharges the runnel, the second the transverse rips associated with LTT, usually as a 'mini-rip' and TBR.

Bar 1 'drains'

The RR system which dominates bar 1 is backed by a shore parallel runnel. Waves overtop the berm, particularly at high tide and during higher waves and water collects in the runnel. This water is discharged back to the surf via drains which transect the ridges. An example of these drains is shown in Figure 5.5b and c and Figure 5.20a. As the drains are often only active during high water, remaining dry and inactive at low water and even during neap tides, they are a 'quasi' rip.

53

Well developed drains were observed on the 1987 and 1988 photographs. Their mean spacing ranged from 407 to 683 m with an overall mean of 505 m, which as will be seen, is the same magnitude as the TBR rips. Within the groyne fields the drains usually locate adjacent to one or both groynes thereby reducing drain spacing (see eg. Fig. 5.18).

The drains may result from two modes of formation. In an accretionary beach phase they may simply represent infilled transverse rips inherited from antecedent beach conditions, the 'mini rips' of the beach model (Fig. 2.2) except partially fronted by the ridge. Secondly, if rips were not previously present the drains may represent a series of runnel breakouts or breaches through the ridge. Whatever their origin the drains, once formed, would exert a positive topographic feedback on the runnel circulation to remain relatively fixed in location. Sequential field observations of drain formation are required to assess the exact mode and mechanism of formation.

5.7.2 Bar 1 transverse rips

Transverse rips consist of a relatively deep rip channel, usually fed by one or two longshore rip feeder channels, separated from adjoining rips by a transverse bar. The bar and ridges may be shore normal or skewed longshore depending on formative wave approach (Fig. 5.20). Transverse rips were most commonly observed on bar 1 usually as mini or small rips in the LTT and also with the TBR system. Their mean spacing ranged from 341-984 m with an overall mean of 502 m, based on bar 1 rips other than drains (Table 5.7). Within the groyne fields the beach type usually shifted to a partially higher type (LTT to TBR, TBR to RBB), and rips were located adjacent to one or both groynes, thereby decreasing rip spacing to the order of 200-300 m (see section 5.6.3, and Figs. 5.18 and 5.19).

The rips were observed to be heavily skewed to the south in 1983, 1984, and 1987, to the north in 1986 and more shore normal in 1985 and particularly 1988. A time series of rip observations is required to accurately assess rip orientation. In the absence of these data the wave rose (Fig. 4.2) would suggest rips should be to the north about 30%, shore normal about 30% and to the south about 40%. Also one would expect wind driven currents and tidal currents to contribute to rip orientation and rip circulation.

The length of the heavily skewed 1983 and 1984 rips were measured from the start of the rip feeder channel/point of transverse bar attachment to the rip neck. This averaged 500 and 400 m respectively, the same magnitude as the rip spacing. During high waves and high tide it is likely that a meandering type surf zone circulation operates (eg. Sonu, 1972).

5.7.3 Bar 2 rips

Bar 2 varies from RR (22%) to LBT (5%) and is modally RBB (40%) and TBR (32%). All these systems possess rips resulting in rip topography being a dominant feature of this system. However, like bar 1 rip currents will only occupy the topography during higher wave conditions.

The aerial photographs reveal bar 2 rips in 1983, 1985, 1986 and 1988 (Table 5.6) and in the 1968, 1970 and 1971 airphoto mosaics (Table 5.5). Their absence in some years and along sections of the coast is more a function of limitations in the sampling technique (see

section 2.3) than their absence alongshore. The air photo samples indicate that the rip spacing ranged from 355 to 909 m with an overall mean of 595 m, about 100 m longer than the bar 1 rips (Table 5.7). Like the bar 1 rips their orientation depends on formative wave approach. Examples of a bar 2 TBR and RBB rips are shown in Figures 5.21 and 5.22.
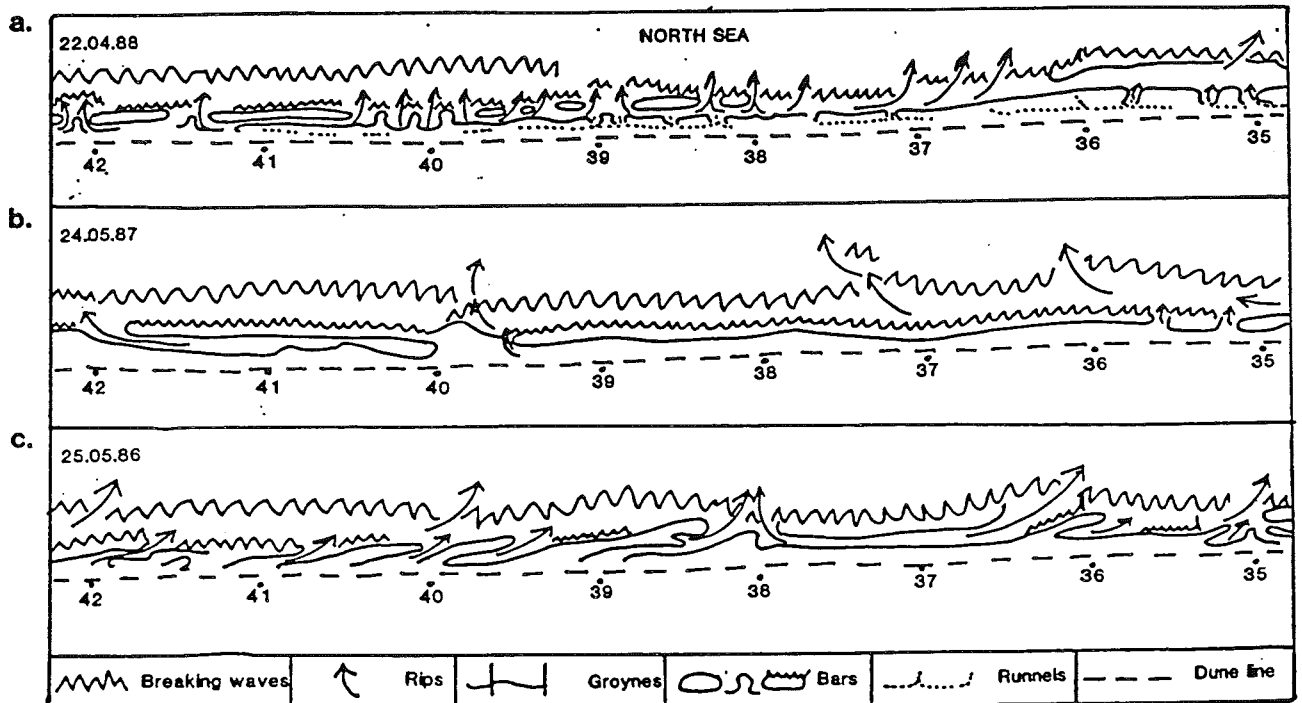
Figure 5.22 Morphological sketch of the coast near Egmond aan Zee based on aerial photographs (dates indicated). In each year rips dominate. 1988 has both small drains and TBR; 1987 has heavily skewed southerly TBR (bar 1) and RBB rips bar 2; while 1986 had rips skewed north with bar 1 TBR and RBB/LBT bar 2.

The bar 2 rips were also intersected by the groyne fields resulting in a similar impact to bar rips. The TBR rips tended to RBB (i.e. bars detached from beach) with rip spacing reducing to groyne spacing (e.g. Fig. 5.19). Under high waves it appears that the topographic controls exerted on these systems resulted in the one or two rips per groyne cell excavating most of the bar 2 from the groyne cell. In other words the groynes enhanced offshore translocation of bar 2 to outside the groynes. The 1971 air photo mosaic however, showed a LBT being lowered to a TBR in the groyne field, the reverse situation. Clearly antecedent wave and beach/bar conditions must also be considered in determining the groyne impact. Whatever the case however more rips result.

5.7.4 Bar 3 rips

Bar 3 is dominated by RBB (44%) and LBT (56%) both characterized by large rip systems. These rips being less topographically controlled are only active during high wave events. This fact combined with the sampling limitations discussed in section 2.3. resulted in the spacing o only four bar 3 rips being recorded (Table 5.7). They give a mean spacing of 900 m almost

twice that of bar 1. This is to be expected particularly if one assumes the rip spacing is determined by edge wave spacing. This aspect will be examined in Section 7.2.
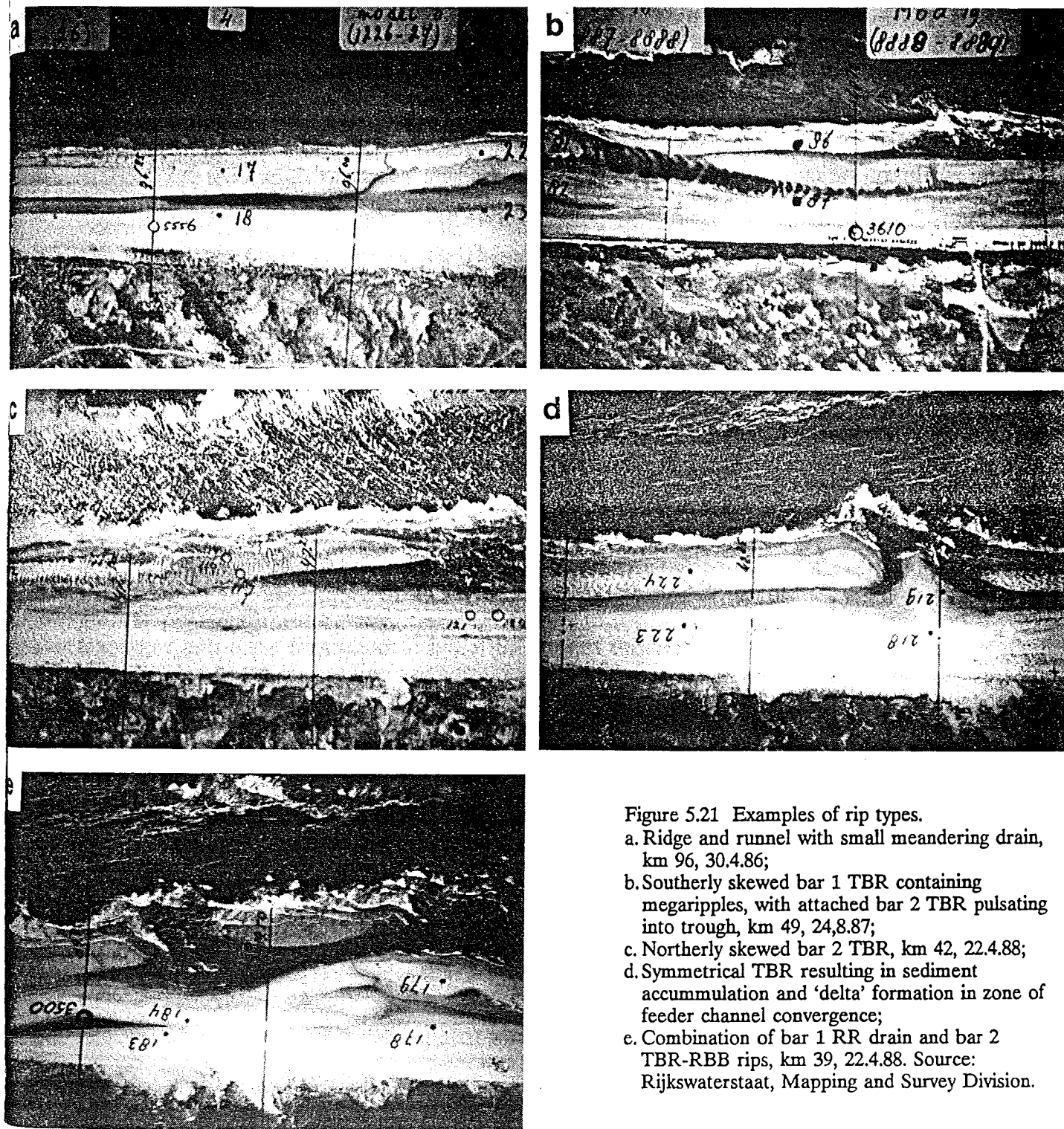
Figure 5.21 Examples of rip types.
a. Ridge and runnel with small meandering drain, km 96, 30.4.86;
b. Southerly skewed bar 1 TBR containing megaripples, with attached bar 2 TBR pulsating into trough, km 49, 24,8.87;
c. Northerly skewed bar 2 TBR, km 42, 22.4.88;
d. Symmetrical TBR resulting in sediment accummulation and 'delta' formation in zone of feeder channel convergence;
e. Combination of bar 1 RR drain and bar 2 TBR-RBB rips, km 39, 22.4.88. Source: Rijkswaterstaat, Mapping and Survey Division.

6. SHOREFACE GRADIENTS

The shoreface includes the beach, surf zone and nearshore seaward to boundary with the inner shelf. Along the central coast its position and characteristics have been mapped by van Alphen and Damoiseaux (1989). They call this zone the coastal slope and note that its boundary with the shelf occurs at around 20 m depth. It consists of a narrow inner slope with a gradient of < 1:100 and a wider lower gradient (1:100 to 1:1000) outer slope. The width of the entire zone decreases from about 10 km in the north and south to 2.5 km in the central region (km 40-85) (Figure 2.1).

Wiersma and van Alphen (1988) suggest there is a correlation between the gradients of the shoreface and the shoreline evolution. The two regions of low outer gradients (north of Bergen km 0-35, and south of Katwijk km 88-120), possess steeper inshore gradients and are experiencing shoreline erosion, while the overall steeper central section is stable to accretionary. They also infer that the "Younger Dunes" of the central section are derived from the sediments of the coastal slopes. These dunes are less developed along the wider lower gradient areas north of Bergen and south of Scheveningen (km 103-120). A possible scenario proposed by Wiersma and van Alphen is that shoreline and shoreface regression in the central section resulted in a steepening of the gradient and consequently higher breaker wave energy. As the regression slowed or stabilized either the higher waves and/or other climatic processes "triggered" shoreline erosion, dune destabilisation and transfer of sediment from the coastal slope to the "Younger Dunes". At the same time the northern and southern sections were 'protected' from the higher waves by the lower shoreface gradients induced by the Den Helder tidal delta and between Katwijk and Hoek van Holland.

Such a model of wave, beach, dune interaction is in general, but not in detail, agreement with the wave-beach-dune model proposed for southern Australia by Short (1987, 1988). In general, he found in southern Australia that higher waves produce more dissipative beaches which inherently have more unstable (wave eroded) backshore and dunes, which coupled with greater potential onshore sand transport (wind) results in more massive aeolian sand transport and dune formation. It is not the aim of this report to persue this question. Rather the present shoreface gradients are important because of their impact on breaker heights and their potential interaction with low frequency standing waves which may inturn influence bar spacing and overall beach morphology (see e.g. Short 1975, Aagaard 1988c).

Table 6.1 Summary of inner slope (surf zone) morphometric characteristics, based on beach profiles

	n	mean	SD	Max	Min
$\tan \beta$	116	0.013	0.004	0.040	0.005
No. bars	118	2.6	0.7	4	0
Net shore width	117	42.7 m	29.2	240	0
Net shore amp.	112	1.4 m	0.5	3	0.5
Area sweep zone	114	1420 m^2	576	3 200	220
Width sweep zone	117	692 m	164	850	190
Area bar 1	110	83 m^2	49	300	5
Amp. bar 2	114	2.0 m	0.6	4	1
Bar 1 migration	110	59 m	23	150	10
Bar 2 migration	112	113 m	45	200	10
Bar 3 migration	82	175 m	64	300	20

Original Source: Rijkswaterstaat, Tidal Waters Division

The gradient of the inshore (to 8 m depth) and overall or outer (15 m depth) coastal slope was obtained from two sources. The inner slope, including the beach and bar systems was obtained from the 118 sets of beach profiles. The results are plotted in Figure 6.1 and summarized in Table 6.1. The overall gradient from the shoreline to the break in slope (mean depth 15 m, sd = 3 m) was obtained from plots of the nearshore profiles spaced at 5 km intervals from km 15-120. The resulting distance to and depth of the break in slope, together with the gradient, are shown in Figure 6.2 and summarized in Table 6.2.
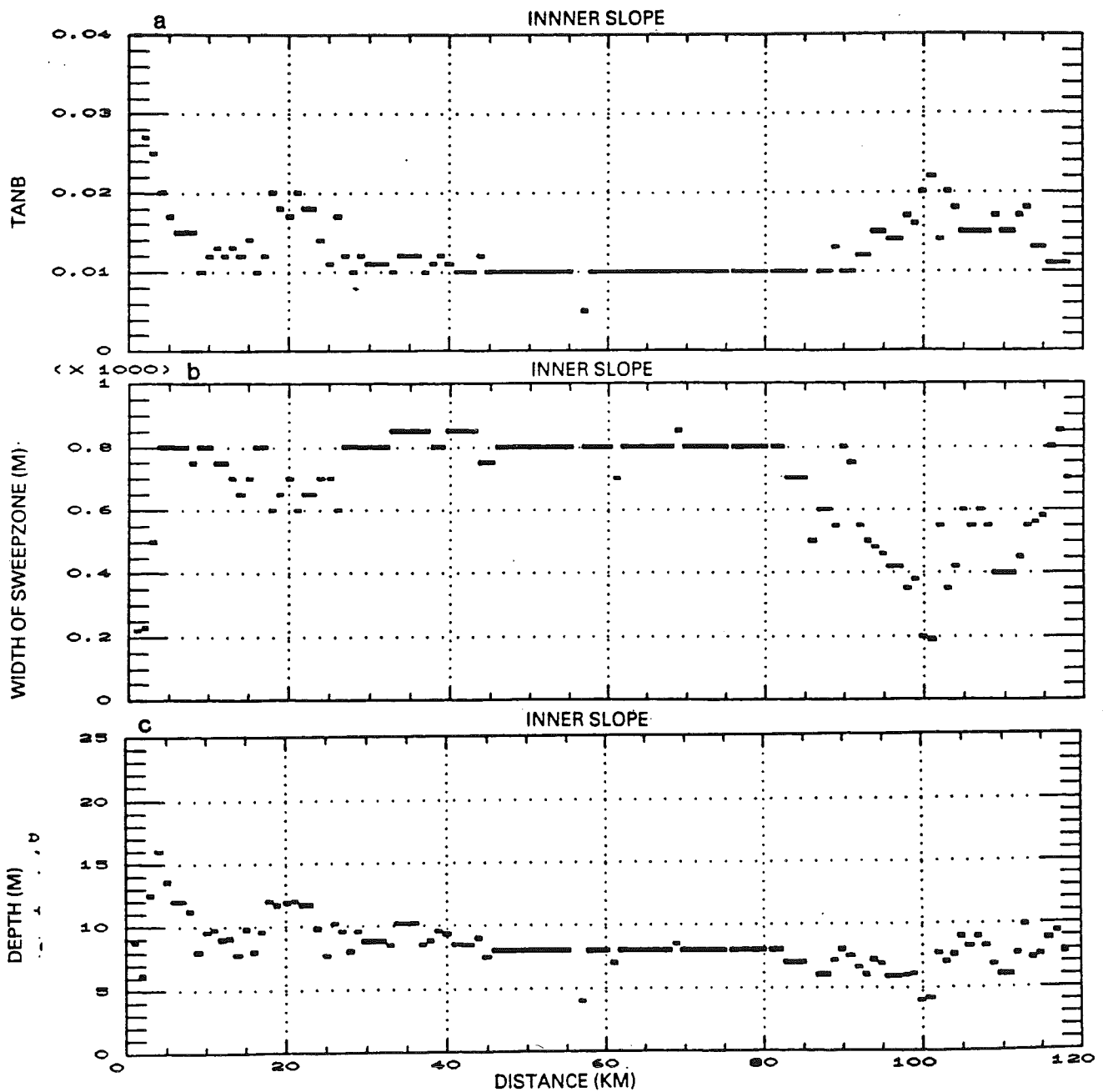
Figure 6.1   Longshore variation in inner slope (surf zone) gradients,
a. slope (tan B);
b. width of active sweep zone; and
c. depth of outer edge of active sweep zone. Based on Rijkswaterstaat beach profile survey 1976-1985.

Table 6.2   Summary of outer (overall shoreface) slope gradient (tan β), width (Xs)
and outer depth

	n	mean	SD	Max	Min
tan β	68	0.0046	0.0013	0.0084	0.003
Xs (m)	68	3569	1178	6850	1100
depth Xs (m)	68	15.3	2.9	20.5	8.0

Original source: 1:10,000 sounding charts, Rijkswaterstaat
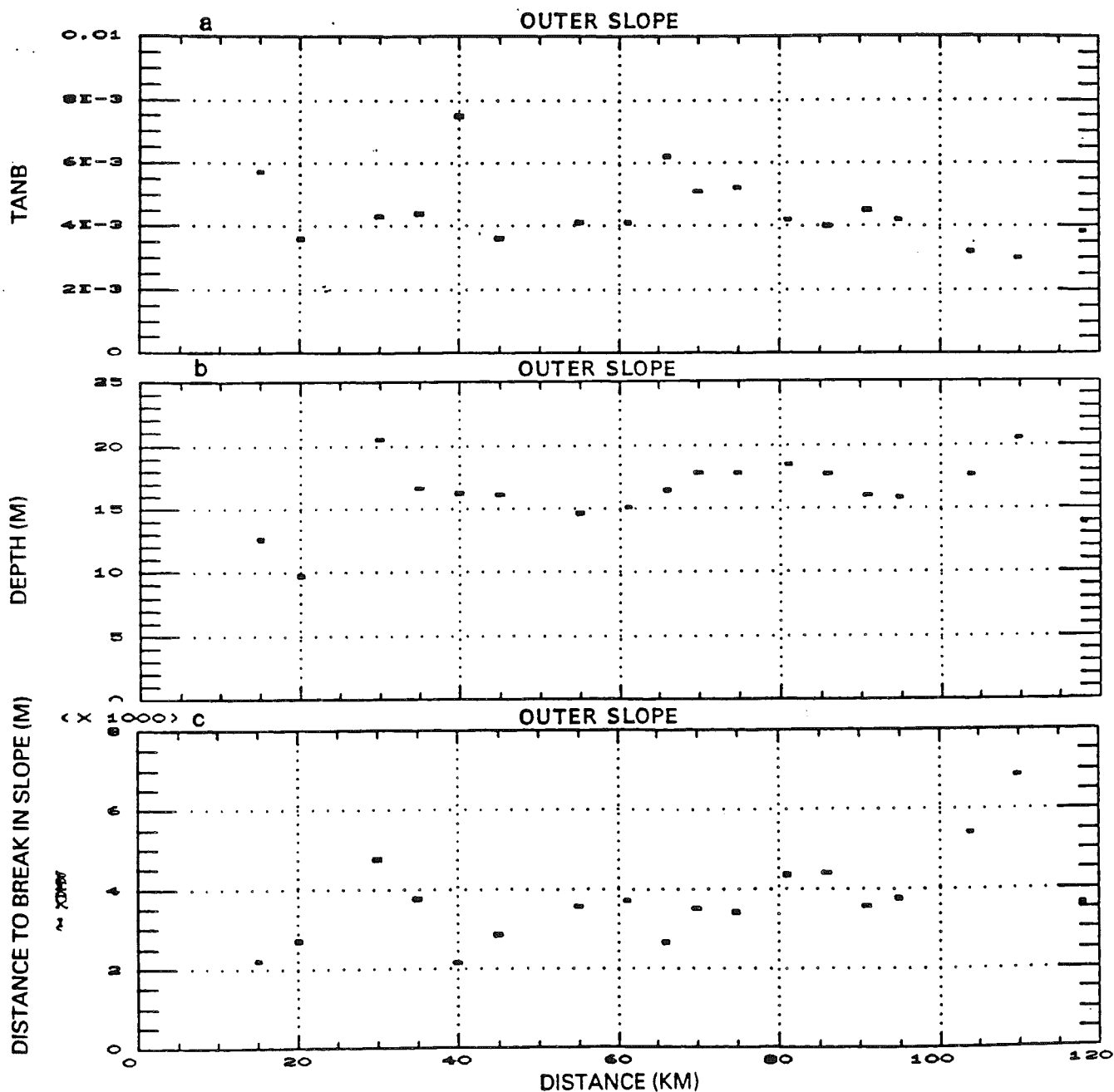
Figure 6.2   Longshore variation in outer slope (overall shoreface) gradients,
a. slope of entire shoreface based on nearshore profiles;
b. depth of outer break in slope; and
c. distance to outer break in slope. Based on Rijkswaterstaat nearshore surveys.

The inshore results correspond to the findings of Wiersma and van Alphen (1988) that the slope is lower (0.01) between km 40 and 90, and increases (0.015) both towards Den Helder (km 0-40) and Hoek van Holland (km 90-118). As previously seen these are also the areas of fewer bars (bars 1 and 2 only) and more stable bar systems (de Vroeg, 1987, see Fig. 5.2).

On the outer slope the more widely spaced samples provide a less distinct trend. They do in general agree with van Alphen and Damoiseaux (1989) with the gradient decreasing south of km 75. The samples are insufficient north of km 40 to detect a trend. However, van Alphen and Damoiseaux (1989) clearly show the impact of the Den Helder ebb tide delta which decreases the overall gradient. This impact is mirrored in a noticable decrease in breaker wave height between km 0-5.

In summary, as Wiersma and van Alphen (1988) have suggested, the regional trends in the inner and outer shoreface gradients may be a product of late Holocene shoreline evolution. Whatever the cause the existing gradients are expected to play a role in contemporary beach-bar morphodynamics. In order to conclusively assess the impact on the present beach system the interaction between incident and low frequency (infragravity) waves across the surf zone and shoreface needs to be monitored to assess the dominance of selected infragravity frequencies. Assuming infragravity standing and/or edge waves are present (e.g. Gerritsen and van Heteren, 1984) their interaction with the shoreface gradient is expected to determine cut off modes and thereby the selection of resonant frequencies, that may in turn control shore parallel bar spacing (standing waves) and shore normal rip spacing (edge waves). Within a general framework of average values listed in Tables 6.1, 6.3 and 6.4, their relationships will be explored in section 7.

Table 6.3 Inner slope (surf zone), width (m), outer depth (m) and slope characteristics used in section 7

Variable	Widsweep	depth	tan β
Sample size	117	116	116
Average	691.966	8.39879	0.0128621
Median	800	8	0.011
Mode	800	8	0.01
Standard deviation	164.171	1.83478	4.41715E-3
Minimum	190	4	5E-3
Maximum	850	16	0.04
Range	660	12	0.035

Table 6.4 Outer slope (shoreface), width (m), outer depth (m) and slope characteristics used in section 7

Variable	Slopebreak	depth	tan β
Sample size	18	18	18
Average	3727.78	16.2889	4.45E-3
Median	3575	16.3	4.2E-3
Mode	3750	20.5	3.6E-3
Standard deviation	1149.96	1.61396	1.11104E-3
Minimum	2150	9.7	3E-3
Maximum	6850	20.5	7.5E-3
Range	4700	10.8	4.5E-3

7. BEACH MORPHODYNAMICS

Beach morphodynamics is concerned with beach and nearshore morphology and sediments interacting with coastal processes to produce beach systems and change. The proceeding sections have described the morphology of the central Netherlands beach systems (section 5), the nearshore gradients (section 6) and beach sediments (section 3) together with waves and other processes (section 4). In this section the contribution of waves, sediments and nearshore gradients to beach morphology and morphodynamics will be assessed using two distinct approaches. The first will apply standing and edge wave theory to explain bar and rip location and spacing; while the second will test the applicability of the parameter (dimensionless fall velocity) for predicting beach type and change. It should be noted at the outset that the presently available data are insufficient to enable conclusive results. However, both approaches are persued in the belief that in identifying how much they can explain together with the gaps in our data and knowledge recommendations can be made as to how to achieve a more robust understanding of these systems.

7.1 Infragravity waves and bars

Infragravity waves are defined as waves with a period between 30-300 sec. In the surf zone they may be derived from an external source such as wave groupiness or generated internally through red shifting during wave breaking of incident wave energy to lower frequency motions, often manifest at the shoreline by surf beat and wave set up and set down. Standing waves are produced in the surf zone when incoming incident and infragravity waves interact with totally or partially reflected waves of a similar period. The standing waves may be two-dimensional, called leaky modes, or they may regularly undulate alongshore and are called edge waves. Edge waves are the trapped modes of longshore wave motions that can occur in the surf zone and may be progressive, that is, move alongshore, or be standing, that is, stationary (Guza and Inman, 1975). In the following discussion it is assumed that standing waves whose wave length is measured perpendicular to shore are responsible for the formation and spacing of shore parallel bars (see Short, 1975), while edge waves whose wave length is measured parallel to shore are responsible for rip spacing and rhythmic transverse bar spacing (see Bowen and Inman, 1969).

Irrespective of their mode of generation the frequency and period of infragravity standing and edge waves at a shoreline will be a function of the period of the formative mechanism and the gradient of the surf zone-nearshore over which they operate. Huntley (1976) first showed that depending on the gradient certain infragravity wave frequencies will be selected or enhanced and thereby dominate the energy spectrum. This mechanism is called the "cut off" mode or frequency, implying longer frequencies will be cut off or not enhanced. Therefore if one knows the prevailing range of infragravity wave frequencies, the slope and theoretical cut off frequencies, then one can predict the likely prevailing or dominant frequency and thereby the scale of the standing and/or edge waves. It is then the scale or length of these waves which is assumed to generate and therefore correlate with bar and rip spacing. It is on the above premises that the following analysis is based.

The theoretical relationship between infragravity standing and edge waves and bar formation is well documentated and will not be reviewed here. Carter (1988) provides a recent overview. The application of this theory to explain actual bar formation has also been utilized by a number of researchers. These are reviewed in a recent study of bars on the Danish and Australian coast by Aagaard (1989).

In order to conclusively test the relationship between infragravity waves and bar formation simultaneous data is required on both, in particular the full wave spectra within, and preferably across the surf zone, together with accurate survey data on bar and slope morphology. Such wave data is not available for this study. However as a surrogate for such data the measured bar and rip spacings and nearshore gradients can be used to calculate the theoretical range of wave frequencies required to produce such spacings. The nearshore gradient can also be used to calculate cut off frequencies and thereby suggest which wave frequencies are most likely to exist within the surf zone. Finally, these results can be compared with predicted long wave (wave groupiness) for the coast together with limited published field results of long wave measurements.

The occurrence of infragravity waves (T > 30 sec) has been documented on the central Netherlands coast by Gerritsen and van Heteren (1984). In a series of winter experiments (December 1982) they recorded surf beat with periods between 41-83 sec (T_o = 6.95-7.5 sec) on 10.12.82, and up to 91 sec (T_o = 9 sec) on 21 and 27.12.82. They found that the infragravity peak frequency was on average eight times the incident wave frequency with a recorded range of 6.2 to 9.9. On the central coast where the modal period is 5 sec, but which can increase to 9 sec during storms this should generate infragravity waves between 40 and 70 seconds, though Gerritsen and van Heteren (1984) concluded even longer periods occur.

Infragravity waves can be generated by several mechanisms, one of which is wave groupiness. For a given wave period and wave amplitude wave group frequency can be predicted using the equation

$$T_g = gT^3/4\pi^2 a = (g/2\pi^2)(T^3/H) \qquad\qquad 7.1$$

where a = ½H, and T is incident wave period.

Table 7.1 lists the T_g for representative combinations of wave height and period for the central coast. For periods of 7 and 8 sec and to a lesser extent 9 sec the T_g is within the range recorded by Gerritsen and van Heteren (1984).

Table 7.1 Predicted wave group periods using equation 7.1

	T (sec)			
	6	7	8	9
H_m (m) 3.0	35.8	56.8	84.8	120.8
3.5	30.7	48.7	72.7	103.5
4.0	26.8	42.6	63.6	90.6

Table 7.2 Characteristics of three slopes used in bar predicitons

Extent (km beach poles)	tan β	Width	No. bars
Outer slope km 0-120	0.004	N.A.	N.A.
Inner slope km 25-85	0.01	700	3
Inner slope km 85-118	0.015	500	2

In order to test the relationship between infragravity waves and bar and rip spacing the coast will be divided into two sectors representing the inner and outer slope. The extent and characteristics of each are given in Table 7.2. They are based on the longshore trends in each illustrated in Figures 6.1 and 6.2. The outer slope is used to check the role of the outer break in slope in contributing to cut off frequencies and standing wave mode selection; while the two inner slopes use the surf zone (ie bar zone) only to calculate cut off frequencies and mode selection. The use of two inner slopes is required to distinguish between the lower gradient three bar system (km 40-90) and the steeper gradient two bar system (km 0-40 and km 90-118). Sample crossections of these bars are illustrated in Figure 7.1a and b. For the two inner slope sectors three representatives beach profiles were chosen to measure bar spacings. The results are given in Table 7.3.
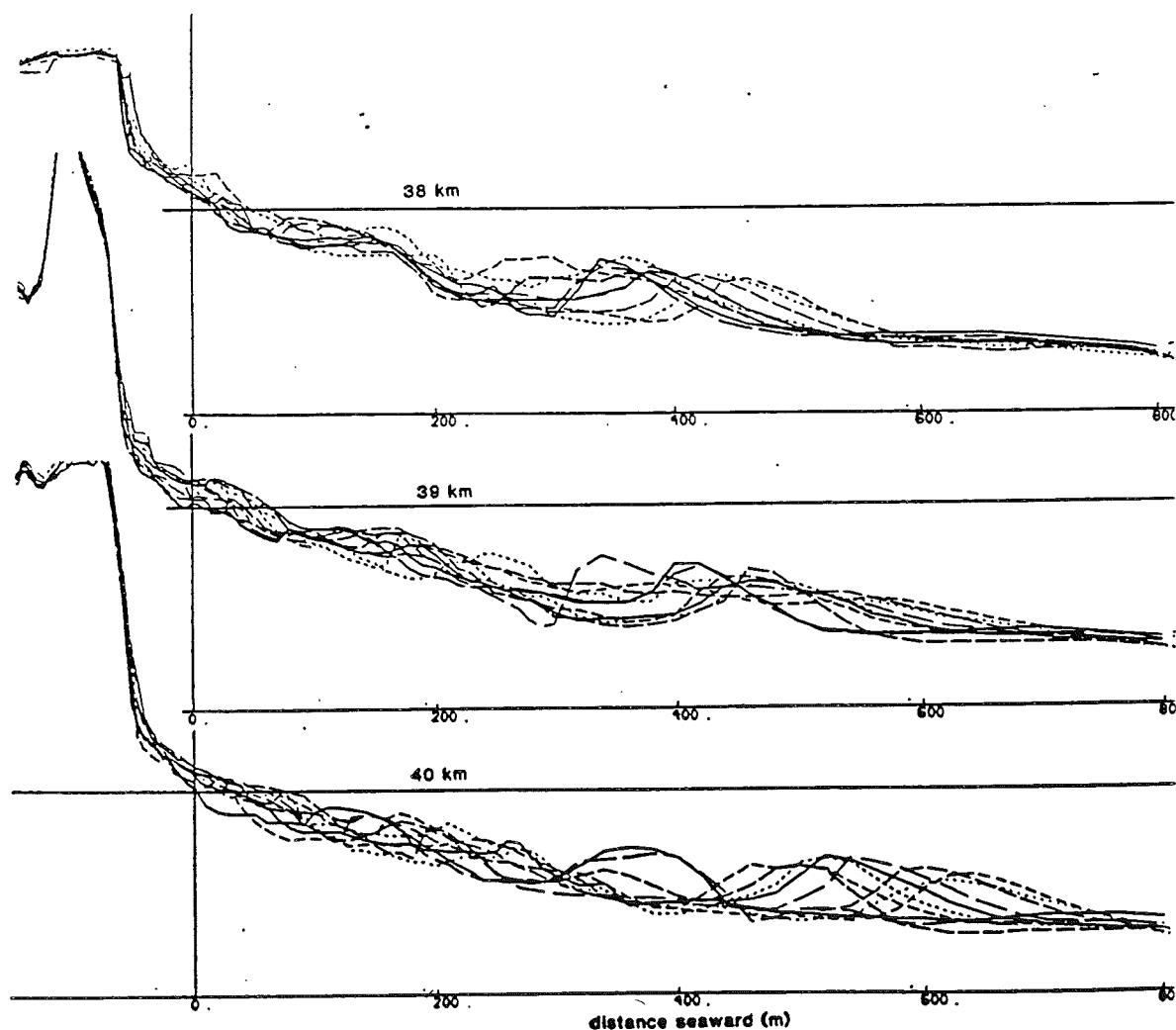
Figure 7.1   Cross-shore beach profiles at
a. northern site showing three bar (km 38, 39 and 40) located immediately south of Egmond aan Zee.

94 km

95 km

96 km

distance seaward (m)
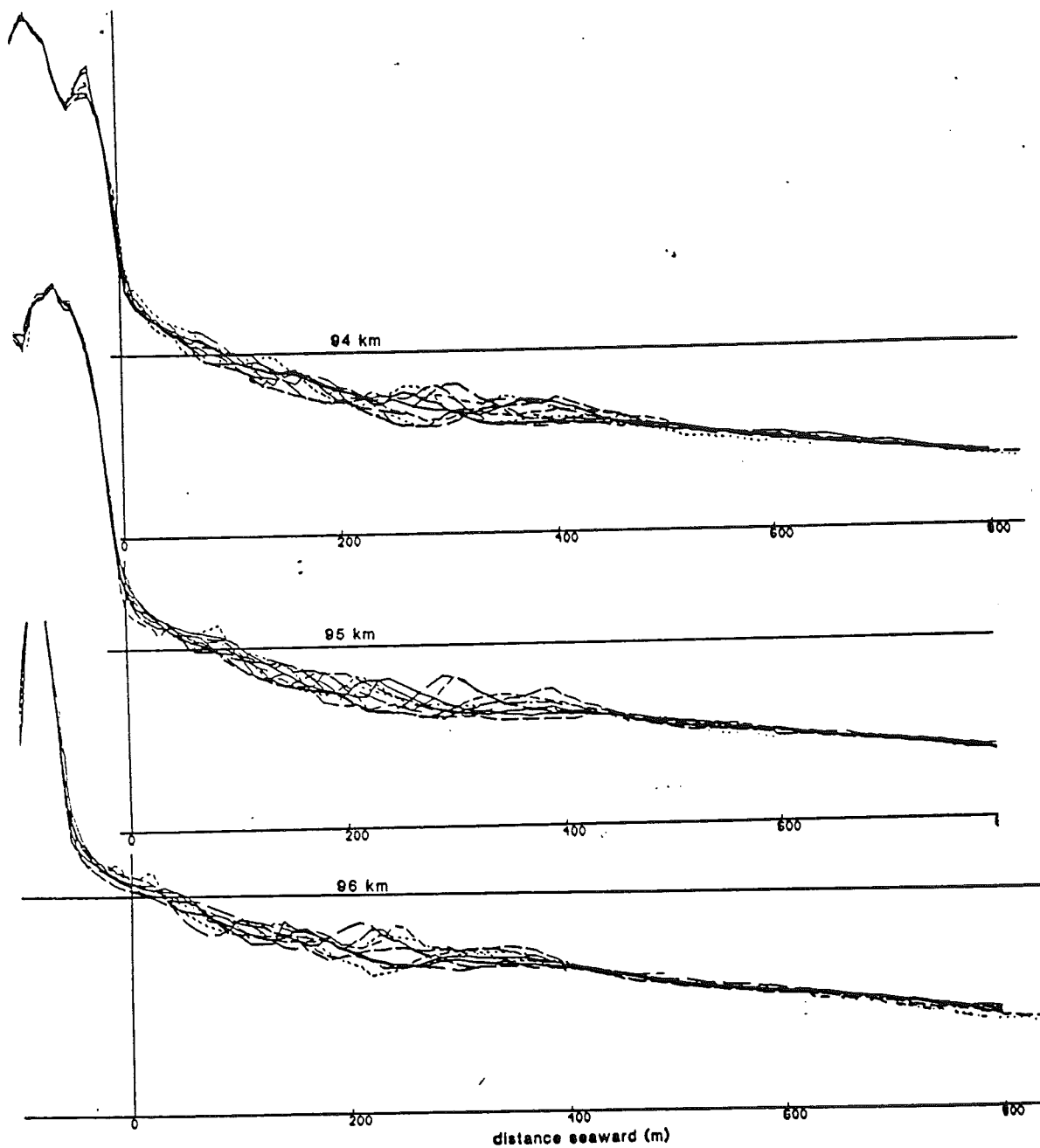
Figure 7.1   Cross-shore beach profiles at
b. southern site showing two bars (km 94, 95 and 96) located north of Scheveningen (The Hague).
These sites were used to test relationships between infragravity waves and bar location. Source:
Rijkswaterstaat beach surveys 1976-1985.

Table 7.3 Observed bar spacing

Location (beachpole, km)	Distance to shoreline (m)		
	Bar 1	Bar 2	Bar 3
38.00 (Egmond aan Zee)	50	180	400
39.00	80	230	500
40.00	100	260	570
Mean	77	223	490
94.00	100	280	
95.00	90	260	
96.00	75	230	
(100.00 Scheveningen)			
Mean	88	257	

The T_g periods (Table 7.1) were then used to predict theoretical bar spacing using the equation

$$X_n = (g \tan \beta / 4\omega^2)\, Z_n^{(r)}; \qquad r = 1,2 \qquad\qquad 7.2$$

where X_n is distance to the bar $(1,2, \ldots n)$, $\tan \beta$ the nearshore gradient, $Z_n^{(r)}$ is obtained from Table 7.4, and $\omega = 4\pi^2/T_g^2$.

Table 7.4   Values of ^{2} the non-dimensional offshore distance for which zero-crossings of drift velocity occur. Zero-crossings at antinodes and nodes of the wave form are defined as $Z_n(1)$ and $Z_n(2)$, respectively. From Aagaard, 1988

n	$Z_n(1)$	$Z_n(2)$
1	13.9	26.3
2	49.2	70.2
3	103	135
4	178	219
5	271	322

The results for each slope scenario are given in Table 7.5. When these are compared with the actual spacings in Table 7.3 it is apparent that the inner slopes provide more realistic spacings. A standing wave period (T_s) of between 80-90 sec is required to produce three bar spacings in general agreement with those observed in Table 7.3. This predicted period is in close agreement with the observations of Gerritsen and van Heteren (1984), and also with the predicted T_g in Table 7.1 for a $H_b = 3$ m and $T = 8$ sec. This range of breakers is again in agreement with the conditions observed by Gerritsen and van Heteren (1984) when recording the 80-90 sec T_s.

Next the theoretical T_s required to generate standing waves capable of producing spacings is given in Table 7.6 for three slope scenarios. Finally for each slope scenarios the cut off frequency X_s was calculated using the equation

$$X_s = \omega\, e^2\, X_s/g \tan \beta \qquad\qquad 7.3$$

The resulting cut off periods for modes 1-3 are also given in Table 7.6.

Table 7.5a Predicted bar spacing, using the outer slope (tan β = 0.004)

T (sec)	n	Antinodes (m) 1	2	3	Nodes (m) 1	2	3
40		6	22	46	12	31	60
50		10	31	72	18	44	94
60		12	44	104	26	71	136
70		17	67	141	36	96	185
80		25	78	184	47	126	242
90		31	111	207	53	159	272

b Predicted bar spacing, using the inner slope (tan β = 0.01)

T (sec)	n	Antinodes (m) 1	2	3	Nodes (m) 1	2	3
40		14	49	102	26	70	134
50		22	76	160	41	109	210
60		31	110	230	59	157	302
70		42	150	314	80	214	411
80		55	196	410	105	279	537
90		70	248	418	132	353	579

c Predicted bar spacing, using the inner slope (tan β = 0.015)

T (sec)	n	Antinodes (m) 1	2	Nodes (m) 1	2
40		21	73	39	105
50		32	115	61	164
60		47	165	88	235
70		63	225	120	321
80		83	293	157	419
90		105	371	199	530

These figures again favour the inner slopes for both providing realistic T_s and cut off modes with a mode 2 or 3 standing wave giving the closest correlation with the observed (Gerritsen and van Heteren, 1984) and predicted T_g (Table 7.1) and T_s (Table 7.5). These are indicated by the asterisks in Table 7.6a and b.

In comparing the results of Tables 7.1, 7.3, 7.4, and 7.5 together with the results of Gerritsen and van Heteren (1984) the following can be concluded.

1. Low frequency (40-90 sec?) infragravity waves occur on the central coast during periods of high (> 3 m) long (5-9 sec) waves. The waves may be generated by wave groups (Table 7.1) and other mechanisms (Gerritsen and van Heteren, 1984).

2. The calculations of T_g (Table 7.1) suggest that waves with H_b > 3 m and T_o > 7 sec are required to generate T_g in the range observed by Gerritsen and van Heteren (1984).

Table 7.6a Predicted infragravity periods, using the outer slope (tan β = 0.004) and observed bar spacings

Location (beachpole km)	Antinodes (m)			Nodes (m)		
	1	2	3	1	2	3
38.00	113	114	118	82	96	103
39.00	114	129	132	104	108	115
40.00	160	137	141	117	115	123
Cutoff periods	690	398	232	690	398	282

b Predicted infragravity periods, using the inner slope (tan β = 0.01) and observed three bar spacings

Location (beachpole km)	Antinodes (m)			Nodes (m)		
	1	2	3	1	2	3
38.00	76	77	79*	55	64	69
39.00	96	87	88*	70	73	77
40.00	108	92	94	78	77	82*
Cutoff periods	201	116	82	201	116	82

c Predicted infragravity periods, using the inner slope (tan β = 0.015) and observed two bar spacings

Location (beachpole km)	Antinodes (m)		Nodes (m)	
	1	2	1	2
94.00	88	78*	64	65
95.00	83	75	61	63
96.00	76	71	55	59
Cutoff periods	138	80	138	80

* possible selected frequencies based on cut-off frequencies

3. Calculations of T_s (Table 7.5) required to explain the bar spacing at Egmond (Table 7.4) indicates that the inshore scenario provides the more reasonable results with predicted T_s in the mean range of 63-98 sec.

4. This is further supported by the theoretical bar spacings produced by standing waves with T_s similar to those predicted (Table 7.3), where again the inshore scenario produces bar spacings in general agreement with those at Egmond. These spacings are generated by T_s of 70-90 sec again in agreement with the observed (Gerritsen and van Heteren) and predicted (Table 7.5) periods.

5. The calculated cut off mode or frequency for the three scenarios (Table 7.5) again favours the inshore scenarios (Table 7.5b), and particularly a mode 3 standing wave ($T_s \sim 80$ sec) for the three bars and mode 2 for the two bar regions.

6. Finally, an explanation of the decrease from three to two bars south of 85 km can be inferred from these results. The steeper slope lowers the cut off to a mode 2 standing wave (Table 7.6c) which permits only two bar formation compared to the mode 3 and three bars north of 85 km. Therefore the slope is self regulating in both the number and spacing of the bars that a particular T_s can generate.

67

It is therefore proposed that the two and three bar systems along the central Netherlands coast may be controlled and maintained by high wave events (H_b > 3 m, T > 7 sec) which generate standing waves of periods of 60-90 sec resulting in the selection of a mode 3 or 2 standing wave based on the inshore slope and resulting cut off frequency, which in turn produces two or three bars located at approximately 70-100 m, 210-280 m and 400-550 m distance offshore.

None of these results however shed any light on the reasons for the northerly bar migration and major bar attachments. The scale and period of these phenomena require an investigation of processes with a lower frequency then storm generated standing waves.

7.2 Edge waves and rips

Edge waves are secondary waves oscillating at right angles to the shore. They can exist at frequencies from subharmonic to infragravity. At subharmonic frequencies (i.e. T_e = 2T) they have been associated with the formation of beach cusps (e.g. Wright et al., 1976; Carter 1988). At infragravity frequencies Bowen and Inman (1969, 1971) first suggested their association with the spacing of crescentic bars and rip currents.

For a given nearshore gradient and rip or crescentic bar spacing the theoretical edge wave period (T_e) required to produce such a spacing can be calculated using the equation:

$$T_e = (4\pi Y_s / g \sin (2n + 1)\beta)^{\frac{1}{2}} \qquad\qquad 7.4$$

where Y_s is the rip spacing, n the mode number (0,1,2, ... n) and the slope in degrees. The predicted wave periods and cut off frequencies required for a range of rip spacings commonly found along the northern and southern sectors of the central Netherlands coast (350-900 m, Table 5.7) are given for the two inner and outer slope scenarios in Table 7.7. The table indicates the T_e required at each mode (0 to 5) to produce edge wave lengths (L_e) comparable to the observed rip spacings Y_s, where Y_s = L_e/2. At the base of the table are the cut off frequencies with possible selected frequencies indicated by an asterisk. Again results support using the inner slope in these calculations. They also suggest that the more closely spaced rips (Y_s = 500-600 m) may be produced by mode 2 or 3 edge waves with periods in order of 80 sec, similar to the standing waves. The larger bar 3 rips (Y_s ~ 900 m), however, either require a lower mode edge wave (n=0) for formation as proposed by Gerritsen and van Heteren (1984), or perhaps as Aagaard (1988) suggests a steeper inner surf zone slope should be used to calculate the theoretical T_e, which would in this case decrease the long wave periods, hence increase the mode required. The resolution and testing of these suggestions will require field investigations.

The slight but unconfirmed tendency for shorter rip spacing in the southern sector (Table 5.7) can be explained by the steeper slope generating both shorter edge wave lengths and lower cut off frequencies.

In summary like the standing waves the spacing of rips along the coast can be roughly correlated with the theoretical and observed edge wave periods based on an inner slope scenario. The correlation could perhaps be improved by using a steeper gradient surf zone slope only, say to 500 or 600 m distance.

Table 7.7a   Predicted infragravity wave period (T_a) using the outer slope (tan β = 0.004)

Rip spacing (λ) n =	0	1	2	3	4	5
350 m	314	181	141	119	105	95
400	336	194	150	127	112	101
500	375	217	168	142	125	113
600	411	328	184	156	137	124
700	432	257	199	168	148	134
800	475	274	213	180	158	143
900	504	291	225	191	168	152
Cutoff periods	0	690	398	282	218	178

b   Calculated infragravity wave periods (T_a) using the inner slope (tan β = 0.01)

Rip spacing (λ) n =	0	1	2	3	4	5
350 m	207	119	93	78*	69	62
400	221	187	99	84*	74	67
500	247	143	111*	93	81	75
600	270	156	121*	102	90	82
700	293	169	131	111	98	88
800	312	180	140	118	104	94
900	330	192	148	125	111	100
Cutoff periods	0	201	116	82	63	52

c   Calculated infragravity wave periods (T_e) using the inner slope (tan β = 0.015

Rip spacing (λ) n =	0	1	2	3	4	5
350 m	169	98	76*	64	56	51
400	181	104	81*	68	60	55
450	192	111	86	72	64	58
Cutoff periods	0	138	80	57	44	36

* possible selected frequencies based on cut-off frequencies

7.3   Non Dimensional Parameters

A number of non dimensional parameters have been proposed for defining the directions of shoreline change (erosion and accretion) and beach morphology. Three well known parameters are the dimensionless fall velocity (Ω) (Gourlay, 1968)

$$\Omega = H_b / _{ws}T \qquad\qquad 7.5$$

the Iribarren number (ϵ_b) (Battjes, 1974)

$$\epsilon_b = \tan \beta (H_b/L_o) \qquad\qquad 7.6$$

and the surf scaling parameter (e) (Guza and Inman, 1975)

$$\epsilon = a^2/g \tan \beta^2 \qquad\qquad .7.7$$

In order to test their applicability to the central Netherlands coast the range of each parameter in relation to beach type and to the central coast wave, slope and sediment characteristics is presented in Table 7.8. Of the three only the predicts anything less than dissipative conditions on the coast. The ϵ_b and ϵ are too insensitive to low waves on the low gradient central coast tan ß (= 0.01). As a result the following discussion will focus on applying the Ω to assess beach types on the coast.

Table 7.8 Reflective intermediate and dissipative domains predicted by Ω, ϵ_b and e

Parameter	Reflective	Intermediate	Dissipative	Modal
Ω	< 1	1-6	> 6	0.6
% predicted	5	33%	62%	
ϵ_b	> 1	1-0.23	< 0.23	0.05
% predicted	0	-1	99%	
ϵ	0.1-2.5	2.5-20	20-200	5232
% predicted	0	-1	99%	

Central Netherlands coast
w_s = 0.027
H_b = 1.3 m
T = 5.1 sec
$\tan \beta$ = 0.01

7.4 Wave regime, Ω and beach state

The wave regime for the central coast can be best characterised using the lower energy MPN station (see section 4.2). The H_{mo} and T_{mo} matrix for this station is presented in Figure 7.2. Overlain on the matrix is the corresponding Ω values for w_s = 0.027 m/sec. This figure shows the deepwater wave conditions that will result in dissipative, intermediate and reflective conditions. The coast is clearly modally dissipative (62%) but with significant periods of intermediate conditions (33%).

It must be understood that these values are based on MPN deepwater values. As the waves move between the 10 km between the 18 m depth at MPN station depth and the 3-5m depth of the bar 3 breaker zone they will be further reduced in height.

Furthermore these figures predict only conditions on the outer bar. As the waves break and reform to break again on bar 2 and eventually the beach/bar 1 they are substantially reduced in wave height. This will produce lower waves on bar 2 and bar 1 respectively, and corresponding lower values and a shift to more intermediate conditions.
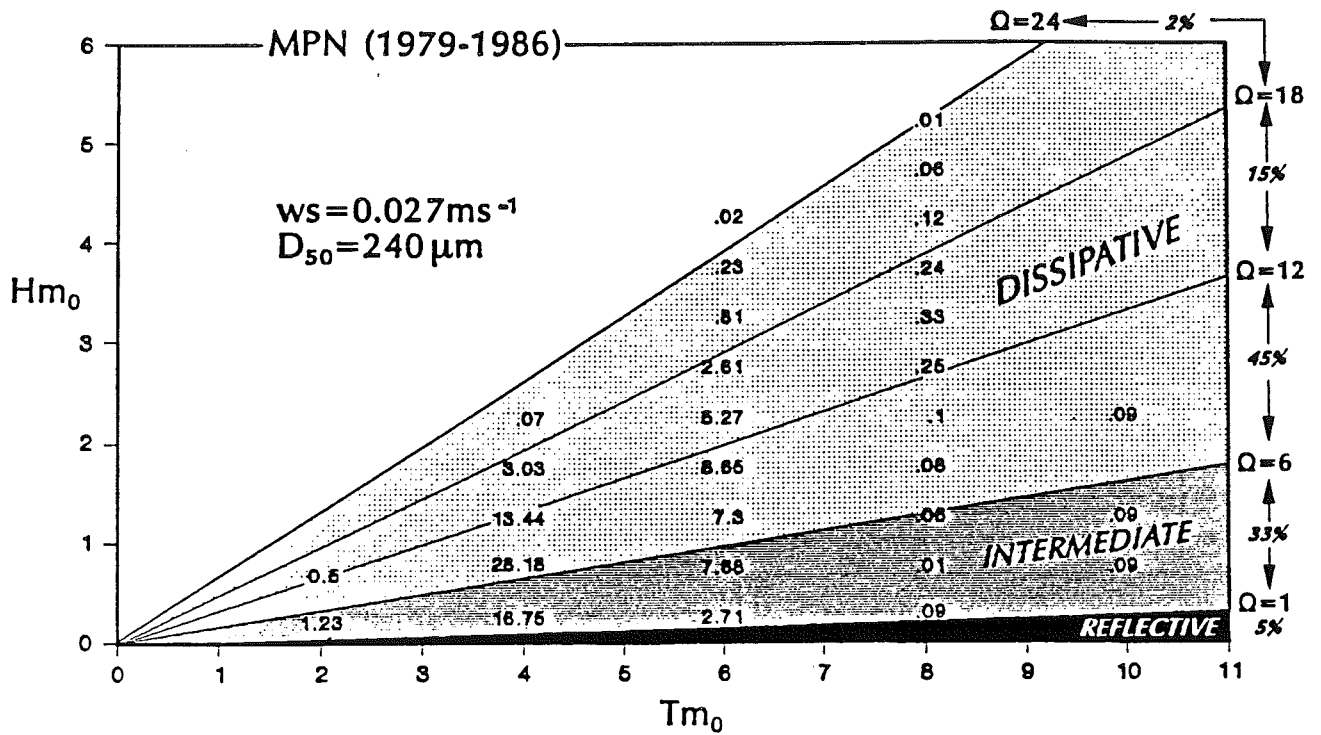
Figure 7.2 A combined plot showing the frequency of occurrence of H_{mo} and T_{mo} matrix for MPN station, overlain with threshold lines of $\Omega = H_o/w_sT_o$, where w_s = 0.027 m/sec. The major threshold values of 1 and 6 along with 12, 18 and 24 are drawn through the H-T matrix. On the right hand side the predicted percentage of occurrence of reflective (5%), intermediate (33%) and dissipative (62%). Ω values on the outer bar are given.

The impact of wave breaking on surf zone wave heights can be estimated using two empirical approaches. Keady and Coleman (1980) proposed the formula:

$$H_r/H_i = 0.58 \, (H_i/d)^{-0.8} \qquad\qquad 7.8$$

to predict the reformed wave height where Hr is the reformed wave height, Hi the initial wave height and d the water depth at wave breaking. Aagaard (1989) used this formula and found that for low waves (H_b < 0.6 m) it predicts an increase in breaker height. He derived an empirical equation, based on regression analysis where:

$$H_r = 0.667 \, H_i + 0.048 \qquad\qquad 7.9$$

In Table 7.9 the two equations are used to calculate H_r on bar 2 and bar 1 for a range of typical wave conditions together with the corresponding values. The results suggest the following:

1. During storm conditions (H_b > 3 m, T = 7 sec) the entire surf zone is dissipative. This is in agreement with the observations of Van den Berg (1977) who observed flat post storm profiles on beach/bar 1 about 7% of the time. In Figure 7.2 this would represent Ω > 16 which occurs approximately 5% of the time.

71

2. During moderate to high waves (H_b = 1.5-3 m) the outer surf zone remains dissipative while the inner surf zone tends towards more intermediate conditions.

3. Under modal and low wave conditions (H_b < 1.5 m) waves first break on bar 2 producing dissipative-intermediate conditions with intermediate conditions dominating at the shoreline.

Table 7.9 Incident (H_i) and reformed (H_r) breaker wave heights using equations 7.8 and 7.9 and predicted Ω at each bar

Wave conditions	Bar 3		Bar 2		Beach/Bar 1	
(T, w_s and d used)	H_i	Ω	H_r	Ω	H_r	Ω
Storm [1]	5	26.4	2.9	15.3	1.7	9
	5		3.38	17.9	2.25	11.9
	4	21.1	2.76	14.6	1.7	9
	4		2.72	14.4	1.8	9.8
	3	15.9	2.61	13.8	1.7	9
	3		2.05	10.8	1.4	7.5
Transition [2]	2	12.3	1.60	9.9	1.11	6.9
	2		1.38	8.5	0.96	5.9
	1.5	9.2	1.04	6.4	0.74	4.6
Modal[3]			1.3	9.6	0.9	6.7
			1	7.4	0.7	5.2
Low[3]			0.5	3.7	0.4	2.8

1 Storm   T = 7, w_s = 0.027, d = 5m (bar 3)/2m (bar 1)
2 Transition   T = 6, w_s = 0.027, d = 3m (bar 2)/2m (bar 1)
3 Modal-low   T = 5, w_s = 0.027

All the above results are likely to be conservative owing to overestimates of the H_i, and consequently one would expect intermediate conditions to prevail more frequently across the inner (bar 1) and midsurf zone (bar 2) under modal and transitional waves (i.e. H_b < 2 m).

The usefulness of Ω in predicting beach type can be gauged from Figure 7.3. This figure plots the observed beach type (bar 1, 2 and 3) for each aerial photograph set, versus the calculated based on the actual wave data, using the formulae:

$$\Omega N = (\Sigma D^{-i/\phi})^{-1} \Sigma (\Omega i D^{-i/k\phi})$$
7.10

from Wright et al. (1987) where ΩN is the predicted Ω value for the day in question, D is the number of antecedent days used to calculate Ω usually 30, i = 0 for the day in question, and i/ϕ is a decay function where ϕ = 5.

Aagaard (1988) proposed a slightly modified version for the eastern Danish coast where:

$$\overline{\Omega}_{10} = (\sum_{i=0}^{D} 10^{-i/\phi})^{-1} \sum_{i=0}^{D} (\Omega_i 10^{-i/\phi})$$
7.11

where D = 10, day i = 0 is used while ϕ remains 5. The lower D value implies the beach responds more rapidly to the Danish sea environment than the Australian swell environment of Wright et al.

The predicted ΩN and ΩH values were calculated based on actual wave conditions for 30 and 10 days prior to each aerial photograph. These are presented in Table 7.10 and plotted in Figure 7.3 together with the observed beach type on each of the bars.

Table 7.10 Predicted Ω values for beach and bar morphology along the central Netherlands coast

Year	D	Predicted Ω				Aerial photographs Observed mean beach types (and standard deviation)		
		0-56 km [1]		56-118 km [2]				
		H [3]	N [3]	H	N	Bar 1	Bar 2	Bar 3
1982	10	4.95	6.22	6.52	2.19	2.06	2.3	
	30	4.95	6.21	6.52	2.17	(0.49)	(0.1)	
1983	10	8.41	9.80	11.08	12.91	2.0	3.3	4.6
	30	8.42	9.81	11.10	12.92	(0)	(0.83)	(0.39)
1984	10	3.68	4.31	4.85	5.67	1.57	2.55	
	30	3.72	4.35	4.89	5.73	(0.49)	(0.72)	
1985	10	7.09	7.56	9.34	9.95	1.95	3.57	4.90
	30	7.08	7.53	9.32	9.92	(0.27)	(0.75)	(0.21)
1986	10	8.26	9.35	10.28	12.31	2.15	4.1	4.7
	30	2.26	9.33	10.88	12.29	(0.32)	(0.47)	(0.27)
1987	10	8.01	9.11	10.55	12.00	2.0	3.24	
	30	8.02	9.12	10.57	12.01	(0)	(0.96)	
1988	10	5.58	4.94	7.35	6.50	2.55	3.61	
	30	5.58	4.94	7.35	6.51	(0.29)	(0.5)	

1 w_s = 0.027 m/s
2 w_s = 0.0205 m/s
3 H = Hald equation
  N = Narrabeen equation

The results indicate that the observed beach types generally lie above the threshold values suggested by Wright and Short (1984). Aagaard (1988) obtained similar results from his Danish coastal sites and suggested the dissipative to intermediate transition values be raised to 12.5. This would improve the results, but the problem remains of accounting for the decreasing Hb and across the surf zone and presumably lower beach state. Using the results of Table 7.9 two additional Ω scales are shown in Figure 7.3. The scales indicated the predicted for bar 2 and bar 1 resulting from the reduced breaker wave height. For example when predicted Ω = 9 on bar 3 it is 6 on bar 2 and 5 on bar 1. Consequently predicted beach type will vary accordingly. The overall result is to leave bar 3 within the predicted dissipative range, to have bar 2 oscillating around the dissipative-intermediate boundary, and to place bar 1 below boundary and increasing in lower intermediate regime. In general this adjustment provides reasonable results, particularly if the ΩH with D = 10 is used.

Figure 7.3 also shows the predicted frequency of occurrence of each beach type for each bar systems based on calculations of Ω made using the reduced breaker wave heights, and the deepwater wave frequencies for Figure 7.2. These can then be compared with the observed beach types based on the aerial photographs in Figure 7.4. As the observed values are based on a biased (spring conditions) and small sample, it is expected that the actual values would lie somewhere between. An estimate of these is given in the third 'expected' columns. These results suggest that the entire system is 'expected' to be dissipative only 5%. It is predominantly intermediate, though the modal beach type ranges from LBT-RBB (bar 3) to RR-LTT (bar 1) (see Table 5.3). The outer bar will never be reflective while the second bar will only be reflective at points of bar attachment.
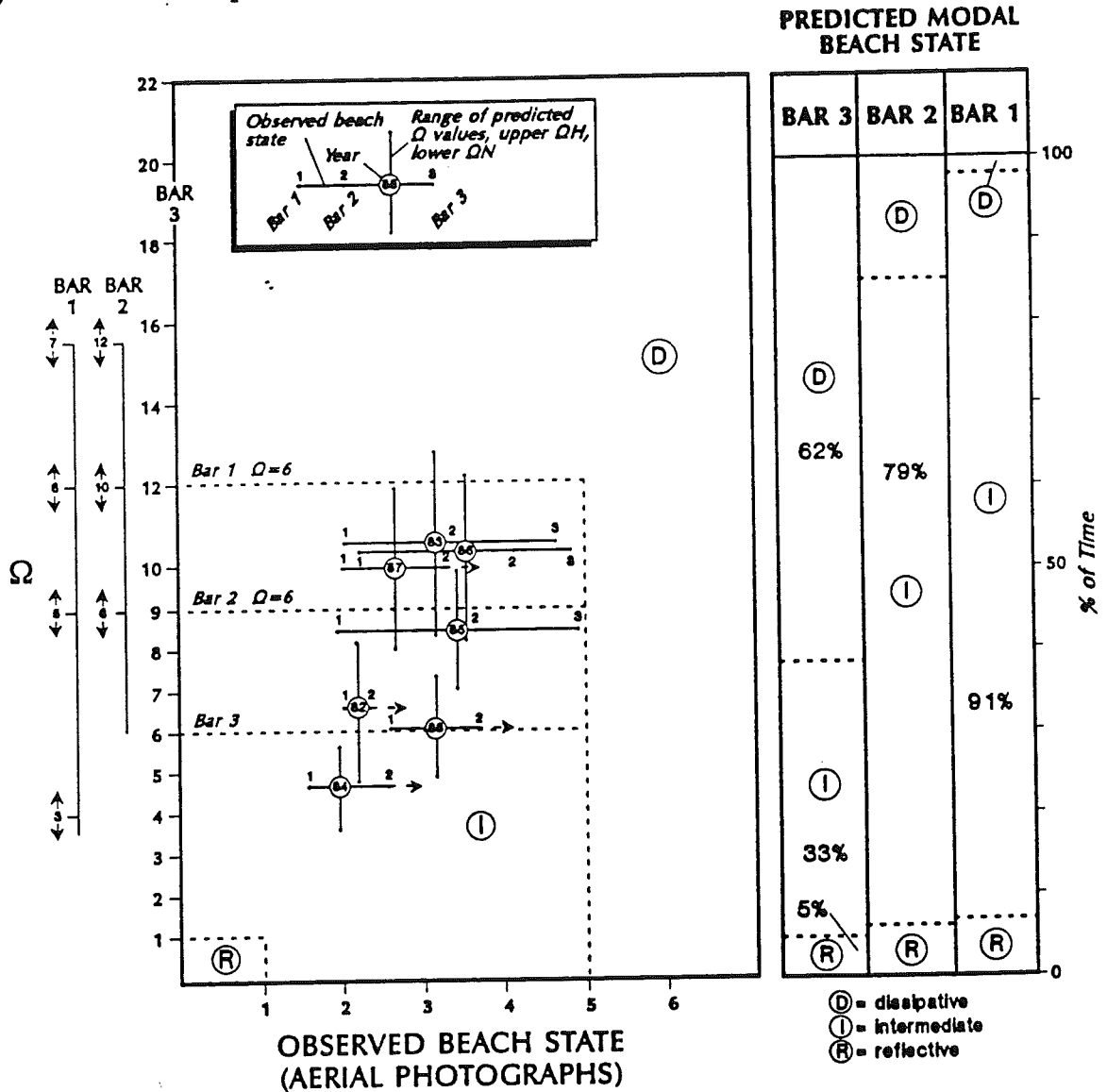
Figure 7.3   The relationship between predicted and observed beach state at time of annual aerial photographs for 1982-1988 based on table 7.10. The three scales for are for each bar as a result of the decreasing wave height based on equations 7.8 and 7.9. The range of predicted Ω is a result of using equations 7.10 and 7.11. Upper range is due to ΩN, lower range to ΩH. Horizontal dashed lines provide thres-hold Ω values between intermediate and dissipative domains for each bar. Bar graphs at right show predicted modal beach states for bar 3 (based on Figure 7.2) and subsequent predictions based on reduced wave heights for bars 2 and 1.

Finally, in reviewing these results it must be stressed that there is much room for variation in the calculation of the values, both in the formula used and the estimates of H_b particularly across the surf zone. The results suggest the best estimate is to use the ΩH estimate and the Aagaard threshold of $D > I$ of ~ 12.5, or to reduce H_b across the surf zone and use the adjustable scale (Fig. 7.4).

Figure 7.4 The relationship shown in Figure 7.3 plotted using only the ΩH values. The bar 2 and bar 1 vertical scales (on left) represent the predicted ΩH values for the corresponding bar 3 value based on H_o and T_o values from Figure 7.2. The predicted beach type for each bar is obtained from Figure 7.2, the observed from aerial photographs (Table 5.3) and the expected which probably lies between the observed and predicted frequencies. See Table 2.3 for explanation of expected beach types.

In order to accurately assess this technique and these proposed beach type frequencies, daily time series of waves and beach morphology is required as was used by Wright et al. (1985) and Aagaard (1988). Such data are not presently available for the Netherlands coast.

8. RESULTS AND DISCUSSION

In considering the results of this study it is important to restate the aims and the data base. This study is solely concerned with the beach morphodynamics of the central Netherlands coast and factors that contribute to its spatial and temporal (months) variation. It is therefore examining the relative shallow (< 10 m), narrow (< 1000 m) inner shoreface containing the beach and bar systems. Apart from some site visits to familiarize the author with the coast made during April to July 1989, the data is based entirely on information and publications available as at June 1989.

This section contains a summary of the results presented in the previous sections, highlighting those most relevant to contemporary beach morphodynamics. This is followed by a discussion and proposal of a preliminary 'beach model' for the central Netherlands coast.

8.1 Results relevant to beach morphodynamics

The central coast barrier system is a mid Holocene regressive barrier system now in a state of transgression. The present beach and shoreface represents the response of these reworked barrier sands to contemporary coastal processes. In the recent past the shoreface has been steepened by these processes as sediment was transferred from the shoreface to the 'Younger Dune' system, particularly in the central section of the coast. This paper is not concerned with the reasons for the present shoreface gradients and sediments or coastal stability. Rather given that such gradients, sediments and processes presently exist along the central coast, this paper addresses their relatively high frequency interactions which contribute to contemporary beach morphodynamics.

8.1.1 Sediments

Sediments along the central coast consist of reworked fluvial and some glacial sands. They are relatively uniform alongshore as indicated in Figures 3.1 and 3.2. A summary of their characteristics is given in Table 3.1 and Appendix 12.1. For the purpose of calculations requiring grain size parameters, two values of D_{50} were adopted for the study. A value of $D_{50} = 200$ um (ws = 0.0205 m/sec) for km 0-56, and $D_{50} = 240$ um (ws = 0.027 m/sec) for km 57-119. This distinction is based primarily on the inner surf zone sediment characteristics (200 and 400 m, Fig. 3.2)

8.1.2 Shoreface gradients

Shoreface gradients are an essential component of beach morphodynamics. They not only determine the level of inshore wave attenuation and refraction, thereby influencing breaker wave height and direction, but also in their interaction with infragravity waves contribute to standing and edge wave lengths and cut off frequencies. They are therefore together with waves and sediment a major determinent in the type and scale of beach processes and morphology.

An examination of both nearshore profiles extending several kilometers offshore and beach profiles extending 1 km offshore was used to assess the morphometric character of the

shoreface. The longshore variation in their character is presented in Figures 6.1 and 6.2 and summarized in Tables 6.1 and 6.2. The surf zone or inner shoreface slope averages 700 m in width extending out to 8 m water depth with a mean gradient of 0.011. It can further be divided into three sectors, a low gradient (0.01) central sector (km 40-90) with steepening (0.014) to the north (km 0-40) and south (km 90-118). The entire shoreface out to the break in slope with the inner shelf has a mean width of 3 600 m, with a mean gradient of 0.0045 out to 15 m depth. In assessing their contribution to standing waves and edge waves all three slopes were used. It was found that the two inner slopes give more realistic results and appears to make a major contribution to bar and rip spacing along the coast.

8.1.3 Waves

Waves moving across the shoreface and breaking in the surf zone interact with the tides, slope and sediment to produce the beach morphodynamic system. Whereas inshore slope and sediments are relatively uniform longshore, and constant over time waves are highly variable.

Longshore variation in wave characteristics is not expected to be great along the central coast given its relatively short length and uniformly in exposure to the North Sea (Fig. 1). Any variation could not, however, be tested in this study owing to the offshore nature of the wave data. It is therefore assumed to be uniform longshore except in the vicinity of the harbour breakwaters (IJmuiden and Hoek van Holland) and the Den Helder ebb tide delta. Each produces in a reduction in breaker wave height. The extent of this impact is indicated in Figure 5.7.

Temporal variation in waves are, however, considerable. A plot of daily wave height (Fig. 4.3) illustrates the extreme daily change in height in response to changing wind conditions over the North Sea. Particularly noticable is the roughly 10 day cycle in higher waves, possibly related to the west to east passage of subpolar low pressure cyclones. When averaged over months and years (Fig. 4.5) two trends are apparent. First there is a définite seasonal variation in mean wave height with the highest and longest waves arriving in winter (January, December), a spring transition of moderate waves (February, March), lower shorter waves during summer (April to August), a fall transition of moderate waves (September, October) then back to winter.

The modal wave height for MPN is 1.3 m with a 5.1 sec period. However, from year to year the monthly and annual mean wave height can vary considerably (Table 4.2) indicating that lower frequency cycles are influencing wave conditions with some years (e.g. 1988) substantially higher than low years (e.g. 1987). Still longer cycles and trends in the North Sea wave climate are presented by Hoozemans and Wiersma (in press).

Finally, waves arrive from south west through north east quandrants with most arriving from the north west and a secondary mode from the south west (Fig. 4.2).

In this study the MPN wave station data, supplemented with YM6 data was used to both assess the breaker wave climate and to calculate its impact on beach morphodynamics.

8.2 Beach morphology

The beach morphology of the central coast is essentially uniform alongshore apart from one natural and several structural effects. The system (Fig. 5.1) consists of a continuous barrier-beach system containing beach/bar 1 and bar 2 for its entire length. A third bar exists from km 0-85, with only two from km 85-119. The km 40-85 section also possesses a lower inner shoreface gradient (Fig. 6.2) and a more stable beach system. The modal beach type of the three bars, their observed and expected ranges are given in Table 8.1 together with the mean spacing of rips in each system, and offshore bar location and mobility.

Table 8.1   Some characteristics of the three bar system along the central Netherlands coast

	Bar 1	Bar 2	Bar 3
Location	km 0-119	km 0-119	km 0-85
Beach Type[1] Modal Range	RR R-TBR	TBR R-LBT	RBB/LBT RBB-LBT
Rip Spacing[2] (m)	500	600	900
Distance to bar[3] (m)	80	250	500
Lateral bar mobility[4] (m)	60	120	180

1 Table 5.3
2 Table 5.7
3 Table 7.3
4 Table 6.1

Manmade structures occupy 42% of the coast consisting of 44 km of groynes, the 4.5 km long Hondsbossche dyke and the major breakwaters at IJmuiden and Hoek van Holland. Each has an impact on the adjacent beach system. The breakwater and their adjacent tidal shoals result in a wave 'shadow' zone with wave height decreasing towards the breakwaters in the shadow zone. Within each zone beach type also changes to either a lower energy type, or inactive modal or even higher energy type (see section 5.6).

The Hondsbossche dyke has replaced the beach/bar 1, (Fig. 5.14) however, bars 2 and 3 still continue seaward of the dyke.

The groynes have two impacts. First they induce more rips either adjacent to one or both groynes, and even mid-groyne rips when they are more widely spaced (Fig. 5.19). As the groyne spacing averages less than half the mean rip spacing the groyne fields produce more numerous, topographically controlled rips. Second, the groynes appear to shift the entire beach-bar 1 up one beach state to a higher energy rip dominated state. At bar 2 however the groynes produce more in rips when it is RR resulting in a shift to a higher state (ie to TBR) and apparently shifting it to a lower states when LBT (ie to RBB or TBR). When bar 2 is TBR or RBB the groynes simply produce more rips at the groyne locations, approximately doubling the number of rips. The groynes do not, however, appear to affect the lower frequency position and migration of bars 2 and 3.

8.3 Beach morphodynamics

The beach morphodynamics of the coast is a function of the wave characteristics interacting with the sediments and shoreface slope. To test the relationship between the observed beach morphology and the wave climate, for a given slope, grain size and tide range, two approaches were used. First measurements of bar and rip spacing and estimates of infragravity wave frequencies based on observations and theory were compared using predicted cut off frequencies and bar and rip spacing. The results suggest the following:

1. The wave climate is capable of producing wave groups with periods during storms of 60-100 sec. Standing wave periods (Ts) required to produce theoretical bar spacings similar to that observed are on the order of Ts = 80-100 sec (Table 7.6b, c).

   Edge wave periods (Te) required to produce rip spacings the same magnitude as those observed are on the order of 100 sec for bar 1, 150 sec for bar 2 and 300 sec for bar 3, (Table 7.7b, c) the latter agreeing with field measurements made by Gerritsen and van Heteren (1984).

   Based on the predicted cut off frequencies it is hypothesised that a mode 3 standing waves with a T_s = 80-100 sec, is responsible for the three bar spacing, while lower frequency edge waves (mode 0-3) are responsible for the variable rip spacing. Both hypothesises require field testing.

2. A method of relating beach morphodynamics to waves, sediments and slope is provided by non-dimensional parameters. The dimensionless fall velocity (Ω) was found to be the most suitable parameter providing reasonable predictions of both modal and predicting beach state for beach/bar 1, bar 2 and bar 3. To obtain the values for bar 1 and 2 emperical values of reformed breaker wave height were calculated (Table 7.8). Figure 7.2 illustrates the Ω domain for the coast, while Figure 7.3 and particularly 7.4 illustrates the relationship between predicted Ω and the observed beach state. The results confirm the threshold values of Wright and Short (1985). Reflective conditions requiring Ω < 1 are expected to prevail < 15% at bar 1 and rarely on bar 2. (Fig. 7.4). Intermediate conditions require $\bar{o}$ = 1-6 which are expected to commonly prevail on bar 3 (85%), bar 2 (85%)and bar 1 (80%), values which roughly correspond with the limited observational data. The modal intermediate beach state however, shifts from LBT on bar 3 to RR on bar 1 (Table 8.1). Dissipative conditions are predicted for the outer bar 62% of the year. However, they were not observed and are expected to prevail about 15% of the year. The low expected frequency of dissipative beach types can be explained by two facts. First the breaker wave height at the outer bar will be lower than that at MPN whose values are presented in Figure 7.2. Therefore $\bar{o}$ will be correspondingly lower; second, most high wave events are of limited duration, normally only 1 to 2 days, whereas beach state requires up to 10 days to fully adjust to changed wave conditions. Therefore modal LBT and RBB states as expected prevail into the highly dissipative domain. Only when full dissipation is achieved on bar 3 can bar 2 and 1 begin to become fully dissipative. The estimated frequencies of 10 and 5% suggest this only occurs during extreme waves and accompanying storm surges. As no observations of dissipative conditions were available, this high energy of the beach domain is highly inferencial and awaits field testing.

Finally, it must be stressed that the above correlations are based on a very small temporal sample of beach morphology. To rigorously test both the relationships between modal and

threshold Ω and beach state, and the prediction of daily beach state using Ω will require longer (months-years) daily time series of beach type together with more accurate measurements of breaker (bar 3) and reformed wave height (bar 2 and bar 1).

8.4 'Beach Model' for the central Netherlands coast

The beach system of the central Netherlands coast was classified using the beach model of Wright and Short (1984) developed for the micro-tidal swell dominated southern Australian coast. While the Australian sediments and tides range are similar to those along the central coast the wave climate is significantly different in several ways. First the North Sea is a storm wave environment generating seas rather than swell. Modal wave period is 5.1 sec and ranges from 3-9 sec, compared to periods of 8-16 sec in southern Australia. Wave heights are also limited ranging from 0-5 m. Of equal importance is the episodic nature of the waves with storms and high waves followed by days, weeks and in summer even months of lower often ineffective wave action. Unlike beaches in the Australian swell environment that are constantly adjusting to changing wave conditions, the sea environment has short periods of high waves when conditions tend toward more dissipative beaches, followed by longer periods of low to no waves when the system slowly shifts towards more intermediate-reflective conditions or remains inactive.

Finally the high angle of wave approach and following winds can produce topography heavily skewed to the north or south as indicated in Table 5.7.

The result is first of all a three bar system whereas the Wright and Short model has one up to two. Secondly the scale of temporal change and beach 'memory' is shorter in the sea opposed to swell environment, a result also reached by Aagaard (1989) on the eastern Danish coast.

These factors have been considered in constructing Figure 8.1 which is a preliminary beach model for the central Netherlands coast. It is preliminary because it is based on a limited morphological data base as indicated by the discrepancy between the observed and expected frequency of occurrence of each type.

The most interesting feature of this model is the hierarchy of bar types within each beach state. Only at the full dissipative (a) and fully reflected (b) states are all bars of a similar type. In the dominant intermediate states a range of bar types is produced by two factors. First the shoreward decrease in breaker wave height (Table 7.9) which produces a shoreward shift to lower energy beach types, and second, the seaward increase in standing and edge wave spacing which produces a seaward increase in bar and rip spacing.

In Figure 8.1a the dissipative end member represents the shape of the beach that is expected to follow storm waves and surges of sufficient duration to permit a fully developed dissipative beach system, containing three shore parallel bars. Flow is essentially onshore at incident wave frequency switching more to infragravity frequency towards the shore, and offshore as a standing wave at infragravity frequencies. Rip circulation if present is relatively weak and suppressed by the shore normal flows. Such a state would probably require a series of closely spaced major storm events and should therefore have a low frequency of occurrence.

F:
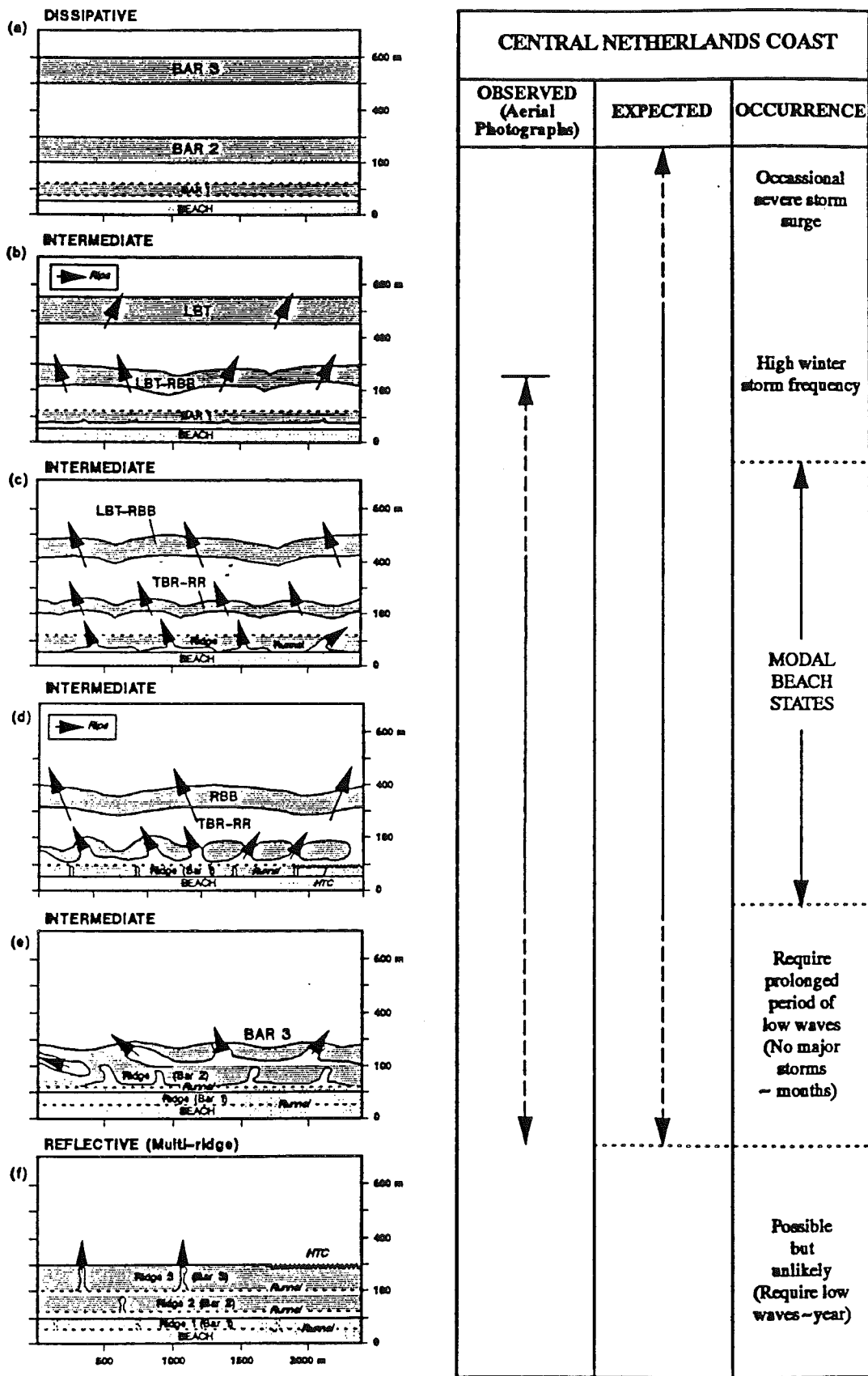
80

Figure 8.1 Possible range of beach types observed on the central Netherlands coast based on 1982-1988 aerial photographs. Types b, c and d were observed on the photographs. Type a is expected following severe storms and storm surges. Types e may occur following prolonged low wave periods and Type f is only probably following extreme periods (months) of low wave conditions and consequently is unlikely to occur.

More usually individual major storm seas or normal winter storms produce a high energy intermediate beach state as illustrated in Figure 8.1b or c, with a continuous outer bar either straight (LBT) or rhythmic LBT-RBB, a highly rhythmic bar 2 and bar 1. Large scale rip circulation dominates across the surf zone. As the three bars move shoreward under post-storm conditions increasing rhythmicity leads to Figure 8.1c and b the modal beach states on the central coast. The outer bar 3 is continuous though broken by widely spaced rips. It is separated from bar 2 by a 100-150 m wide trough. Bar 2 is highly rhythmic and dominated by detached (RBB) or attached (TBR) bars and rip systems. The inner bar 1 attaches to the beach as TBR in Figure 8.1c and welds to the beach as a ridge and runnel by Figure 8.1d.

If prolonged periods of no storms and/or low waves occur, continued onshore bar migration could lead to an attachment of the three bars in Figure 8.1e with bar 3 being RBB-TBR, bar 2 TBR-RR and bar 1 RR/R. It is possible that an unusually long period of low waves could produce Figure 8.1f when all three bars well as a series of ridge and runnels. However the latter (f) and possibly (e) are more likely theoretical end members rather than actual scenarios. Only long term monitoring of beach behaviour will permit refinement of both the bar patterns and frequency of occurrence of the states illustrated in Figure 8.1.

While Figure 8.1 represents a major conclusion of this report it is in fact only a starting point for a more rigorous analysis of the Netherland beach systems. Such an analysis commenced at Egmond aan Zee in 1989 with a cooperative Rijkswaterstaat-University of Utrecht study of the bar morphodynamics and sediment transport (project leaders Aart Kroon (University of Utrecht) and Leo van Rijn (Delft Hydraulics)). No doubt when the results of their detailed study of beach and surf zone morphodynamics is complete it will be able to both rigorously test the conclusions reached in this study and build a more robust model of the central Netherland beach systems.

9. CONCLUSIONS AND RECOMMENDATIONS

9.1 Conclusion

The 120 km long central Netherlands coast is a sandy transgressive barrier containing a beach and multi-bar (two or three) system for most of its length. The beach-bar system is exposed to a highly episodic seasonal storm wave environment with high frequency (~ 30 per year), short duration (2-3 days) storm waves (H_s = > 1.5 m, T = 5 sec) being followed by longer period of calms particularly during summer.

The waves interact with a shoreface consisting of two steeper gradient zones (tan ß = 0.014, km 0-40 and 90-118) containing double bar systems, separated by a lower gradient (tan ß = 0.015, km 40-90) zone containing three bars. All three zones are typified by an inner beach-bar 1 usually attached to the beach as a ridge and runnel. The outer bar 2 is characterised by TBR and RBB, ranging from RR to LBT while the bar 3 is typically LBT to RBB. The number and spacing of the bars can be approximated using infragravity wave theory.

All bars are characterised by rips. The bar 1 has RR or TBR rips averaging 500 m in spacing, bar 2 has TBR rips averaging 600 m while bar 3 has RBB-LBT rips averaging 900 m. The rip spacing can be approximated using predicted low mode edge waves.

The central coast consists of a micro-tidal, multi-bar, storm driven beach system. A tentative model illustrating the range of beach types associated with this system is presented including end member types which rarely, if ever, are achieved on the Netherlands coast (Fig. 8.1)

Man-made structures occupy 48 km (40%) of the coast. The 4 km long Hondsbossche dyke while replacing the beach - bar 1 has little apparent impact on the surf-zone - bar 2.

Two groyne fields (km 0-30 and km 97-115) intersect the beach-bar 1 and occasionally bar 2 and result in a shift to more intermediate beach conditions, typically producing groyne controlled TBR and RBB. The rips usually exit adjacent to one or both groynes, resulting in more frequent rips occurrence and doubling of their number when they are present.

The harbour moles at IJmuiden and Hoek van Holland have resulted in up to 200 m of shoreline progradation as well as a reduction in wave height and changing beach type toward the moles.

9.2 Recommendations

The foregoing results and conclusions could only be reached because of the excellent data base that exists for the Netherlands coast. The fact however that the results are preliminary and some conclusions tentative indicates the need for additional information. Specifically the following is required to fully understand the beach morphodynamics.

1. *Sediments.* Sediment data is adequate.

2. *Waves.* Deepwater wave data is adequate. However the sampling interval should be extended to permit the recording of sufficient waves to enable spectral analysis to identify the presence of infragravity waves, particularly related to wave groupiness. This would require a 15 to 20 minute 0.5 sec sample each hour.

2. *Waves.* Deepwater wave data is adequate. However the sampling interval should be extended to permit the recording of sufficient waves to enable spectral analysis to identify the presence of infragravity waves, particularly related to wave groupiness. This would require a 15 to 20 minute 0.5 sec sample each hour.

Breaker wave data is presently lacking. This can be recorded by placement of a nearshore wave rider and wave tower seaward of the outer bar, such as for the 1989 Egmond aan Zee field experiments. Breaker wave height within the surf zone is far more difficult to monitor on a long term basis due to the hostile environment. However the coupling of a permanent nearshore wave station and short term experiments will permit empirical observation and subsequent deviation of cross shore wave breaking. In all cases waves must be recorded to allow identification of incident and infragravity wave spectra.

3. *Beach Morphology.* The aerial photographs provide an excellent annual spatial snapshot of the beach morphology. However there is a need to expand this in time. This can be achieved using the video recording method of Lippman and Holman (1989). This would provide quantifable daily changes in the morphology of all three bars. A system could be installed in a safe, high location such as the top of the Egmond lighthouse.

Beach morphodynamics. In order to test some of the tentitative correlations presented in this report between infragravity standing wave and edge waves and shore parallel and shore normal bar and rip spacing the following is required. First, simultanous recording of prebreaking, surf zone and swash wave spectra and cross spectra, preferably with simultaneous current spectra. Second, a record of the three dimensional surf zone morphology (air photo, surveying, video) and its change in time.

The investigation of short term field experiments such as the 1989 Egmond work together with long term daily breaker wave and morphological monitoring will enable a rigorous model of the beach system to be developed, one that should be capable of predicting changes in meso scale, three dimensional surf zone dynamics and morphology.

5. *The Wadden Sea and Delta coasts.* The wave, sediment and photographic data presently exists to conduct identical preliminary investigations of the beach-bar systems of the Wadden Sea barrier islands and Delta coasts. A more comprehensive investigation would require an effort identical to that recommended for the central coast.

Structures. At the meso scale level of observations the groyne fields appear to have no positive impact on the coast. Their mean spacing usually less than half that of the natural rip spacing results in the forcing of more intermediate, rip dominated surf zone morphodynamics. This in turn may result in accelerated long and offshore transport, particularly during storms. The groynes and natural sections of identical coast do however provide an ideal natural laboratory for rigorously assessing the actual impact of groynes, particularly during storm events.

10. ACKNOWLEDGEMENTS

11. REFERENCES

Aagaard, T., 1988a. A study on nearshore bar dynamics in a low-energy environment; Northern Zealand, Denmark. J. Coastal Res., 4, 115-128.

Aagaard, T., 1988b. Rhythmic beach and nearshore topography: examples from Denmark. Geogr. Tidsskr, 88, 55-60.

Aagaard, T., 1988c. Nearshore bar morphology on the low-energy coast of Northern Zeeland, Denmark. Geogr. Ann., 70A, 59-67.

Aagaard, T., 1989. Infragravity waves and nearshore bars. PhD Thesis, Inst. Geog., Univ. of Copenhagen, 234 pp.

Aagaard, T., in press. Infragravity waves and nearshore bars in protected, storm-dominated coastal environments. Mar. Geol.

Aagaard, T., in press. The evolution of nearshore bar morphology under the influence of low frequency edge waves. (Abstract) Coastal Sediments 91, ASCE, Seattle.

Alphen, J. van, 1987. De morfologie en lithologie van de brandingszone tussen Terheijde en Egmond aan Zee. Rijkswaterstaat, notitie NZN87.28, 22 pp. (The morphology and lithology of the surfzone between Terheijde and Egmond aan Zee.)

Alphen, J.S.L.J. van and Damoiseaux, M.A., 1988. Geomorfologische kaart van de Nederlandse kustwateren, schaal 1 : 250,000. K.N.A.G. Geografisch Tijdschrift, 22, 161-167. (Geomorphological map of the Dutch coastal zone).

Alphen, J.S.L.J. van and Damoiseaux, M.A., 1989. A geomorphological map ofthe Dutch shoreface and adjacent part of the continental shelf (1 :250,000). Geologie en Mijnbouw 68, 333-   .

Baak, J.A., 1936. Regional Petrology of the Southern North Sea. Thesis, Leiden, 128 pp.

Bakker, W.T. and de Vroeg, J.H., 1988. Coastal modelling and coastal measurement in the Netherlands. In: de Graaw, A. and Hommen, L. (eds.), Prototype measurements to validate numerical models of coastal processes, Grenoble, 5-25.

Battjes, J.A., 1974. Surf similarity. Proc. 14th Intl. Conf. Coastal Engr., ASCE, 466-480.

Bemmelen, C.E. van, 1988. De korrelgrootte-samenstelling van het strandzand langs de Nederlandse Noordzee-kust. Rijksuniversiteit Utrecht. Vakgroep Fysische Geografie Report Geopro 1988-01. Utrecht, 38 pp. (The grain size composition of the beach sand along the Dutch North Sea coast.)

Beets, D.J., Roep, Th.B. & de Jong, J., 1981. Sedimentary sequences of the sub-recent North Sea coast of the western Netherlands near Alkmaar. Spec. Publ. Int. Ass. Sediment, 5, 113-145.

Berg, J.H. van den, 1977. Morphodynamic development and preservation of physical sedimentary structures in two prograding recent ridge and runnel beaches along the Dutch coast. Geologie en Mijnbouw, 56, 185-202.

Bowen, A.J. and Inman, A.L., 1969. Rip currents. 2 Laboratory and field observations. J. Geophys. Res., 14, 5479-5490.

Bowman, D. and Goldsmith, V., 1983. Bar morphology of dissipative beaches: an empirical model. Mar. Geol., 51, 15-33.

Carter, D.J.T. and Draper, L., 1988. Has the north-east Alantic become rougher? Nature, 3327, 494.

Carter, R.W.G., 1988. Coastal Environments. Academic Press, London, 617pp.

Dillingh, D. and Stolk, A. 1989. A short review of the Dutch coast. Nota GWIO-89.004, Tidal Waters Division, Rijkswaterstaat, 30pp plus 14 photos.

Doeglas, D.J., 1954. The origin and destruction of beach ridges. Leidse Geologische Mededelingen, 20, 34-47.

Edelman, T., 1967. Systematic measurements along the Dutch coast. Proc. 10th Conf. Coast Engr., 489-501.

Eisma, D., 1968. Composition, origin and distribution of Dutch coastal sands between Hoek van Holland and the Island of Vlieland. Neth. J.Sea Res., 4, 123-267.

Gerritsen, F. and van Heteren, J., 1984. Low frequency oscillations on the Dutch coast. Proc. 19th Coastal Engr. Conf., ASCE, 625-641.

Gourlay, M., 1968, Beach and dune erosion tests. Delft Hydraulics Laboratory, Report No. M935/M936.

Guza, R.T. and Inman, D.L., 1975. Edge waves and beach cusps. J. Geophys. Res., 80, 2997-3012.

Hoopen, H.G.H. ten & van Driel, G.B., 1979. Rapportage fotovluchten muistroom-onderzoek. Rijkswaterstaat, Nota WWKZ-79G.013, 13 pp. (Report on photoflights rip current investigation.)

Hoozemans, F. and Wiersma, J., in press. Is the mean wave height in the North Sea increasing? Nature. (prepublished as Nota GWAO-89.004, Rijkswaterstaat, North Sea Directorate, PPA).

Huntley, D.A., 1976. Long period waves on a natural beach. Journ. Geophys. Res., 81, 6441-6449

Jelgersma, S., de Jong, J., Zagwijn, W.H. & van Regteren-Altena, J.F.,1970. The coastal dunes of the western Netherlands: geology, vegetational history and archeology. Med. Rijks. Geol. Dienst, N.S., 21, 93-167.

Keady, and Coleman, 1980., In 'Shoreline Past and Present', Tanner, W.F. (ed), Coastal Res., Florida State Univ., Tallahessee, 249-168.

K.N.M.I. (1982-1989). Monthly Bulletin North Sea. (Metereological and wave conditions.)

Knoester, D., 1987. Beschrijving databestand Delflandlodingen van 1900-1960. Notitie GWAO-87-407, 9 pp. (A description of the database, Delfland soundings 1900-1960).

Kohsiek, L.H.M., 1984. De korrelgrootte karakteristiek van de zeereep (stuifdijk) langs de Nederlandse kust. Rijkswaterstaat, nota WWKZ-84G.007, 38 pp. plus figures. (The grain size characteristic of the most seaward range of dunes along the Dutch coast.)

Lippmann, T-C. and Holman, R.A., 1989, Quantification of sand bar morphology: A video technique based on wave dissipation, Journ. Geophys. Res., 94, 995-1011.

Postma, R. and Kroon A., 1986. Mathematische profielanalyse van de onderzeese oever de aansluitende zeebodem voor de Nederlandse kust. Rijkswaterstaat dienst Getijdewateren notitie: GWAO-86.375, 21 pp. plus appendices. (Mathematical profile analysis of the Shoreface off the Dutch coast.)

Rijkswaterstaat. Noordzeekust van Nederland. Fotodocumentatie 1950-1954 (Archive 5/c/117). (The Dutch North Sea coast, photography documentation 1950-1954 Archive 5/c/117).

Rijkswaterstaat. Oblique colour aerial photographs: Zeeland-IJmuiden4.7.87, IJmuiden-Den Helder 2.7.87, Texel-Rottum 18.10.87.

Roep, Th.B., 1984. Progradation, erosion and changing coastal gradient in the coastal barrier deposits of the western Netherlands. Geologie en Mijnbouw, 63, 249-258.

Roep, Th.B., 1986. Sea level markers in coastal barrier sands: examples from the North Sea coast. In: V.d. Plassche, O., Sea-level Research, 97-128.

Roep, Th.B. & Beets, D.J., 1988. Sea level rise and paleotidal levels from sedimentary structures in the coastal barriers of western Netherlands since 5600 BP. Geologie en Mijnbouw, 67, 53-60.

Roep, Th.B., Beets, D.J. & Ruegg, G.H.J., 1975. Wavebuilt structures in subrecent beach barriers of the Netherlands. Proc. 9th Int. Sed. Congress, Nice, 141-146.

Roskam, A.P., 1988. Golfklimaten voor de Nederlandse kust. Rijkswaterstaat, Nota GWAO-88.046, 21 pp. (Wave climate of the Dutch part of the North Sea).

Short, A.D., 1979. Three dimensions beach stage model. Journ. Geol., 87, 553-571.

Short, A.D., 1985. Rip current type, spacing and persistence, Narrabeen Beach, Australia. Mar. Geol., 65, 47-71.

Short, A.D., 1986. A note on the controls of beach type and change, with examples from south east Australia. J. Coast. Res., 3, 387-395.

Short, A.D., in press, Macro-meso tidal beach morphodynamics - an overview, Journ. Coastal Res..

Short, A.D. and Wright, L.D., 1983. Physical variability of sandy beaches. In Mclachlan, A. and Erasmus, T. (eds.), Sandy Beaches as Ecosystems. (he Hague, 133-144.

Sonu, C.J., 1972, Field observations of nearshore and meandering currents. Journ. Geophys. Res., 77, 3232-3247.

Stolk, A., 1989. Zandsysteem kust; een morfologische karakterisering. Technisch rapport 1, Kustverdediging na 1990. Rijksuniversiteit Utrecht, Vakgroep Fysische Geografie, Rapport GEOPRO 1989.02, 97 pp. (Sand system coast - a morphological characterization, Technical Report No. 1 - coastal defence after 1990).

Stolk, A., Wiersma, J. and Zitman, T.J., 1987. Kustgenese. Grootschalige vorming en ontwikkeling van de Nederlandse kust. Rijkswaterstaat Fase 1, 1987, Deelrapport III, 120 pp. (Coastal genesis - large scale formation and development of the Dutch coast).

Vessem, P. van, 1988. Een eerste benadering van de verplaatsing van de Nederlandse kustlijn in 1990-2000, 1990-2020 en 1990-2090. Nota GWAO.88.356. (A first approach of the shifting of the Dutch shoreline position in 1990-2000, 1990-2020 and 1990-2090.)

Vroeg, J.H. de, 1987. Schematisering brandingsruggen met behulp van jaarlijkse kustmetingen. Vakgroep Waterbouwkunde, Technische Universiteit Delft, 37 pp. (A schematic representation of surf zone bars based on annual coastal survey.)

Wiersma, J., 1989. Kustgenese; van kustregiem tot kustregie. De Levende Natuur, 5, 102-105 (Coastal Genesis)

Wiersma, J. and Van Alphen, J.S.L.J., 1988. The morphology of the Dutch shoreface between Hook of Holland and Den Helder (The Netherlands). In: De Boer, P.L. et al. (eds.) Tide-influenced sedimentary environments and facies, D. Reidel Publ. Co., 101-111.

Wright, L.D. and Short, A.D., 1984. Morphodynamic variability of surf zones and beaches: a synthesis. Mar. Geol., 56, 93-118.

Wright, L.D., Nielsen, P., Shi, N.C. and List, J.H., 1986. Morphodynamics of a bar-trough surf zone, Mar. Geol., 70, 251-285.

Wright, L.D., Nielsen, P., Short, A.D. and Green, M.O. 1982. Morphodynamics of a macrotidal beach, Mar. Geol., 50, 97-128.

Wright, L.D., Short, A.D., Boon, J.D. III., Hayden, B., Kimball, S., and List, J.H., 1987, The morphodynamic effects of incident wave groupiness and tide range on an energetic beach, Mar. Geol., 74, 1-20.

Zagwijn, W.H., 1984. The formation of the younger dunes on the west coast of the Netherlands (AD 1000-1600). Geologie en Mijnbouw, 63, 259-268.

Appendix 12.1

Summary statistics of surf zone sediment characteristics.
Source: Van Alpen (1987).
a. all data
b. D_{50}
c. sorting
d. percent $CaCO_3$
e. percent mud

a. Surf zone - nearshore: all samples

Variable	D_{50} um	SdD_{50}	$D_{90}D_{10}$
Sample size	344	53	53
Average	230.727	14.4717	1.87981
Median	220	14	1.83
Mode	230	15	1.61
Standard dev.	67.0524	8.48665	0.221572
Minimum	133	3	1.54
Maximum	615	37	2.34
Range	482	34	0.8

Variable	$SdD_{90}D_{10}$	Sort	$CaCO_3$
Sample size	53	98	98
Average	0.111038	0.425612	12.3002
Median	0.097	0.42	11.85
Mode	0.054	0.42	15
Standard dev.	0.0744128	0.0561674	3.27675
Minimum	7E-3	0.32	4.2
Maximum	0.45	0.65	23.7
Range	0.443	0.33	19.5

Variable	Mud	W_sM_s
Sample size	179	344
Average	2.43531	0.0258052
Median	1.1	0.24
Mode	0.9	0.024
Standard dev.	4.30697	0.0112525
Minimum	0.2	0.01
Maximum	34	0.091
Range	33.8	0.081

b. Surf zone - nearshore: D50 um

Variable	100 m	200 m	300 m
Sample size	3	29	5
Average	217	228.517	266.8
Median	222	209	262
Mode	199	209	230
Standard dev.	16.0935	61.3553	46.0945
Minimum	199	174	219
Maximum	.230	431	332
Range	31	257	113

Variable	400 m	500 m	600 m
Sample size	35	2	36
Average	189.4	201	185.833
Median	177	201	168.5
Mode	168	203	150
Standard dev.	40.5029	2.82843	60.2326
Minimum	151	199	150
Maximum	382	203	489
Range	231	4	339

Variable	800 m	1000 m
Sample size	34	35
Average	201.324	212.143
Median	169	174
Mode	148	148
Standard dev.	77.9292	108.626
Minimum	147	133
Maximum	466	615
Range	319	482

92

c. Surf zone - nearshore: sorting

Variable	100 m	200 m	300 m
Sample size	2	14	4
Average	0.435	0.421429	0.48
Median	0.435	0.43	0.43
Mode	0.44	0.43	0.41
Standard dev.	7.07107E-3	0.0253763	0.114018
Minimum	0.43	0.37	0.41
Maximum	0.44	0.45	0.65
Range	˙0.01	0.08	0.24

Variable	400 m	500 m	600 m
Sample size	19	2	19
Average	0.398947	0.475	0.393684
Median	0.41	0.475	0.39
Mode	0.41	0.53	0.42
Standard dev.	0.0478301	0.0777817	0.03876
Minimum	0.32	0.42	0.34
Maximum	0.49	0.53	0.48
Range	0.17	0.11	0.14

Variable	800 m	1000 m
Sample size	19	19
Average	0.428421	0.466842
Median	0.44	0.5
Mode	0.48	0.41
Standard dev.	0.0460993	0.0594468
Minimum	0.36	0.38
Maximum	0.49	0.56
Range	0.13	0.18

93

d. Surf zone - nearshore: CaCO₃

Variable	100 m	200 m	300 m
Sample size	2	14	4
Average	10.7	10.1643	11.675
Median	10.7	9.85	9.6
Mode	11.8	9.9	4.2
Standard dev.	1.55563	2.24623	8.37073
Minimum	9.6	4.9	4.2
Maximum	11.8	14.4	23.3
Range	2.2	9.5	19.1

Variable	400 m	500 m	600 m
Sample size	19	2	19
Average	11.5947	9.65	12.1158
Median	10.7	9.65	11.6
Mode	10.4	10.5	11.6
Standard dev.	3.45036	1.20208	2.02602
Minimum	6.4	8.8	9.9
Maximum	17.9	10.5	16.6
Range	11.5	1.7	6.7

Variable	800 m	1000 m
Sample size	19	19
Average	13.9368	13.7063
Median	14.2	13.7
Mode	15	12.4
Standard dev.	2.34265	3.26352
Minimum	9.8	7.5
Maximum	17.5	23.7
Range	7.7	16.2

e. Surf zone - nearshore: D_{50} um

Variable	100 m	200 m	300 m
Sample size	35	2	36
Average	2.56286	2.45	1.89167
Median	0.9	2.45	1.3
Mode	0.69	4.1	0.7
Standard dev.	4.0377	2.33345	2.1968
Minimum	0.3	0.8	0.7
Maximum	15.2	4.1	13.1
Range	⁻14.9	3.3	12.4

Variable	400 m	500 m	600 m
Sample size	3	29	5
Average	1.3	0.893103	1.1
Median	1.4	0.6	1
Mode	0.7	0.5	0.9
Standard dev.	0.556776	0.649687	0.620484
Minimum	0.7	0.2	0.3
Maximum	1.8	2.8	2
Range	1.1	2.6	1.7

Variable	800 m	1000 m
Sample size	34	35
Average	2.28529	4.57771
Median	1.3	1.5
Mode	1.1	1
Standard dev.	2.287	7.91923
Minimum	0.4	0.4
Maximum	11.8	34
Range	11.4	33.6

95

12.2.1.a
Deepwater wave height and period matrix for meetpost-Noordwijk (MNP)
Source: Roskam (1988)

Station: Meetpost-Noordwijk
Relative distribution without differentiation on direction
3 hourly series (1.1.1979 - 31.12.1986)
Number of values in this sector = 18005

H_{mo}	T_{mo1} (sec)								
(cm)	< 1.0	1.0-3.0	3.0-5.0	5.0-7.0	7.0-9.0	> 9.0	all	y mean	cum.
0-50	.000	1.227	16.751	2.710	.089	.000	20.778	4.16	100.000
50-100	.000	.505	28.176	7.681	.094	.006	36.462	4.40	79.222
100-150	.000	.000	13.441	7.298	.061	.006	20.805	4.71	42.760
150-200	.000	.000	3.027	8.653	.083	.000	11.741	5.49	21.955
200-250	.000	.000	.072	5.276	.100	.006	5.437	6.01	10.214
250-300	.000	.000	.000	2.610	.250	.000	2.710	6.07	4.776
300-350	.000	.000	.000	.805	.333	.000	1.055	6.47	2.066
350-400	.000	.000	:.000	.233	.244	.000	.567	7.18	1.011
400-450	.000	.000	.000	.022	.117	.000	.267	7.83	.444
450-500	.000	.000	.000	.000	.056	.000	.117	8.00	.178
500-550	.000	.000	.000	.000	.006	.000	.056	8.00	.061
550-600	.000	.000	.000	.000	.000	.000	.006	8.00	.006
600-650	.000	.000	.000	.000	.000	.000	.000	.00	.000
650-700	.000	.000	.000	.000	.000	.000	.000	.00	.000
70-750	.000	.000	.000	.000	.000	.000	.000	.00	.000
> 750	.000	.000	.000	.000	.000	.000	.000	.00	.000
all	.000	1.733	61.466	35.290	1.494	.017	100.000	4.73	100.000
x mean	.00	43.13	78.77	151.53	316.00	141.67	107.39		

Appendix 12.2

12.2.1.b
Deepwater wave height and period matrix for IJmuiden-06
Source: Roskam (1988)

Station: IJmuiden-06
Relative distribution without differentiation on direction
3 hourly series (1.1.1979 - 31.12.1986)
Number of values in this sector = 14784

H_{mo}	T_{mo1} (sec)								
(cm)	< 1.0	1.0-3.0	3.0-5.0	5.0-7.0	7.0-9.0	> 9.0	all	y mean	cum.
0-50	.000	.379	12.500	1.292	.007	.000	14.177	4.13	100.000
50-100	.000	.047	25.358	5.621	.169	.000	31.196	4.38	85.823
100-150	.000	.000	16.633	7.508	.081	.000	24.222	4.63	54.627
150-200	.000	.000	5.459	8.300	.081	.000	13.839	5.22	30.404
200-250	.000	.000	.392	7.224	.135	.007	7.758	5.94	16.565
250-300	.000	.000	.000	4.072	.142	.014	4.228	6.08	8.807
300-350	.000	.000	.000	1.995	.311	.000	2.307	6.27	4.579
350-400	.000	.000	.000	.710	.386	.000	1.096	6.70	2.273
400-450	.000	.000	.000	.135	.534	.000	.670	7.60	1.177
450-500	.000	.000	.000	.007	.284	.007	.298	8.00	.507
500-550	.000	.000	.000	.000	.129	.007	.135	8.10	.210
550-600	.000	.000	.000	.000	.041	.007	.047	8.29	.074
600-650	.000	.000	.000	.000	.020	.000	.020	8.00	.027
650-700	.000	.000	.000	.000	.007	.000	.007	8.00	.007
70-750	.000	.000	.000	.000	.000	.000	.000	.00	.000
> 750	.000	.000	.000	.000	.000	.000	.000	.00	.000
all	.000	.426	60.342	36.864	2.327	.041	100.000	4.82	100.000
x mean	.00	35.00	89.48	178.28	353.50	391.67	128.25		

windrich tingen graden	klasse midden graden	frequentie van voorkomen van windrichtingsklasse in procenten							
		K13	SON	ELD	YM6	MPN	LEG	SWB	alle
0-30	15	7,0	6,5	5,9	6,2	6,0	6,5	6,1	6,3
30-60	45	6,1	6,9	7,3	5,3	6,7	8,3	8,0	6,9
60-90	75	5,7	7,8	8,3	7,9	7,3	6,6	5,7	7,0
90-120	105	6,9	7,4	8,2	9,6	5,6	5,2	6,4	7,1
120-150	135	4,8	6,4	6,5	5,6	6,0	5,0	5,5	5,7
150-180	165	5,6	6,2	7,3	7,2	4,7	5,4	6,8	6,2
180-210	195	10,3	11,4	9,7	9,5	9,8	11,7	12,2	10,8
210-240	225	14,4	13,3	12,2	14,0	18,0	18,1	17,4	15,3
240-270	255	12,6	10,6	11,1	11,1	10,9	11,3	10,2	11,1
270-300	285	10,7	9,0	8,9	8,6	8,9	8,6	8,5	9,0
300-330	315	8,1	8,2	7,6	7,5	10,0	7,1	6,7	7,9
330-360	345	7,9	6,4	7,0	7,5	6,1	6,3	6,5	6,8

Appendix
12.2.3 a

Monthly, annual and mean deepwater wave height and period from Ijmuiden station (YH6). Based on data supplied by
Rijkswaterstaat 1979-1986 (A.P. Roskam) and KNMI, Division of Oceanographic Research, 1987-1988.

|		JAN	FEB	MAR	APR	MAY	JUN	JUL	AUG	SEP	OCT	NOV	DEC	ALL
1979	HMO	146	162	139	0	96	90	106	107	127	141	180	212	139
	TM01	4.8	5.2	5.1	0	4.4	4.4	4.5	4.5	4.9	4.5	5.1	5.3	4.8
	NR.	140	55	54	0	83	57	92	238	199	58	105	171	1252
1980	HMO	153	97	115	133	95	104	157	148	107	182	0	212	135
	TM01	4.8	4.2	4.6	4.9	4.5	4.3	4.6	4.9	4.3	5.5	0	5.4	4.7
	NR.	137	154	159	186	240	161	133	177	183	140	0	203	1873
1981	HMO	203	115	132	114	82	127	95	99	110	197	153	0	125
	TM01	5.6	4.5	4.8	4.6	4.3	4.7	4.2	4.5	4.4	5.5	5.1	0	4.7
	NR.	111	168	212	240	230	229	190	200	235	240	7	0	2062
1982	HMO	71	91	137	121	68	81	87	112	101	128	192	194	119
	TM01	3.8	3.9	5.0	4.8	4.4	4.7	4.5	4.5	4.6	4.6	5.2	5.4	4.7
	NR.	107	207	244	213	221	185	248	220	236	224	233	244	2582
1983	HMO	243	104	135	98	102	93	66	92	156	191	142	153	131
	TM01	5.7	4.4	4.9	4.7	4.6	4.6	4.3	4.4	5.1	5.4	5.2	4.7	4.8
	NR.	236	149	248	239	247	240	244	247	180	240	250	153	2663
1984	HMO	323	101	82	59	104	98	88	64	129	157	116	154	120
	TM01	6.4	4.3	4.4	4.3	4.7	4.8	4.7	4.1	4.7	4.9	4.3	4.7	4.7
	NR.	116	110	5	136	244	227	243	221	84	231	168	205	1990
1985	HMO	0	0	0	87	0	67	95	127	132	54	183	148	136
	TM01	0	0	0	5.5	0	4.6	4.6	4.7	5.0	3.8	5.6	5.9	5.0
	NR.	0	0	0	14	0	11	139	204	49	4	203	24	648
1986	HMO	209	129	103	105	82	85	86	114	64	135	212	178	127
	TM01	5.6	4.7	4.6	5.0	4.3	4.4	4.6	4.8	5.5	5.1	5.7	5.4	4.9
	NR.	199	160	174	197	113	140	166	188	12	188	70	107	1714
1987	H	149	111	141	71	130	94	121	105	122	141	162	137	121 (22)
	T	5.9	5.6	5.6	5.3	5.6	5.0	4.6	5.2	5.1	0	0	0	5.3 (.4)
1988	H	176	226	157	91	77	127	121	112	160	102	154	180	149 (52)
	T	5.1	6.2	6.	5.5	5.0	5.7	5.1	5.4	5.7	5.5	6.3	5.9	5.6 (.4)
	H	186	126	127	98	93	97	102	108	121	143	166	174	129 (10)
	O	71	41	22	22	17	18	24	21	26	41	27	26	
	T	5.3	4.8	5.0	4.8	4.6	4.7	4.6	4.7	4.9	5.0	5.3	5.3	4.9 (.3)
	O	0.8	0.7	0.5	0.4	0.4	0.4	0.2	0.4	0.4	0.6	0.6	0.5	

Appendix 12.2

12.2.3.b Monthly, annual and mean deepwater wave height and period for Meetpost - Noordwjk (MPN) wave station. Source A.P. Roskam (pers. comm.) Rjkswaterstaat

S T A T I O N :   MPN   (MEETPOST NOORDWIJK)

		JAN	FEB	MAR	APR	MAY	JUN	JUL	AUG	SEP	OKT	NOV	DEC	ALL
1979	HM0	100.	100.	122.	84.	73.	73.	80.	85.	111.	61.	138.	167.	99.
	TM01	4.6	5.0	4.9	4.4	4.4	4.2	4.5	4.4	4.7	4.0	4.8	5.0	4.6
	NR.	209.	223.	245.	215.	219.	225.	203.	181.	226.	226.	204.	209.	2585.
1980	HM0	101.	67.	90.	115.	78.	84.	89.	98.	107.	153.	165.	163.	107.
	TM01	4.5	4.2	4.6	4.7	4.4	4.3	4.3	4.6	4.6	5.5	5.0	5.2	4.6
	NR.	224.	220.	228.	234.	236.	126.	201.	165.	147.	144.	151.	211.	2287.
1981	HM0	161.	101.	85.	84.	64.	104.	66.	124.	65.	159.	166.	143.	112.
	TM01	5.4	4.4	4.5	4.4	4.2	4.5	4.6	4.9	4.3	5.3	5.3	5.2	4.7
	NR.	189.	207.	206.	197.	192.	156.	19.	82.	111.	141.	178.	123.	1801.
1982	HM0	87.	55.	119.	106.	69.	89.	81.	100.	68.	85.	149.	159.	96.
	TM01	4.4	3.7	4.9	4.6	4.5	4.6	4.4	4.5	4.5	4.4	4.9	5.3	4.5
	NR.	209.	211.	199.	240.	238.	123.	247.	238.	239.	222.	201.	196.	2563.
1983	HM0	196.	136.	124.	82.	88.	74.	56.	81.	119.	153.	63.	143.	108.
	TM01	5.4	4.9	4.7	4.6	4.5	4.4	4.2	4.2	5.1	5.2	4.4	5.1	4.7
	NR.	225.	164.	182.	232.	237.	214.	232.	247.	142.	209.	97.	91.	2272.
1984	HM0	182.	99.	86.	71.	88.	95.	88.	66.	123.	125.	115.	107.	108.
	TM01	5.3	4.4	4.6	4.6	4.6	4.8	4.8	4.4	4.9	4.8	4.5	4.5	4.7
	NR.	225.	131.	165.	139.	98.	205.	195.	132.	223.	145.	198.	211.	2067.
1985	HM0	122.	78.	86.	128.	73.	98.	92.	115.	118.	54.	152.	129.	108.
	TM01	5.0	4.4	4.5	5.2	4.5	4.5	4.5	4.7	4.9	3.8	5.2	5.1	4.7
	NR.	236.	171.	188.	201.	190.	195.	193.	160.	46.	45.	214.	191.	2030.
1986	HM0	168.	87.	115.	96.	84.	94.	84.	114.	97.	135.	139.	161.	116.
	TM01	5.2	4.1	4.7	4.9	4.2	4.5	4.5	4.7	4.9	5.0	4.9	5.2	4.8
	NR.	202.	200.	168.	174.	137.	189.	219.	236.	229.	204.	228.	214.	2400.
ALL	HM0	139.	89.	104.	97.	76.	88.	81.	97.	100.	118.	140.	147.	106.
	SIGMA	40.	23.	17.	18.	8.	11.	11.	17.	21.	38.	26.	21.	6.
	TM01	5.0	4.4	4.7	4.7	4.4	4.5	4.4	4.5	4.7	4.8	4.9	5.1	4.7
	SIGMA	.4	.4	.2	.3	.1	.2	.2	.2	.2	.5	.3	.3	.1
	NR.	1719.	1527.	1581.	1632.	1547.	1433.	1509.	1441.	1363.	1336.	1471.	1446.	18005.

12.2.4.a

Periodogram for WAVESM87.AVGS

(X 100000)
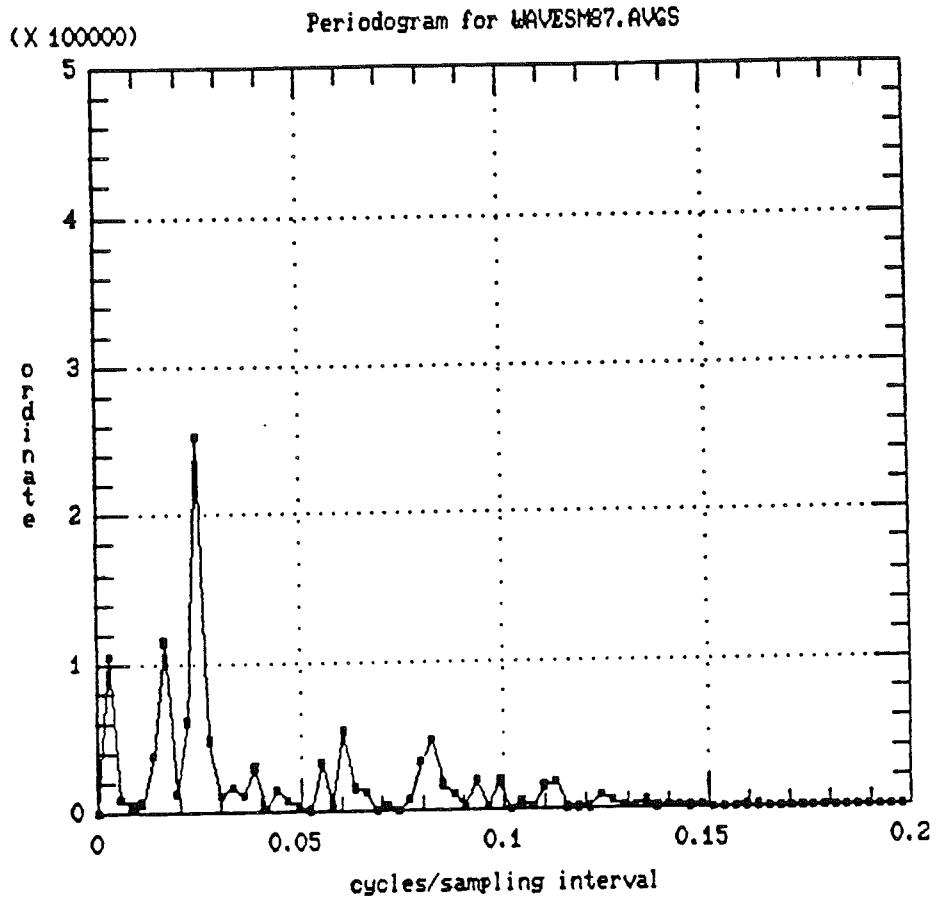
Estimated periodogram ordinates for WAVESM87.AVGS

Frequency	Ordinate	Frequency	Ordinate	Frequency	Ordinate
0.00000	0.69904	0.00275	105179.	0.00549	9597.55
0.00824	5212.06	0.01099	6540.28	0.01374	38079.8
0.01648	114584.	0.01923	12694.5	0.02198	61191.1
0.02473	252673.	0.02747	48126.5	0.03022	11176.6
0.03297	17080.2	0.03571	11352.4	0.03846	29901.9
0.04121	2179.53	0.04396	14575.5	0.04670	7665.93
0.04945	4412.76	0.05220	964.173	0.05495	32499.2
0.05769	3652.93	0.06044	53226.9	0.06319	15823.6
0.06593	12666.5	0.06868	465.832	0.07143	3859.33
0.07418	770.328	0.07692	7715.76	0.07967	33088.3
0.08242	46854.0	0.08516	17453.0	0.08791	10785.8
0.09066	2449.98	0.09341	20063.2	0.09615	1897.44
0.09890	19243.1	0.10165	187.782	0.10440	5175.47
0.10714	1771.79	0.10989	15449.7	0.11264	18639.6
0.11538	1636.08	0.11813	1530.05	0.12088	1213.50
0.12363	9039.08	0.12637	6196.77	0.12912	1988.99

Appendix 12.2

12.2.4.b

Periodogram for WAVES88.AVGS
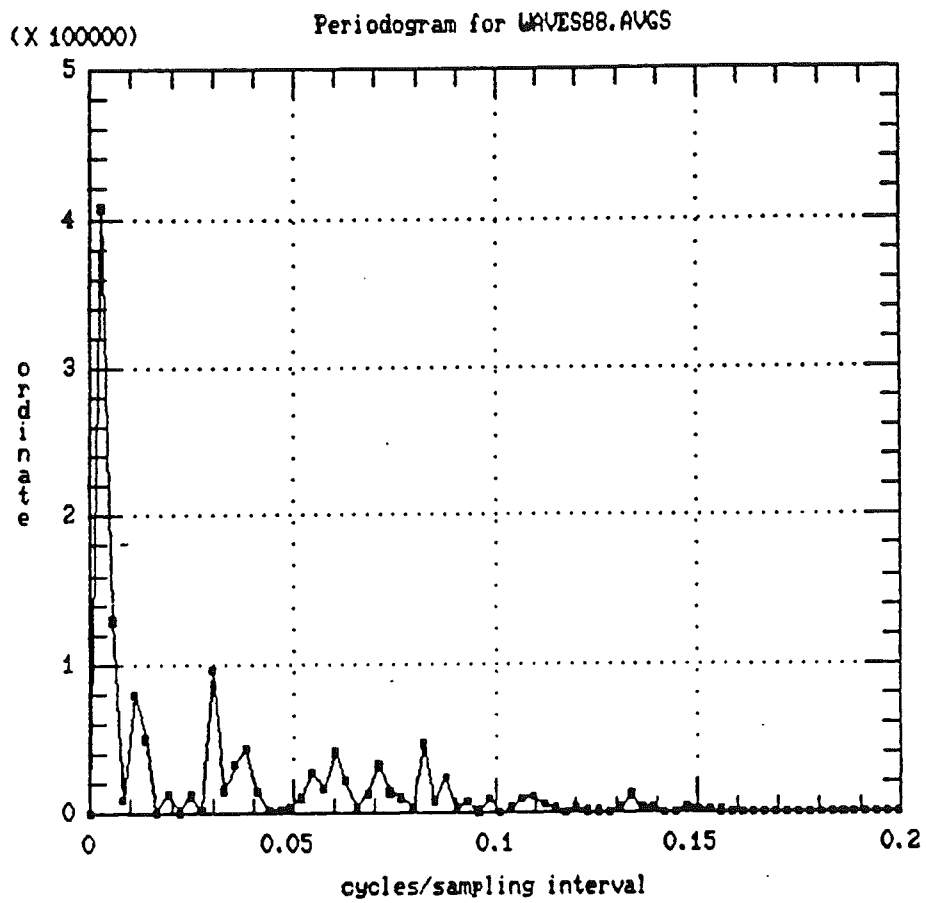
Estimated periodogram ordinates for WAVES88.AVGS

Frequency	Ordinate	Frequency	Ordinate	Frequency	Ordinate
0.00000	0.00000	0.00273	407473.	0.00546	129621.
0.00820	9100.03	0.01093	79973.5	0.01366	50148.7
0.01639	258.535	0.01913	13178.8	0.02186	1576.59
0.02459	11960.4	0.02732	1850.88	0.03005	96394.1
0.03279	15556.8	0.03552	33177.2	0.03825	44175.6
0.04098	14830.1	0.04372	2480.53	0.04645	2165.78
0.04918	3257.78	0.05191	10384.5	0.05464	27670.2
0.05738	16781.7	0.06011	41333.6	0.06284	22461.2
0.06557	4124.42	0.06831	12901.1	0.07104	32161.1
0.07377	14069.9	0.07650	10633.7	0.07923	3962.44
0.08197	46186.3	0.08470	8878.18	0.08743	24316.4
0.09016	3046.01	0.09290	7716.20	0.09563	969.587
0.09836	9559.80	0.10109	893.549	0.10383	3000.71
0.10656	9249.24	0.10929	11236.4	0.11202	5933.26
0.11475	4417.11	0.11749	583.616	0.12022	3395.63
0.12295	1083.30	0.12568	986.167	0.12842	465.094

Appendix 12.3
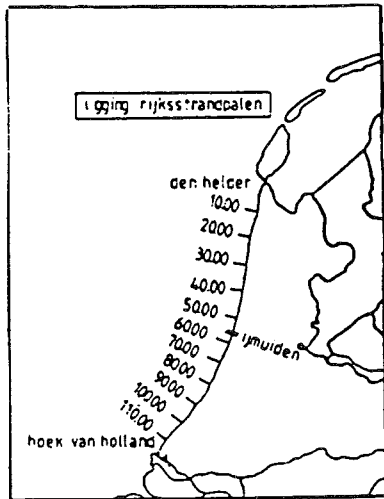
BIJLAGE II.a   3-D-TIJD WEERGAVEN VAN KUST
TEN NOORDEN VAN IJMUIDEN
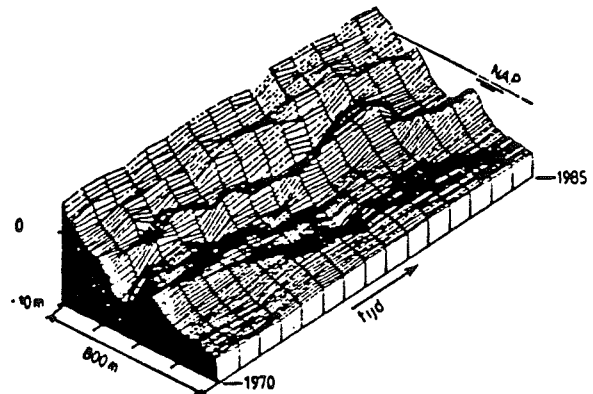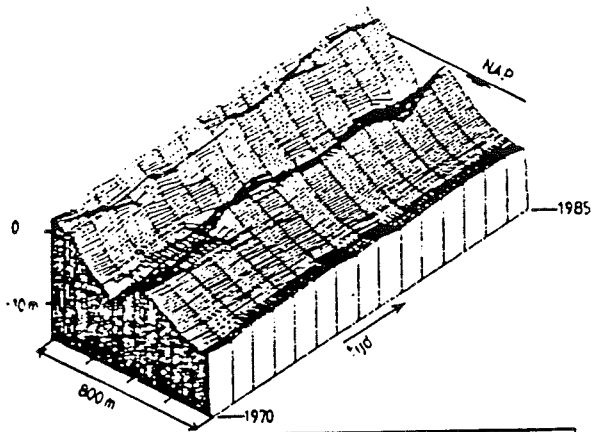
103

Appendix 12.3
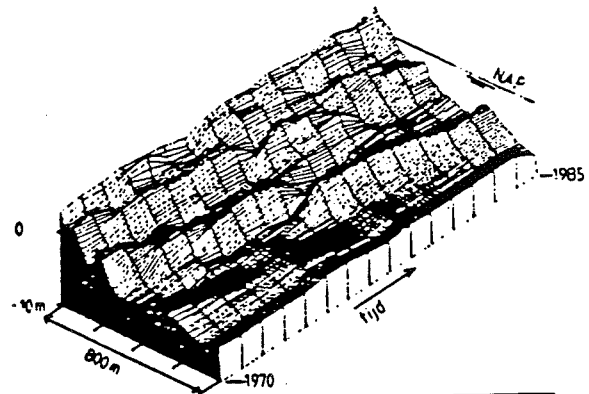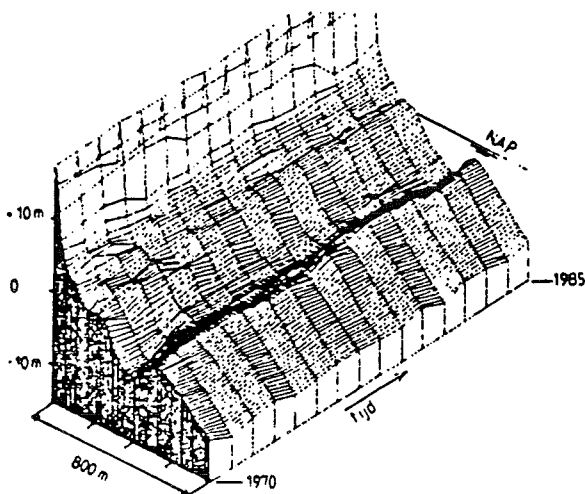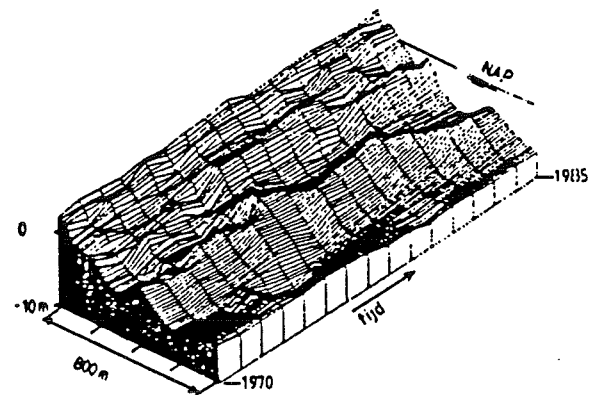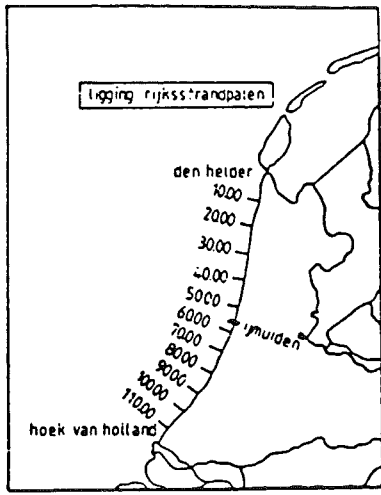
BIJLAGE II.b
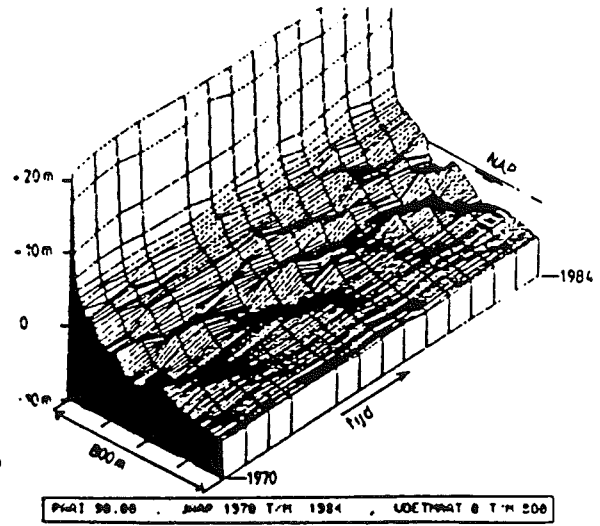
3-D-TIJD WEERGAVEN VAN KUST
TEN ZUIDEN VAN IJMUIDEN

a GROYNE SPACING 0-20KM

b GROYNE SPACING 25-30KM

105

GROYNE SPACING 97-115KM

c

GROYNE SPACING (M)

GROYNE SPACING

d

GROYNE SPACING (M)